The great tragedy of Science –
the slaying of a beautiful hypothesis by an ugly fact

Thomas Henry Huxley

FUNCTIONAL ANALYSIS OF PROTEINS OF THE PEX11-FAMILY IN HUMAN CELLS AND THEIR ROLE IN PEROXISOME PROLIFERATION

Johannes-P. M. KOCH

universität wien

DIPLOMARBEIT

Titel der Diplomarbeit

FUNCTIONAL ANALYSIS OF PROTEINS OF THE PEX11-FAMILY IN HUMAN CELLS AND THEIR ROLE IN PEROXISOME PROLIFERATION

angestrebter akademischer Grad

Magister der Naturwissenschaften (Mag. rer.nat.)

Verfasserin / Verfasser:	Johannes-P. M. KOCH
Matrikel-Nummer:	0247695
Studienrichtung (lt. Studienblatt):	A419
Betreuerin / Betreuer:	Ao.Univ.Prof. Dr. Andreas Hartig

Wien, am 15.08.2008

for Mum

ACKNOWLEDGEMENTS

The last year has been a journey for me aimed at, of course, the diploma thesis and the title Mag. rer. nat. However, things change a lot while under way, so did they for me. The last year has rather become an initiation-rite, getting the feeling how science is like.

I want to thank Cécile Brocard for being the leader during my journey, for always being open for discussion, offering a helping hand and being critical. She has never run out of ideas, supported and engaged me to develop my own strategies and visions. Eventually I agree with her: Science is nothing than sacrifice, the major part of it being frustrating. Still, the few highlights, those little breakthroughs one experiences overrule all bad times by far.

I am very grateful for the all the discussions, coffee sessions and short talks I had with Andreas Hartig about science, the political and universitarian ("dys")system in Austria or just about every-day stuff. He always knew an answer on every question raised, being inspiring and helpful. I thank Sophie Merich and Wolfgang Benetka ("The Elder") for the warm welcome and integration in the "Lab 9- family", for sharing ideas (yes, of course scientific ones … and on how to better play "Gothic"), strong coffees, experience or just time. The same is true for Anja Huber, who had instructed me during my first weeks and prepared me for working on my own. I want to thank her and Veerle de Wever. They have always been willing to listen to my problems.

I would also like to acknowledge Kornelija Pranjic, Karin Großschopf and Fritz Kragler.

Furthermore, I want to thank our administrative and very supportive staff Harald Nierlich, Erna Huber and Silvia Tömö; always accurate and friendly.

I want to deeply thank Beatrice for always standing by me, supporting me, sustaining my moans, sharing my happiness; simply for being her. My thanks go to my family as well, especially to my dear Omi.

You all made my last year a very good one!

And the story goes on …

August 2008

TABLE OF CONTENT

1 Introduction

1.1 Peroxisomes – essential organelles

One of the biggest advantages eukaryotic cells have is their compartmentalization, optimizing the metabolic fluxes. Additionally, the separation of enzymatic pathways such as the catabolism and anabolism of fatty acids provides an easy way of regulating different reactions efficiently. A variety of organelles has evolved to make this possible. Among those are peroxisomes, small compared to other organelles such as the endoplasmic reticulum (ER) or mitochondria since their size ranges from 0.1 to 0.5µm in diameter. Peroxisomes are single membrane-bound organelles and do not contain DNA. Together with glyoxysomes and glycosomes they belong to the microbody family.

Peroxisomes enclose several biochemical pathways, and are essential for most organisms. They oxidize very long chain fatty acids (VLCFA) through β-oxidation, they participate in the metabolism of ether lipids, such as plasmalogens and nitrogen bases (Figure 1, van den Bosch et al., 1992, Lazarow, 1995, Subramani, 1998, reviewed by Wanders and Waterham, 2006). Moreover, peroxisomes contain enzymes involved in the catabolism of reactive oxygen species (ROS) or derivatives, compounds, which accumulation has been correlated with ageing (reviewed by Perichon et al., 1998). The ability to degrade H_2O_2 with catalase gave rise to the name peroxisomes (De Duve and Baudhuin, 1966).

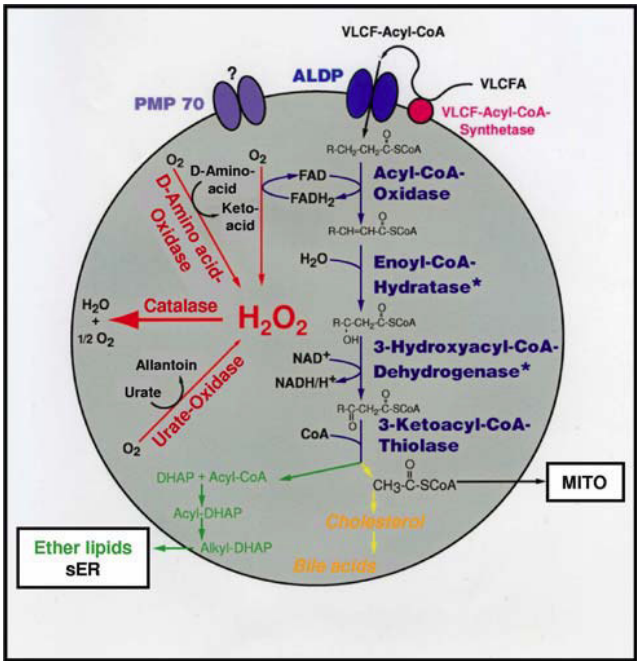

Figure 1: Major metabolic pathways in peroxisomes of the mammalian liver, from Schrader and Fahimi, 2008

These multiple tasks make it clear that peroxisomes need to be versatile in order to adapt to the varying cellular requirements. In the yeast *Saccharomyces cerevisiae*, the need for peroxisomal function arises when fatty acids are provided as sole carbon source. As compared to fermenting cells using glucose, these cells do require peroxisomal β-oxidation to grow. This requirement for peroxisomal function leads to biogenesis and proliferation of these organelles (Veenhuis et al., 1987). Despite the fact that mammalian cells always contain many peroxisomes, their number, size and shape can vary in different tissues or cellular conditions. Moreover, in rodents peroxisomes are highly inducible by hypolipidemic drugs such as fibrates or plasticizers. (Nakajima et al., 2002).

In human, the loss of functional peroxisomes leads to dramatic disorders. This can be due to either an aberrant formation of peroxisomes (peroxisomal biogenesis disorders-PBDs) or to the deficiency of one specific peroxisomal protein (e.g. hyperoxaluria 1, Gould and Valle, 2000; Moser et al., 1995). The PBDs have been classified into 13 complementation groups (CGs) with mutations at different loci. Some broadly known diseases are the Zellweger syndrome, Refsum disease or neonatal adrenoleukodystrophy (Wierzbicki et al., 2002, Moser et al., 1984, Santos et al., 1988). Although some pharmacological advances have been made (such as dietary supplementation with peroxisomal proliferators, McGuinness et al., 2000; Wei et al., 2000, Kemp et al., 1998), these recessive hereditary diseases are mostly lethal.

The use of yeasts as model organisms has allowed to perform genetic screens and led to the identification of genes coding for proteins involved in the biogenesis and proliferation of peroxisomes (Erdmann et al., 1989, Vizeacoumar Vizeacoumar et al., 2004). Today, 31 of these proteins are known, that have been called peroxins and are encoded on the PEX genes (Table 1, Distel et al., 1996, reviewed by Platta and Erdmann, 2007, Brocard and Hartig, 2007). Note, that not all peroxins are present in every organism as listed in Table 1.
Additionally, signal sequences were discovered to traffic newly synthesized proteins to the peroxisomal matrix (Gould et al., 1988; Subramani, 1998; Subramani et al., 2000). Most peroxisomal proteins are targeted to peroxisomes through the peroxisomal targeting signal 1 (PTS1), which originally was thought to consist of the consensus tripeptide (S/A/C)-(K/R/H)-(L/M) at the extreme C-terminus of the cargo protein (Gould et al., 1989).

Gene	Functional orthologs	Identified in *Sc*	*Yl*	*Hs*	Function in biogenesis	Characteristics	Molecular function	Correlated diseases
PEX1		+	+	+	Matrix protein import	AAA-type ATPase	ATP-dependent dislocation of Pex5	ZS/NALD/IRD
PEX2		+	+	+	Matrix protein import	RING-finger		ZS
PEX3		+	+	+	PMP-targeting; *de novo* formation		Membrane anchor of Pex19	NALD
PEX4		+	-	-	Matrix protein import	Ubc	Mono-ubiquitination of Pex5	
PEX5		+	+	+	Matrix protein import	WxxxF-motifs; TPR; ubiquitinated	PTS1-receptor	ZS/NALD/IRD
PEX6		+	+	+	Matrix protein import	AAA-type ATPase	ATP-dependent dislocation of Pex5	ZS/NALD/IRD
PEX7		+	+	+	Matrix protein import	WD40- domain	PTS2-receptor	RCDP
PEX8		+	+	-	Matrix protein import	coiled-coil domain, leu-zipper	Connection of docking- and RING-complex; cargo release (?)	
PEX9		*Eliminated, wrong ORF*			Matrix protein import		*ORF of YlPex9 misidentified; corresponds to HsPex26*	
PEX10		+	+	+	Matrix protein import	RING-finger		ZS/NALD/IRD
PEX11	PEX25/PEX27	+	+	+	Proliferation		Elongation of peroxisomes	
PEX12		+	+	+	Matrix protein import	RING-finger		ZS/NALD/IRD
PEX13		+	-	+	Matrix protein import	SH3- domain	Member of docking complex	ZS/NALD
PEX14		+	+	+	Matrix protein import	PxxP- motif, phosphorylated	Member of docking complex	ZS
PEX15	PEX26	+	-	-	Matrix protein import	Phosphorylated	Membrane anchor of Pex6	
PEX16		-	+	+	PMP-targeting; *de novo* formation; proliferation			ZS
PEX17		+	-	-	Matrix protein import		Member of docking complex	
PEX18	PEX20	+	-	-	Matrix protein import	WxxxF-motifs;ubiquitinated	PTS2-co-receptor in Sc	
PEX19		+	+	+	PMP-targeting; *de novo* formation	CAAX-box, farnesylated	PMP class I receptor and chaperone	ZS
PEX20	PEX18/PEX21	-	+	-	Matrix protein import	WxxxF-motifs;ubiquitinated	PTS2-co-receptor in most fungi	
PEX21	PEX20	+	-	-	Matrix protein import	WxxxF-motifs;ubiquitinated (?)	PTS2-co-receptor in Sc	
PEX22		+	-	-	Matrix protein import		Membrane anchor of Pex4	
PEX23	PEX30/31/32	-	+	-	Proliferation	DysF	Growth regulation in Yl	
PEX24	PEX28/29	-	+	-	Proliferation		Separation of peroxisomes in Yl	
PEX25	PEX11	+	-	-	Proliferation		Elongation of peroxisomes	
PEX26	PEX15	+	-	+	Matrix protein import		Membrane anchor of Pex6 in Hs	ZS/NALD/IRD
PEX27	PEX11	+	-	-	Proliferation		Elongation of peroxisomes	
PEX28	PEX24	+	-	-	Proliferation		Separation of peroxisomes in Sc	
PEX29	PEX24	+	-	-	Proliferation		Separation of peroxisomes in Sc	
PEX30	PEX23	+	-	-	Proliferation	DysF	Growth regulation in Sc	
PEX31	PEX23	+	-	-	Proliferation	DysF	Growth regulation in Sc	
PEX32	PEX23	+	-	-	Proliferation	DysF	Growth regulation in Sc	

Table 1: *The Peroxins*; AAA: ATPase associated with diverse cellular activities; CAAX-box: farnesylation motif; DysF: Dysferlin domain; PXXP: class II SH3 interacting motif; RING: really interesting new gene; SH3: Src homology 3; TPR: tetratricopeptide repeat; Ubc: ubiquitin-conjugating enzyme; WD40: 40 amino acid long domain containing conserved Trp-Asp; ZS: Zellweger syndrome, NALD: neonatal adrenoleukodystrophy, IRD: infantile Refsum disease, RCDP: rhizomelic chondrodysplasia punctata; adapted from Brocard and Hartig, 2007; Platta and Erdmann, 2007

A minor part of matrix proteins is targeted through PTS2, an N-terminal nonapeptide with (R/K)-(L/I/V)-X_5-(Q/H)-(L/I/V) as consensus sequence (Osumi et al., 1991, Swinkels et al., 1991). Interestingly, the presence of one of these signals does not necessarily imply the localization to peroxisomes. For instance, despite exhibiting a PTS1, phosphomevalonate kinase was shown to be cytosolic (Hogenboom et al., 2004). Furthermore, recent studies have revealed, that PTS1 should rather be considered as dodecamer able to interact with the tetratricopeptide repeat (TPR) domain of Pex5, the PTS1 receptor, than the simple C-terminal tripeptide SKL originally described (Brocard et al., 1994; Neuberger et al., 2004; Neuberger et al., 2003, McCollum et al., 1993, reviewed by Brocard and Hartig, 2006).

1.2 The lifecycle of a peroxisome

The lifecycle of a peroxisome is a multi-step process which involves 1) import of membranes and membrane proteins (PMPs) via the ER, 2) import of matrix proteins, 3) growth and subsequent elongation, 4) fission and 5) degradation and inheritance.

1.2.1 Protein import

The peroxisomal matrix protein import can be divided into four steps: i) cargo recognition by a cytosolic receptor (Pex5 and Pex7 for PTS1 and PTS2, respectively), ii) interaction with the docking machinery, iii) translocation and iv) recycling of the receptor (reviewed by Platta and Erdmann, 2007). While Pex5 directly interacts with Pex14, Pex7 needs an additional adaptor (Pex18/Pex21 in yeast, the splice variant Pex5L in mammalians) to interact with Pex14 (Figure 2, Albertini et al., 1997, Brocard et al., 1997; Einwachter et al., 2001, Williams et al., 2005, Niederhoff et al., 2005).

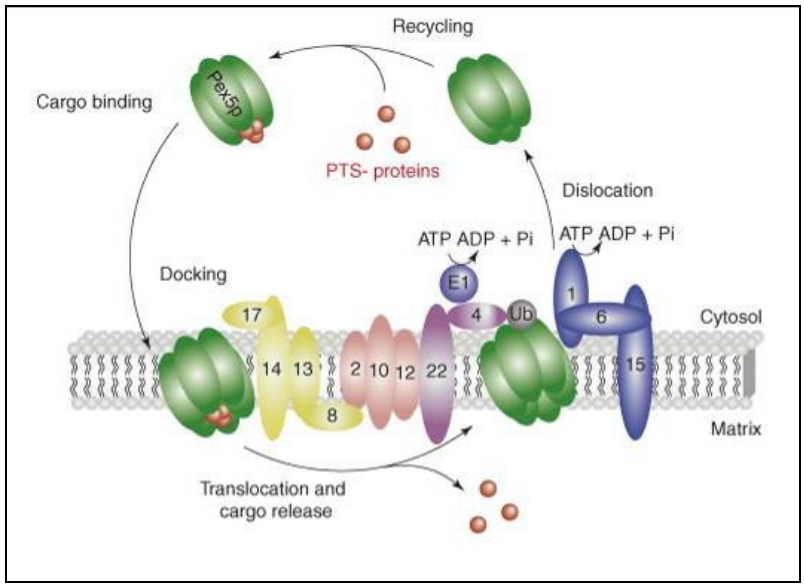

Figure 2: PTS1-dependent protein import in the peroxisomal matrix; from Platta and Erdmann, 2007

Little is known about the import of peroxisome membrane proteins (PMPs). There exist two classes of PMPs, one is believed to be directly targeted and inserted in the peroxisomal membrane (Class I), the other being routed via the ER to its final destination (Class II, Fang et al., 2004). The import machinery is thought to consist of Pex16, Pex3 and Pex19, the latter may perform a chaperone-like activity (Hettema et al., 2000, Purdue and Lazarow, 1995, South and Gould, 1999). Moreover, the identification of a targeting sequence for the

peroxisomal membrane (mPTS) has been an issue (Dyer et al., 1996, Honsho and Fujiki, 2001, Wang et al., 2001, Pause et al., 2000, Rottensteiner et al., 2004). Different consensus sequences and domains were shown to be necessary for correct import. It is believed that not only a short targeting sequence but at least one transmembrane domain (TMD) contribute to a fully functional mPTS. This implies that the mPTSs greatly vary between PMPs (reviewed by Brown and Baker, 2003).

1.2.2 Biogenesis and Proliferation

There exist two ways for the biogenesis of organelles: i) autonomous replication with the ability to proliferate by fission of preexisting organelles (ER, mitochondria, chloroplasts) or ii) non-autonomous biogenesis (lysosomes, endosomes). The origin of peroxisomes has long been a matter of discussion. An endosymbiotic theory was proposed (De Duve, 1969). However, evidence pointed at a model by which peroxisomes proliferate by fission of preexisting organelles. The finding that peroxisomal membrane proteins are synthesized on free polysomes (Lazarow and Fujiki, 1985) supported this model. Additionally, genetic screens, mostly in the yeast *S. cerevisiae*, led to the identification of genes coding for proteins, which are components of the division machinery, with Pex11 as the most abundant protein. Disruption of Pex11 leads to few and enlarged peroxisomes in yeast (Erdmann and Blobel, 1995). In this organism it is believed that Pex11 drives the elongation of the organelle in combination with Pex25 and Pex27. Recent evidence suggests that Pex25 may recruit the GTPase Rho1 to control actin assembly at the peroxisomal membrane. Marelli et al. used a novel approach by combining classical subcellular fractionation with large-scale quantitative mass spectrometry to identify peroxisomal proteins, among those Rho1 was identified. GST-immobilized Rho1 was shown to interact with Pex25 in an *in vitro* binding assay (Marelli et al., 2004).

Among the proteins involved in the peroxisomal fission event Vps1, Dnm1 and Fis1, are also known from mitochondrial fission. Fis1 recruits Dnm1, a dynamin-related protein, to the peroxisomal membrane (Kuravi et al., 2006). There might exist an adaptor protein involved similar to the proteins Mdv1 or Caf4 found in mitochondria (Zhang and Chan, 2007) In mammalian cells, a similar mechanism has been described: The C-terminal tail-anchored membrane protein, Fis1, seems to be recruited by HsPex11β to the peroxisomal membrane, which then interacts with the dynamin-like protein Dlp1, the orthologue of Dnm1 (Li and Gould, 2003, Koch et al., 2004). Even ternary complexes comprising Fis1, Dlp1 and

HsPex11β were detected in a coimmunoprecipitation assay (Kobayashi et al., 2007). A lately discovered membrane protein, Mff, plays a role in mitochondrial and peroxisomal fission, but coimmunoprecipitation experiments revealed that Mff belongs to a different complex than Fis1 implying a more distinct role of Mff in the proliferation machinery (Gandre-Babbe and van der Bliek, 2008). After fission peroxisomes tend to remain clustered, the dissociation seems to require the function of the proteins Pex28 and Pex29 (Vizeacoumar et al., 2003).
The close correlation between the mitochondrial and peroxisomal fission process is evident. Additionally, a cargo-selected vesicular transport from mitochondria to peroxisomes strengthens the interplay between these two organelles (Neuspiel et al., 2008).

The model of autonomous proliferation has become controversial with the finding that mutant cells lacking functional peroxisomes could develop peroxisomes *de novo* upon insertion of the missing gene (Kragt et al., 2005, Haan et al., 2006). Several studies on Pex3 showed the possibility of a *de novo* synthesis of peroxisomes: In *Yarrowia lipolytica* unsynchronized biogenesis happens in temperature-sensitive *pex3*-mutants. These new, immature peroxisomes associate closely with the ER (Bascom et al., 2003). A further proof that Pex3 plays a critical role in the early steps of biogenesis was shown in *Hansenula polymorpha.* The synthesis of the N-terminal 50 amino acids of Pex3 in *pex3*-mutant cells resulted in the formation of vesicular structures containing Pex14, which could be released upon reintroduction of full length Pex3. Here, the nucleus seems to donate the membrane compartment (Veenhuis et al., 1996). Similar experiments using a truncated version of Pex3 in *S. cerevisiae* led to the conclusion that the ER may represent the donor rub for peroxisome biogenesis (Tam et al., 2005). *In vivo* experiments in *S. cerevisiae* underlined these findings (Hoepfner et al., 2005). Interestingly, already decades ago electron microscopy images from Novikoff et al. showed an association between the ER and peroxisomal structures (Novikoff and Novikoff, 1972). Moreover, high resolution immuno-electronmicroscopy and electron tomography led to the suggestion that the ER membrane was the origin of the newly synthesized peroxisomes (Tabak et al., 2003).
In contrast to fungi, in mammalian or in plant cells, Pex3 could not be detected alone in association with the ER (Fang et al., 2004, Hunt and Trelease, 2004). Indeed, these cells seem to require the presence of the protein, Pex16, which then works in concert with Pex3 and Pex19 (Kim et al., 2006). Additionally, the involvement of Arf and coatamer in the process of peroxisome proliferation propose a retrograde transport from the peroxisomes to the ER in mammalian cells (Lay et al., 2006). Moreover, the observation of protein translocation from peroxisomes to the ER makes this retrograde transport also likely in plant and trypanosomes

(McCartney et al., 2005, Subramanya and Mensa-Wilmot, 2006). Today peroxisomes are being considered to derive from the ER and to have the ability to proliferate and divide upon induction (Figure 3).

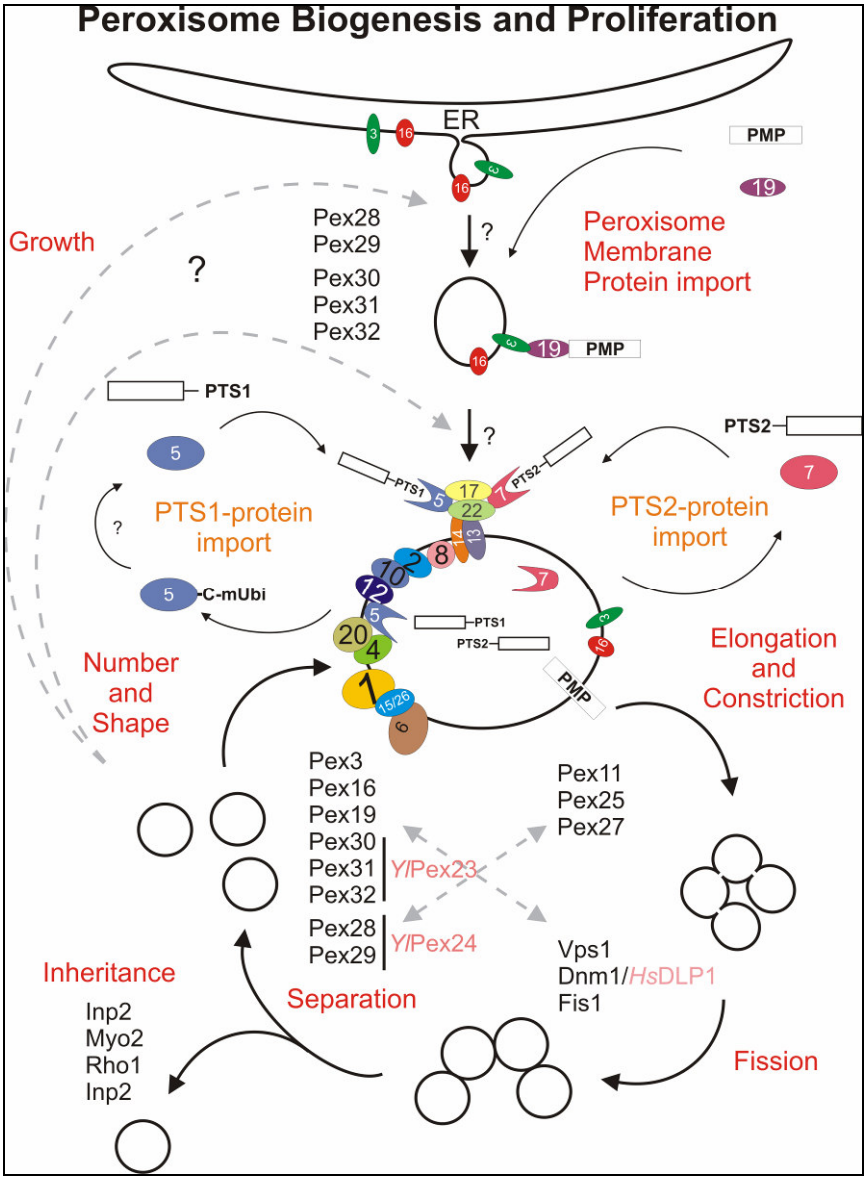

Figure 3: Division and proliferation of peroxisomes - an overview, designed by Brocard C., 2007 (unpublished data)

1.2.3 Peroxisomal induction

Peroxisomes are very adaptable organelles. In order to quickly adapt their manifold enzymes, they must react to various stimuli. Peroxisomes proliferate upon stimulation by herbicides, xenobiotics, ozone or during senescence (Pastori and Del Rio, 1997, Lazarow and Fujiki, 1985). The alpha form of the peroxisome proliferator activator receptor (PPARα) plays a critical role in regulating genes for the lipid homeostasis (Green, 1995). It binds to the

peroxisome proliferator response element (PPRE), which then activates the transcription of several genes (Lemberger et al., 1996). PPARα is stimulated by many ligands such as hypolipidemic drugs (Issemann and Green, 1990). While some studies showed that HsPex11α- expression is affected by PPARα (Shimizu et al., 2004), others postulated that this peroxin is dispensable for PPARα-mediated proliferation. However, HsPex11α expression is affected upon sodium 4-phenylbutyrate induced proliferation (Li et al., 2002a). It has recently been shown that in plant cells even light induces peroxisome proliferation through phytochrome A, HY5 homologue and finally AtPex11b (Desai and Hu, 2008).
In yeast, peroxisome proliferation is induced by the presence of fatty acids (e.g. oleic acid) in the culture medium (Rottensteiner et al., 2003, Tam et al., 2003). In *S. cerevisiae* an oleate-responsive-element (ORE) in the promoter sequence of oleate-inducible genes binds the transcription factor dimer Oaf1/Pip2 (Rottensteiner et al., 1997).

1.2.4 Pexophagy and inheritance

The rapid reaction of peroxisomes on cellular demands requires a robust turnover machinery. The removal of peroxisomes is similar to autophagy, and was called pexophagy (Yokota, 1993, Sakai et al., 2006). Today, two distinct pathways i) the macropexophagy and ii) the micropexophagy contribute to peroxisome homeostasis. In micropexophagy, the lysosome engulfs the peroxisome, whereas in macropexophagy individual peroxisomes are sequestered by multiple membrane layers, which then fuse with lysosomes (Sakai et al., 2006).
Not only biogenesis and proliferation, but also inheritance of peroxisomes to daughter cells is critical in order to maintain peroxisomal function. In budding yeast, Inp2 an integral membrane protein of peroxisomes, works as the receptor for Myo2, a motor protein for actin, and ensures the transport along the actin filaments towards the bud (Fagarasanu et al., 2006). On the opposite, the protein Inp1 serves to retain the peroxisomes due to its strong intrinsic affinity for the cell cortex (Fagarasanu et al., 2005). The delicate interplay between these two proteins is responsible for the correct partitioning of peroxisomes between the mother and the daughter cell during cell division.

1.3 Proteins of the PEX11- family

Because all Pex11 proteins of higher organisms are orthologues of ScPex11, the focus of the introduction will concentrate on the yeast Pex11 family first.

1.3.1 Yeast PEX11 proteins

ScPex11 (formerly Pmp27) is the most abundant peroxin and has always been cited in context with proliferation (Marshall et al., 1995). The implication of this protein to peroxisome proliferation was first suggested by Erdmann et al.: Yeasts lacking the *PEX11* gene were still able to grow on glucose or on ethanol, but failed to grow on oleate as the sole carbon source. Microscopy revealed that these yeast cells contain only few, but giant peroxisomes (Erdmann and Blobel, 1995). Soon after, experiments on the localization, orientation and protein interaction of ScPex11 suggested that ScPex11 localized on the inner surface of the membrane and that it may form homodimers. The monomeric form was proposed to be the active one, whereas dimer formation was anticipated to inhibit further division since immature peroxisomes have a lower dimer to monomer ratio than mature ones (Marshall et al., 1996). The finding that ScPex11 is required for β-oxidation of medium chain fatty acids led to the hypothesis that proliferation is regulated metabolically (van Roermund et al., 2000).
Later, the identification and analysis of two ScPex11 related proteins, ScPex25 and ScPex27 (Rottensteiner et al., 2003; Smith et al., 2002; Tam et al., 2003) complicated this simple view of peroxisome proliferation. Interestingly, growth on oleate of *pex25pex27*-mutant yeast cells was not inhibited. Additional deletion of ScPex11 completely abolished growth but it could be restored by overexpression of ScPex25 only. Yeast two hybrid assays confirmed the known interaction of ScPex11 with itself and further showed that ScPex25 and ScPex27 can interact with each other and themselves.
Although ScPex11, ScPex25 and ScPex27 amino acids sequences are quite similar (~10% identity and ~18% similarity), ScPex25 and ScPex27 exhibit an extended N-terminus as compared to ScPex11 and are both peripheral membrane proteins. ScPex25 is thought to recruit Rho1 to the peroxisomal membrane (Marelli et al., 2004).

1.3.2 Plant PEX11 proteins

Five orthologues of ScPex11 have been identified in the plant *Arabidopsis thaliana*, AtPex11a to e (or AtPex11-3,-4,-1,-5,-2). No obvious homologues sequences of ScPex25/27 or ScPex28-32 were reported, so far. The Pex11 proteins can be divided into three phylogenetically distinct subfamilies AtPex11-3, AtPex11-4 and AtPex11-1,-2,-5, further divided into two classes. Class I AtPex11 are highly similar (>90%, AtPex11-1,-2,-5), class II AtPex11 are more divergent (~50% similarity, AtPex11-3,-4). All localize to peroxisomes and induce proliferation. Only AtPex11-4 is not an integral membrane protein. AtPex11-3, -1 and -2 are constitutively expressed with AtPex11-1 and -2 having the highest expression levels, whereas AtPex11-4 seem to be rather upregulated in senescent tissue. Moreover, AtPex11-4 is thought to play a role in leaf peroxisome photorespiration in young seedlings (Lingard and Trelease, 2006, Orth et al., 2007).

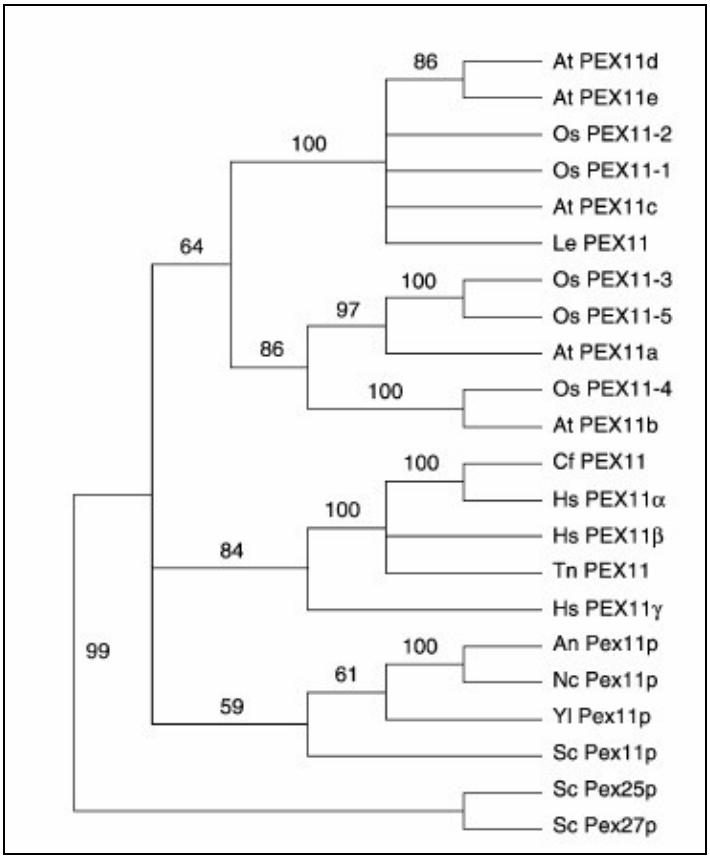

Figure 4: Neighbor-Joining Tree of PEX11 Protein Sequences. Numbers at the nodes are bootstrap values from 1000 trials; An,Aspergillus nidulans; At, Arabidopsis thaliana; Cf, Canis familiaris; Hs, Homo sapiens; Le, Solanum lycopersicum (formerly Lycopersicon esculentum); Nc, Neurospora crassa; Os, Oryza sativa; Sc, Saccharomyces cerevisiae; Tn, Tetraodon nigroviridis; Yl, Yarrowia lipolytica; from Orth et al., 2007

Additionally, the orientation of myc-tagged versions of the five AtPex11 proteins was investigated in *A. thaliana*. Both, N- and C-termini of AtPex11-1,2,4 and -5 were facing the cytosol, just AtPex11-3 exposed its C-terminus to the peroxisomal matrix (Lingard and Trelease, 2006). Recent data showed a cooperative role for AtPex11-1,-5 and -2 during the G2 phase of the cell cycle. Similar to the findings in mammalians and yeast, Fis1b is recruited to the peroxisomal membrane by oligomeric AtPex11 proteins, which then indirectly bind Drp3a to initiate the fission process (Lingard et al., 2008).

1.3.3 Human PEX11 proteins

Three *PEX11* genes have been identified in mammalian cells, coding for HsPex11α (HsPex11A), HsPex11β (HsPex11B) and HsPex11γ (HsPex11C), respectively (Abe and Fujiki, 1998; Abe et al., 1998; Tanaka et al., 2003). Phylogenetic analysis revealed that HsPex11α is more closely related to HsPex11β than both are to HsPex11γ, though interestingly HsPex11α is more similar to the Pex11 protein of *Canis familiaris* (Figure 4).
This tree suggests that all known Pex11 proteins form a monophyletic group. HsPex11α is 11 amino acids longer than ScPex11 with 25% identity, it contains two hydrophobic regions as well as a dilysine motif at its C-terminus. HsPex11β has 12 amino acids more than HsPex11α and shares 40% identity with HsPex11α and 20% with ScPex11.

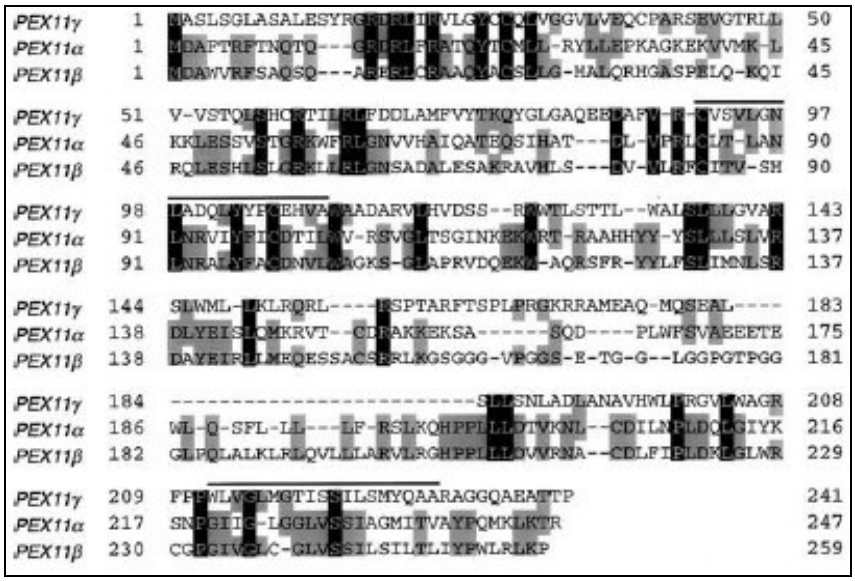

Figure 5: Amino acid sequence alignment of human PEX11α , PEX11β, nd Pex11γ. Sequences were aligned by the CLUSTAL W method. Putative transmembrane spanning segments are overlined; from Tanaka et al., 2002

Between these human Pex11 proteins a higher level of identity was found in the C- terminal region (57% compared to 43%). HsPex11β also contains two hydrophobic domains and a

RxKx motif, similar to the KxKxx motif of HsPex11α. Both proteins have a potential N-glycosylation site (HsPex11α at Asn9 and HsPex11β at Asn134). HsPex11γ is 241 amino acids long has two putative transmembrane segments and shows 22% and 23% amino acid identity to HsPex11α and HsPex11β, respectively (Figure 5).
In contrast to HsPex11α both, HsPex11β and HsPex11γ are constitutively expressed and not inducible by fibrate (Abe et al., 1998).

1.3.3.1 The human Pex11α

The membrane protein HsPex11α exposes both N- and C-terminal ends to the cytosol as revealed by immunofluorescence microscopy experiments. Mutations either changing the dilysine motif (^{243}KLK→LLL) or eliminating the potential N-glycosylation site (^{9}N→D) did not disturb the correct localization to peroxisomes. Moreover, the ^{9}N→D mutation did not change the electrophoretic mobility implying that human HsPex11α was not glycosylated under the conditions tested (in CHO cells, Abe et al., 1998).
An interaction between HsPex11α, Arf and coatomer was reported, suggesting the recruitment of the coatomer by HsPex11α (Passreiter et al., 1998). However, it was later demonstrated, that the binding to the coatomer is not required for the function of HsPex11α in proliferation (Maier et al., 2000). Maybe the mentioned KXKXX motif is responsible for an involvement of the coatomer only under certain circumstances.
No complementation group of peroxisomal deficiencies exist in which HsPex11α is mutated (Abe et al., 1998). Interestingly, a Pex11α$^{-/-}$ mouse has no significant physiological changes compared to a Pex11α$^{+/+}$ mouse. Moreover, normal peroxisome abundance was detected, though a tendency to form peroxisome clusters was observed. The general peroxisome metabolism was unaffected. The highest expression level was measured in the liver. Although HsPex11α is strongly inducible by 4-PBA and fibrates, it was described to be dispensable for PPARα-mediated peroxisome proliferation (Li et al., 2002a).

1.3.3.2 The human Pex11β

Peroxisomal localization of HsPex11β, another membrane protein was proven by immunofluorescence microscopy. Northern blot analysis revealed that this protein is constitutively expressed and could not be induced by clofibrate treatment (Abe and Fujiki,

1998). Pex11β$^{-/-}$ mice displayed neonatal lethality, hypotonia, reminiscent of the human Zellweger syndrome and intrauterine growth retardation (Li et al., 2002b). Additionally, defects in the neuronal migration in coronar sections were observed in these Pex11β null mice. Among the other symptoms were enhanced neuronal apoptosis, delayed renal development and calvarium ossification. However, the peroxisomal protein import and mitochondrial structure were not affected. Likewise, VLCFA accumulation was not the reason for the neuronal abnormalities.

Investigations of double homozygous mice Pex11α$^{-/-}$Pex11β$^{-/-}$ revealed mostly the same phenotypes as homozygous Pex11β$^{-/-}$ mice. Speaking of peroxisome abundance, both the single and the double mutant had approximately half the numbers of peroxisomes as the wild type control mice (Li et al., 2002a).

Biochemical analysis revealed that the C-terminal region of HsPex11β is essential for a direct interaction with Fis1, whereas the N-terminus is indispensable for homo-oligomerization and function. Overexpression of HsPex11β in CHO-K1 cells led to a significant increase in the number of peroxisomes. Kobayashi et al. isolated ternary complexes comprising of HsPex11β, Fis1 and Dlp1 by means of coimmunoprecipitation after chemical crosslinking (Kobayashi et al., 2007). No direct interaction of HsPex11β with Dlp1 was detected, furthermore it could not be shown in association with HsPex11α (Li and Gould, 2003).

Moreover, speculations on a regulation of Pex11β-mediated proliferation by the β-oxidation fell off as Zellweger cells though lacking all peroxisomal metabolic function still contain peroxisomes. In these cells peroxisome abundance was 30 times higher than in wild type cells after transfection with a plasmid coding for HsPex11βmyc. This demonstrates that these peroxisomal membrane remnants are able to proliferate (Li and Gould, 2002).

1.3.3.3 The human Pex11γ

This membrane protein exposes both termini to the cytosol, comparable to HsPex11α. Similar to HsPex11β, it is not inducible by fibrates, but it is constitutively expressed (Tanaka et al., 2003). Indeed, it was reported that the overexpression of HsPex11γ does not induce peroxisomes proliferation, but produces large and clustered peroxisomes (Li et al., 2002a). So far, only speculations about its function remain, since not much biochemical analysis of this protein is available, yet. Therefore, it represents a very good target for further investigations on the molecular mechanisms of peroxisome proliferation.

2 Aim of the Thesis

The peroxisomal biogenesis machinery executes an important process, as deficiencies within this mechanism are lethal for humans. The Pex11 protein family plays a central role in the proliferation of peroxisomes – in yeast, plant and human tissue.

The project, this thesis is embedded in, aims to elucidate the function of the various Pex11 families in yeast, plant and human cells. We work on the analysis of the different and the common elements of the Pex11 proteins and compare these within three kingdoms. This will help to understand the molecular role of Pex11.

This thesis focuses on the analysis of the dynamics of the peroxisomal proliferation in human cells. To address the issue of membrane dynamics we raised the question, whether any correlation exists between the number of peroxisomes and area of peroxisomal membranes. Furthermore, we aim to understand the regulation of the different human Pex11 proteins as well as the importance of the domains of these proteins. A key goal to specifically analyze the molecular function of a protein lies in the identification of interaction partners and the characterization of a potential assembly into complexes. This requires a suitable tag for labeling the proteins of interest.

In order to achieve our aims, we investigated the localization and function of all Pex11 proteins in human cells at various time points. To present statistically relevant data, we counted the number and area of peroxisomes. We analyzed the protein expression of mutated versions of Pex11, where either mutations on two putative phosphorylation sites were introduced or whole domains were truncated.

Additionally, we established a novel technique for labeling our proteins of interest. This tag, called SNAP tag or human alkylguaninetransferase (hAGT) covalently binds its substrate. We modified this tag to introduce a tobacco etch virus (TEV) protease site in order to release our protein of interest from the tag. Consequently, this enables to use this tag conveniently for both, live cell imaging and immunoprecipitation. These analyses all require stably transfected cell lines, which were generated during the work of the thesis.

Live cell imaging will enlighten the role of Pex11 in terms of the peroxisomal proliferation dynamics. The identification of interaction partners by means of coimmunoprecipitation and complex isolation of membrane proteins will certainly provide new insights. As no human cell line mutated in the genes coding for any Pex11 is known, we plan to compare the overexpression phenotype to the knock-down phenotype through siRNA experiments.

The deep scrutiny of the human Pex11 family will bring forth new aspects of complex isolation, organelle proliferation and membrane dynamics.

3 Results

3.1 Ectopic expression of Yeast and Plant Pex11 proteins lead to peroxisome proliferation in human cells

Understanding the evolution of Pex11 will help to pinpoint its function. The Pex11 protein families in human and plant cells were originally found as orthologues of ScPex11 (Abe et al., 1998, Lingard and Trelease, 2006). We sought to clarify whether the function of the various Pex11 proteins are conserved throughout three kingdoms. The localization of yeast or plant Pex11 to the human peroxisomal membrane would give a first hint towards a conserved function of the investigated proteins. Changes in peroxisomal number, size or morphology serve as read out to scrutinize the molecular function of Pex11.

We performed colocalization experiments to address this question. In order to analyze the wild-type phenotype, we cotransfected plasmids encoding two peroxisomal marker proteins in human embryonic kidney cells (HEK293T), a red fluorescent protein appended with a PTS1 (mCherry-SKL, Shaner et al., 2004) and Sterol carrier protein 2, a known peroxisomal protein carrying a PTS1 appended with GFP at its N-terminus (GFP-Scp2, Frolov et al., 1996). We observed complete colocalization of these two proteins (Figure 6D). Herewith, the size, abundance and morphology of peroxisomes did not change compared to singly transfected cells. Significantly, many round-shaped peroxisomes were present throughout the whole cell. Most of those were well separated, though some seemed to be connected, an artifact due to the projection in the z- dimension (see section 3.2 & appendix for details). These findings confirmed our experimental setup.

To compare all known Pex11 proteins, we first evaluated the effect of the overexpression of human Pex11α, β and γ on peroxisome number and size. We used N-terminally GFP- tagged versions of each Pex11 protein under the control of the cytomegalovirus (CMV) promoter (see appendix for detailed information). Our results show that all, GFP-HsPex11α, β and γ fusion proteins colocalized with the peroxisomal marker mCherry-SKL. Furthermore, cells overexpressing GFP-HsPex11α presented significantly more small peroxisomes than wild type cells (Figure 6A). Even more pronounced was the effect of GFP-HsPex11β overexpression (Figure 6B). In both experiments, the cells had at least doubled the number of peroxisomes as compared to HEK293T cells transfected with mCherry-SKL only. In contrast, in about 80% of the cells overexpression of GFP-HsPex11γ led to tubule-formation and

clustering of peroxisomes (see Figure 6C). This however was not accompanied by an increase in the peroxisomal number.

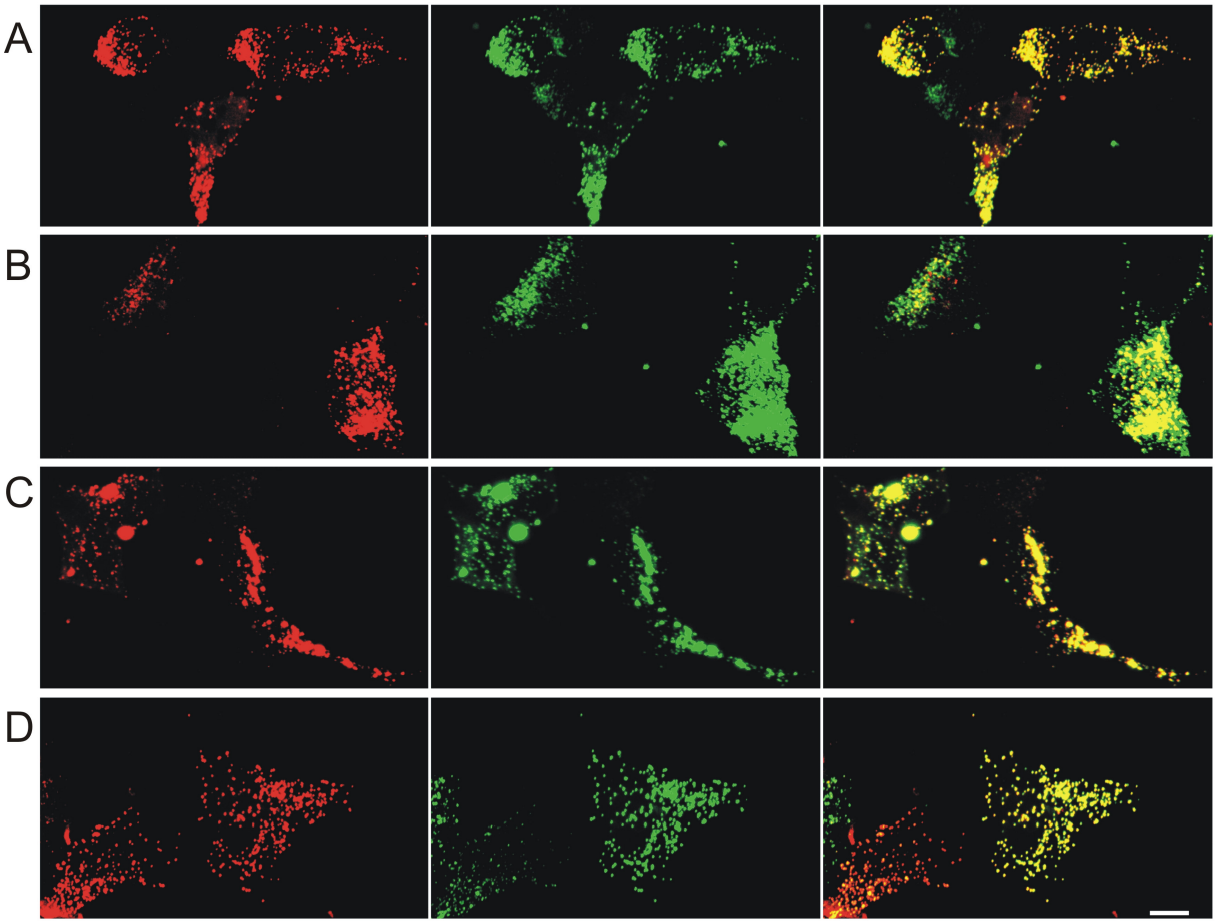

Figure 6: Ectopic overexpression of the three human Pex11 proteins in HEK293T cells 24h after transfection, (A) GFP-HsPex11α induces proliferation, (B) GFP-HsPex11β strongly promotes division, (C) GFP-HsPex11γ leads to formation of large and clustered peroxisomes, (D) wild type peroxisomes with GFP-Scp2; red channel (A-D): mCherry-SKL, images are projected stacks; bar: 10µm

Indeed, it seems as if with an excess of GFP-HsPex11γ the peroxisomes formed clusters, but the final fission and separation steps in proliferation are hampered. In cells that did not contain clustered peroxisomes, those present looked like in wild-types (see Figure 19C, 22h). Taken together, our experiment show that all GFP-tagged Pex11 proteins used are efficiently targeted to peroxisomes and that each of these proteins may have a different effect on peroxisome proliferation.

The overexpression of yeast and plant GFP-Pex11 proteins revealed some similarities compared to the overexpression of the human GFP-Pex11 proteins. Overexpression of GFP-ScPex11 clearly led to far more peroxisomes per cell than the expression of proteins of the Pex11-family from any other organism analyzed (Figure 7). In contrast, overexpression of the yeast GFP-ScPex25 led to enlarged and clustered peroxisomes, which resembles the

observations with GFP-HsPex11γ. However, each cluster formed appeared to be smaller than those visualized through overexpression of the human GFP-HsPex11γ. Overall, in presence of GFP-ScPex25 individual cells contain slightly fewer peroxisomes as compared to cells transfected with the mCherry-SKL only.

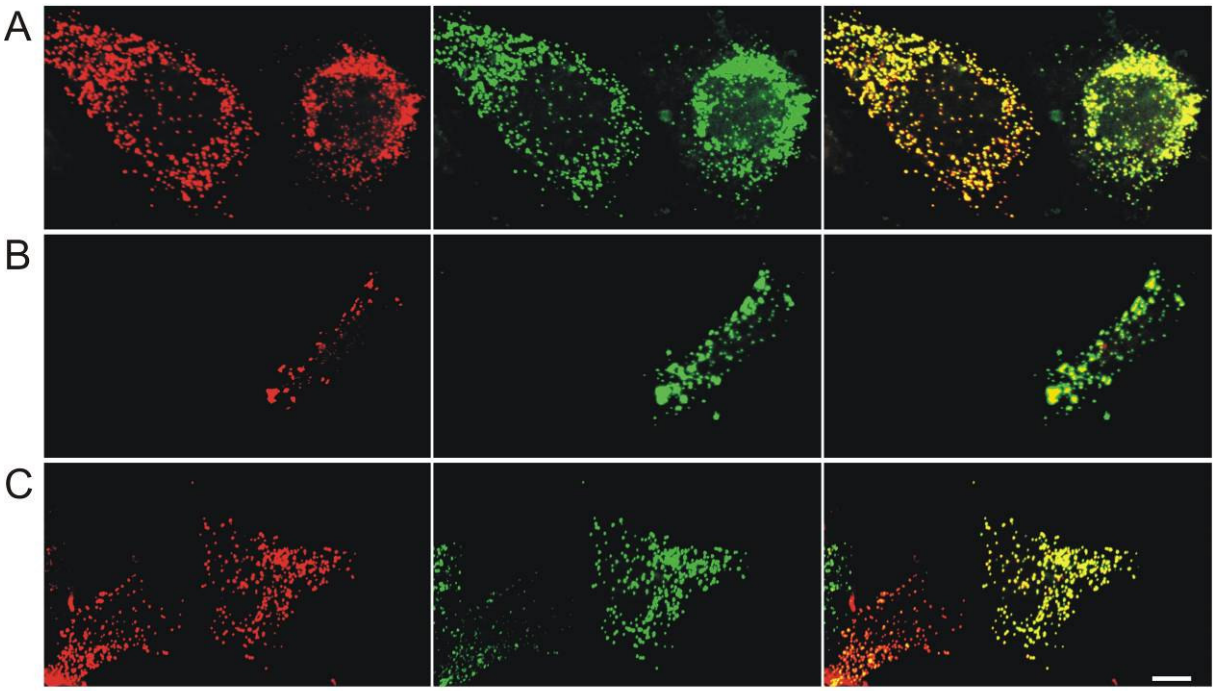

Figure 7: Ectopic overexpression of the yeast Pex11 proteins in HEK293T cells 24h post transfection; (A) GFP-ScPex11 strongly induces proliferation, (B) GFP-ScPex25 forms clustered, larger peroxisomes, (C) wild type peroxisomes with GFP-Scp2; red channel (A-C): mCherry-SKL, images are projected stacks; bar: 10µm

All plant GFP-tagged Pex11 proteins localized to peroxisomes, and in some cases peroxisomes appeared clustered as illustrated through overexpression of GFP-AtPex11-1 to a minor part and GFP-AtPex11-2 to a major part (Figure 8). Noteworthy, cytosolic accumulation of the peroxisomal matrix marker mCherry-SKL seemed to correlate with the overexpression of GFP-AtPex11-4 and GFP-AtPex11-5. Peroxisome clustering has previously been reported in plant cells overexpressing GFP-AtPex11-1,-2 and -5 (Orth et al., 2007). The same group reported the induction of proliferation without clustering for GFP-AtPex11-3 and -4. In our experiments, we cannot confirm a clustering for GFP-AtPex11-5, since the overexpression of GFP-AtPex11-5 led to so many peroxisomes that it is nearly impossible to distinguish between single separated and clustered peroxisomes.

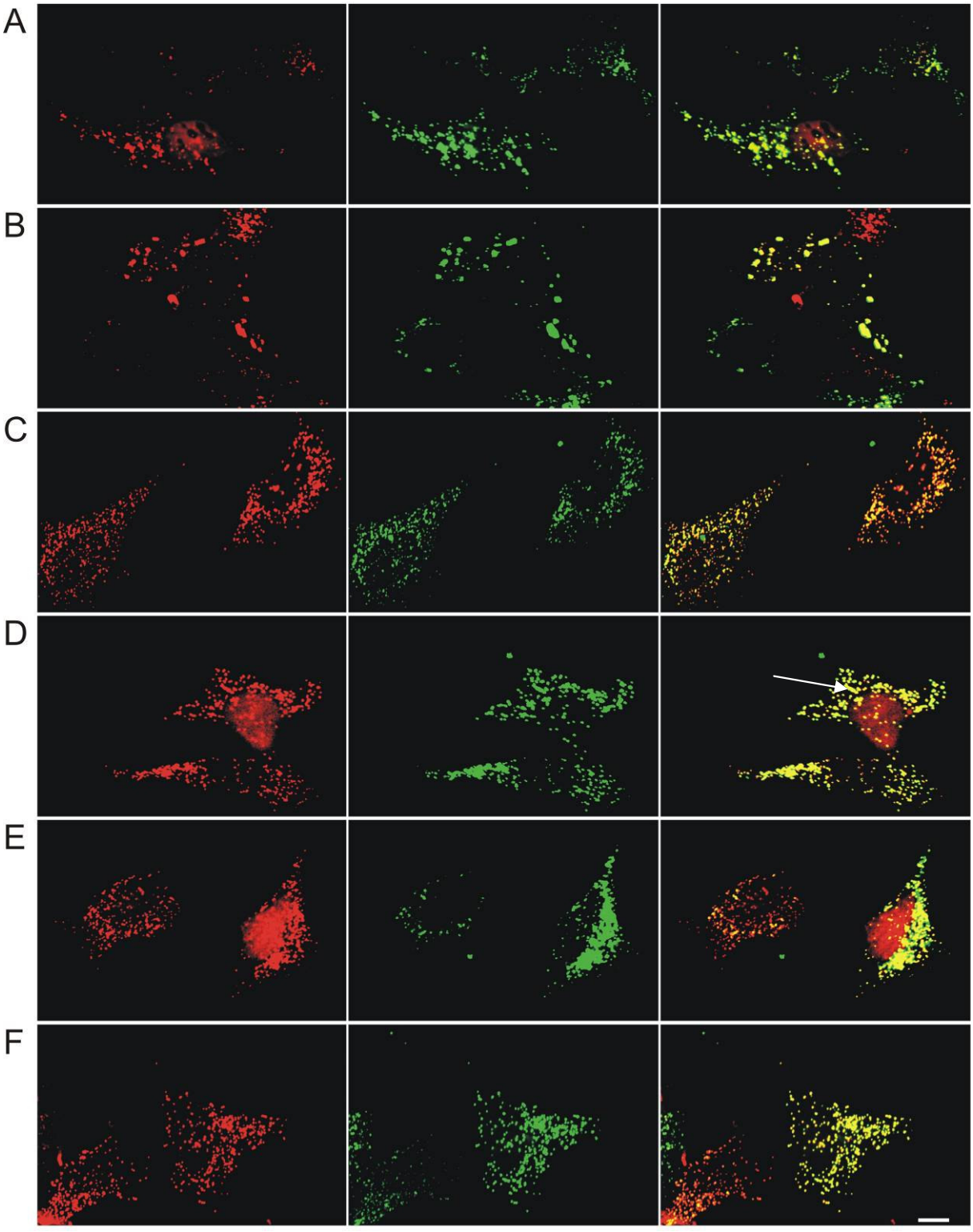

Figure 8: Ectopic overexpression of the plant Pex11 protein family in HEK293T 24h post transfection; (A) GFP-AtPex11-1 partially and (B) GFP-AtPex11-2 induces the formation of enlarged and clustered peroxisomes, (C) GFP-AtPex11-3 and (D) GFP-AtPex11-4 induce proliferation, (E) GFP-AtPex11-5 slightly promotes fission of peroxisomes, (F) wild type peroxisomes; red channel (A-F): mCherry-SKL; images are projected stacks, bar: 10µm

Cells overexpressing GFP-AtPex11-2 presented a dramatically reduced number of peroxisomes. The overexpression of GFP-AtPex11-3 and -4 had only slight effects on the peroxisome number. Still, an increase in the peroxisome abundance was detected. In contrast, overexpression of GFP-AtPex11-4 led to the induction of tubule-formation or elongation of peroxisomes (arrow in Figure 8). A detailed analysis will be presented in section 3.2.

3.1.1 A functional relationship between yeast, plant and human Pex11 proteins

The colocalization of all Pex11 fusion proteins expressed with the peroxisomal matrix marker mCherry-SKL demonstrates that they all localize to peroxisomes. Moreover, the various effects observed on peroxisome number and size suggest that they all may be functional in human cells. At least one protein from each model organism showed an induction of tubules, clusters or, generally enlarged peroxisomes (e.g. GFP-HsPex11γ, GFP-ScPex25, GFP-AtPex11-2). This could represent an early step in the proliferation process. Indeed, it has been reported in the yeast *S. cerevisiae* that peroxisomes tend to remain associated after the fission event. Their separation requires the presence of the proteins ScPex28 and 29 (Vizeacoumar et al., 2003). The fact that this happens with the Pex11 proteins from each studied kingdom might suggest a conserved mechanism for peroxisome proliferation or at least a conserved function for proteins of the Pex11-family.

Our study demonstrates that all proteins of the Pex11-family have an effect on peroxisome number. However, despite the fact that the cells remained viable more than 50 hours after transfection, it remains to be demonstrated whether the peroxisomes are fully functional in cells overexpressing Pex11 proteins with regard to protein import or oxidative stress response. A potential redox-sensitive homodimerization of ScPex11 had been reported which could negatively influence the regulation of ScPex11 function (Marshall et al., 1996). Therefore, it will be extremely informative to test whether the overexpression of Pex11 proteins in human cells confronted with oxidative stress leads to similar observations on peroxisome proliferation.

Overall, overexpression of HsPex11α led to more, smaller peroxisomes, but to a smaller extent than that of HsPex11β. In contrast, HsPex11γ overexpression led to the formation of large clusters. Notably, these phenotypes have already been reported. HsPex11α and β were overexpressed in CHO-K1 and mouse cells presenting similar effects. Only HsPex11γ was investigated in human fibroblasts (Li et al., 2002a). Interestingly, all yeast and

plant fusion proteins localize to peroxisomes. This colocalization cannot be explained with the presence of a simple PTS, since all Pex11 are membrane proteins exhibiting an mPTS. As reported, the mPTS is not fully understood, yet (Brown and Baker, 2003). However, at least one transmembrane is required for correct localization. This excludes random artifacts, that just any protein such as for instance soluble proteins could be inserted by chance.

The fact that overexpression of Pex11 proteins leads to morphological changes of peroxisomes in several ways suggests that they are functional. This is especially fascinating for the plant Pex11 proteins. Ectopic expression of GFP-AtPex11-2 resulted in the formation of larger and clustered peroxisomes, which are however smaller than those observed upon overexpression of GFP-HsPex11γ or GFP-ScPex25. Expression of GFP-AtPex11-1 in human cells resulted in the formation of only few clustered peroxisomes. Apparently, the effect of GFP-ScPex25 expression in human cells is very similar to that of GFP-HsPex11γ (Figure 6C & Figure 7B). Still, their physiological role may be more distinct since the phylogenetic analysis of the genes coding for HsPex11γ and ScPex25 reveals only a weak correlation (Figure 4, Orth et al., 2007). They share the same origin; however, several rounds of divergence could have led to different tasks within the peroxisomal proliferation machinery. The amino acid sequences of AtPex11-1 and -2 are even less similar than those of HsPex11γ and ScPex25. However, these bioinformatics data are always based on mathematical algorithms controlled by manually set parameters, which tends to be error-prone.

3.2 3D reconstruction of peroxisomes

In the colocalization experiments, we observed several kinds of peroxisomes, enlarged and clustered as well as smaller ones. However, to better perceive the variations of peroxisome number and size attributed to the expression of each Pex11 protein we sought to analyze the three dimensional structure of peroxisomes in transfected cells. The projection of a z-stack may produce artifacts, vesicles seem to adhere to each other, but are well separated in the third dimension. Moreover, the colocalization can be judged in three dimensions as well.

We deconvolved a representative z-stack (d=0.5µm) with a calculated point-spread function (PSF). The deconvolved stack was then rendered using VolumeJ (Abramoff and Viergever, 2002, see Methods section for details) and turned around the y-axis. This results in a plastic view of the structures, while the shading gives an impression of the third dimension.

Figure 9 shows a region of a cell transfected with mCherry-SKL and GFP-Scp2 our wild-type phenotype. Note, that even in such a cell some peroxisomes are elongated, which could be a hint for ongoing proliferation.

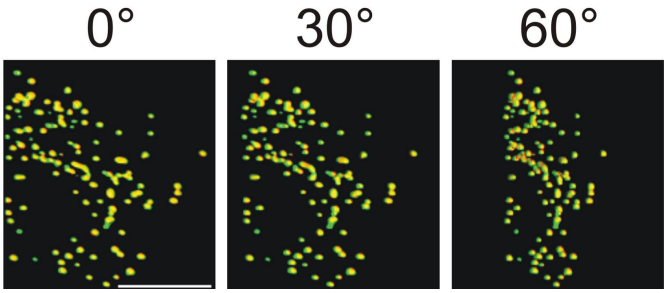

Figure 9: 3D reconstruction of a selected area of HEK293T cells overexpressing mCherry-SKL and GFP-Scp2; image stacks (d=0.5µm) were deconvolved and rendered resulting in a 3D view revealing the fine-structures of peroxisomes; bar: 10µm

Figure 10 shows the three human Pex11 fusion proteins in HEK293T cells. While some of the peroxisomes are always interconnected, most of them are separated. Only GFP-HsPex11γ shows both, enlarged (arrow in Figure 10) and clustered peroxisomes.

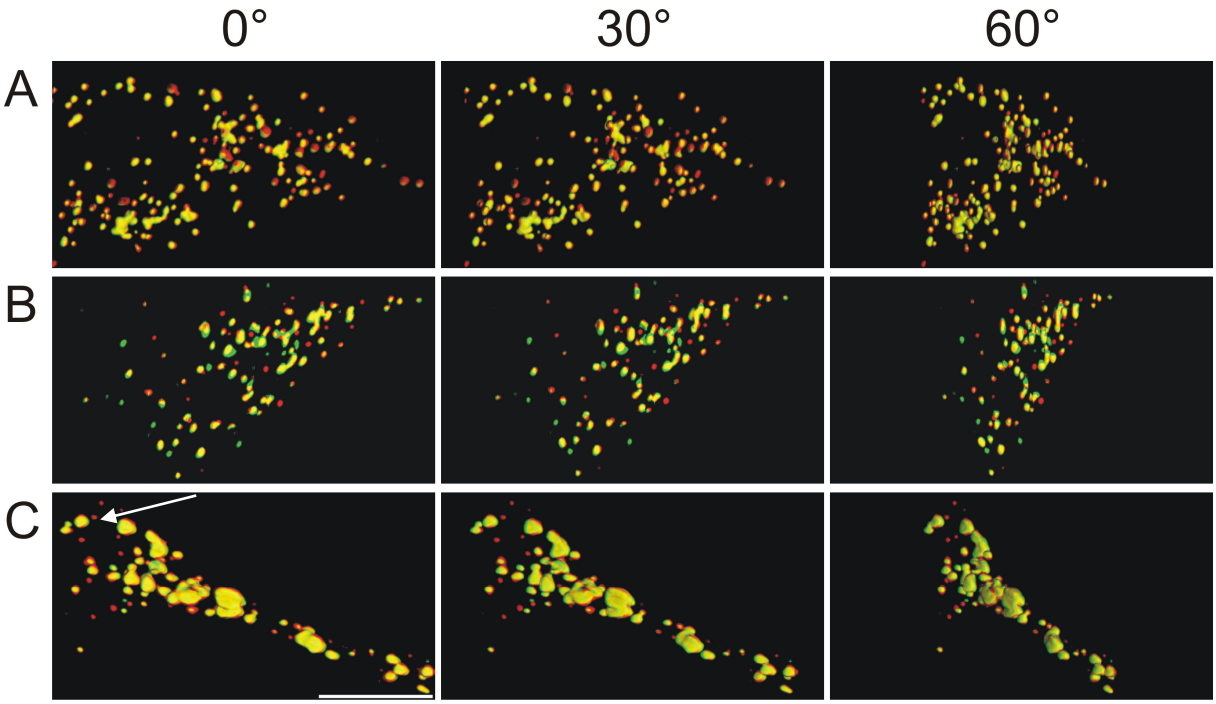

Figure 10: 3D reconstruction of a selected area of HEK293T cells overexpressing human (A) GFP-Pex11α, (B) GFP-Pex11β and (C) GFP-Pex11γ N-terminally GFP tagged; image stacks (d=0.5µm) were deconvolved and rendered resulting in a 3D view revealing the fine-structures of peroxisomes; bar: 10µm

The fine-structures in the clusters suggest that indeed more than one peroxisome is present. Expression of the yeast constructs showed similar structures (Figure 11). GFP-ScPex11

resulted in an increase in peroxisome interconnection, which seems to correlate with proliferation (see Figure 7). In Figure 11B, the strong background fluorescence produced by the marker protein mCherry-SKL still does not disturb the 3D view.

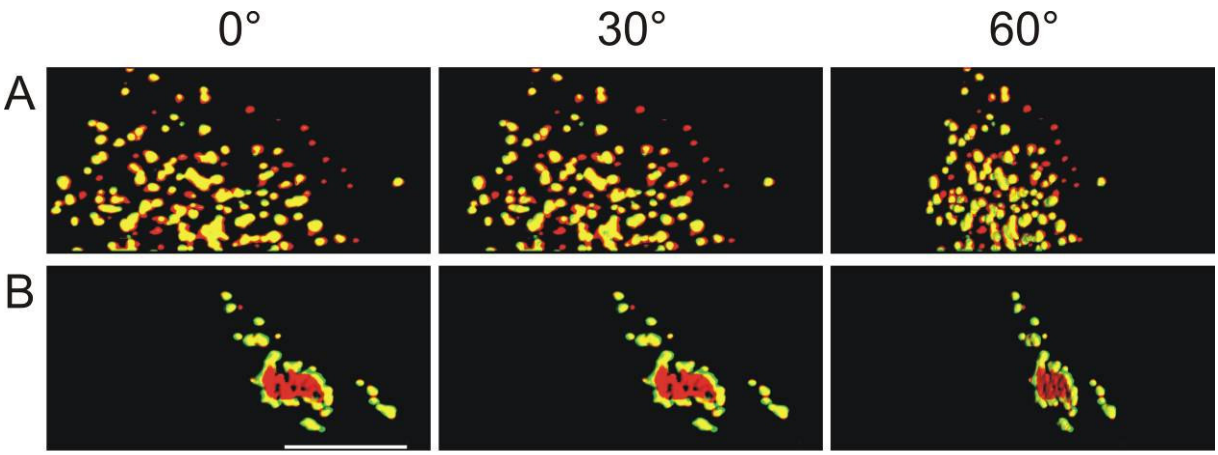

Figure 11: 3D reconstruction of a selected area of HEK293T cells overexpressing (A) GFP-ScPex11, (B) GFP-ScPex25 N-terminally GFP tagged; image stacks (d=0.5µm) were deconvolved and rendered resulting in a 3D view revealing the fine-structures of peroxisomes; bar: 10µm

The 3D reconstructions of the overexpressed GFP-AtPex11-1 to -5 correlate with the colocalization images (Figure 8, Figure 12). Upon ectopic overexpression of GFP-AtPex11-2, human cells contained fewer peroxisomes; especially the clusters are smaller and seem to be more compact. When GFP-AtPex11-3 was overexpressed, a reported inductor of proliferation (Orth et al., 2007), many small peroxisomes were produced that were well separated.

GFP-AtPex11-4 might act as proliferator, since its expression in human cells resulted in the appearance of more elongated peroxisomes as compared to GFP-AtPex11-3, but some are interconnected and form tubules (arrow in Figure 12D). These “sausage-like” structures were reported in yeast cells deleted for a protein of the fission machinery (Schauss et al., 2006, Kuravi et al., 2006). Additionally, Koch et al. have reported similar observations in COS-cells knocked down by siRNA for Dlp1, a protein involved in the mitochondrial and peroxisomal fission process (Koch et al., 2004). We propose that these structures represent ongoing proliferation. Since those “sausage-like” structures are not present throughout the whole cell, is it unlikely that these observations can be attributed to a defect in the peroxisomal fission process. GFP-AtPex11-5 seems to be the most potent proliferator of all plant Pex11 proteins in HEK293T cells. The high number of peroxisomes combined with only little distance in between makes the deconvolution and 3D rendering procedure difficult to achieve properly. However, the peroxisomes seem to remain separated and appear clustered only due to their high density.

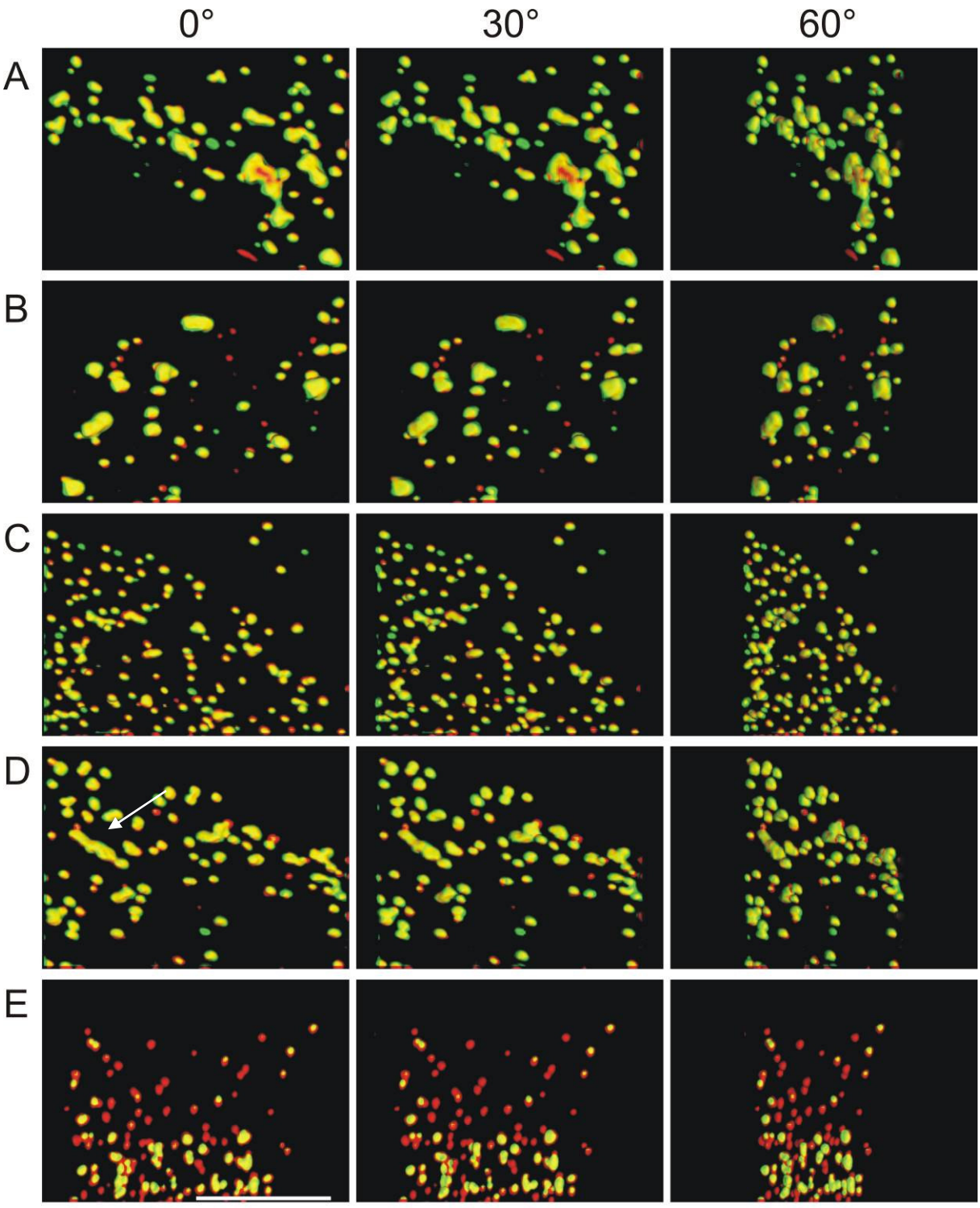

Figure 12: 3D reconstruction of a selected area of HEK293T cells overexpressing (A) GFP-AtPex11-1, (B) GFP-AtPex11-2, (C) GFP-AtPex11-3, (D) GFP-AtPex11-4 and (E) GFP-AtPex11-5; image stacks (d=0.5µm) were deconvolved and rendered resulting in a 3D view revealing the fine-structures of peroxisomes; bar: 10µm

3.3 Statistical analysis of the influence of Pex11 proteins

The observation of confocal laser scanning microscopy (CLSM) images is always accompanied by personal bias, which is usually moderated by evaluating the reproducibility and imaging many coverslips of different experiments. Representative image stacks are shown in Figure 6-Figure 8.

A statistical analysis therefore provides a more profound basis for the quantitative evaluation of microscopy data.

We used and expanded established counting techniques (Kim et al., 2006). Briefly, we collected images of at least 50 cells for the expression of each Pex11 protein 22 hours after transfection. All images were taken in the widest focal plane of a cell containing the most peroxisomes. These images were handled as described (see Methods for details). Images were filtered, converted to 8-bit and a threshold was applied to highlight the peroxisomal fluorescence. Then, each cell was encircled manually and the peroxisomes were counted by using the Particle Analysis package of ImageJ[1]. A z-stack would certainly enable us to consider all peroxisomes of one cell, but the problem of spatial discrimination would emerge.

	category I	category II	category III	category IV
diameter [µm]	**0-0.35**	**0.36-0.66**	**0.67-0.95**	**0.96-10**
area [µm²]	**0-0.1**	**0.11-0.34**	**0.35-0.71**	**0.72-78,54**

Table 2: four categories of peroxisomal size: category II represents the normal peroxisome, category I the small ones, whereas enlarged peroxisomes are found in categories III and IV

Additionally, we measured the total area covered by all peroxisomes of each category. Certainly, the acquisition of large amount of data may lead to a strong bias. To avoid this we sought to compare relative trends for each sample. We divided the peroxisomes into four categories with increasing diameter (Table 2). The normal-sized peroxisomes are found in category II. Categories I and III represent boundary regions since the size of peroxisomes varies even in wild type cells. Nevertheless, fission of peroxisomes into smaller ones would shift the majority of the peroxisomes from category II to I. Category IV encloses all bigger, clustered or enlarged peroxisomes, though some might be found in category III as well.

[1] Rasband, W.S., ImageJ, National Institutes of Health, Bethesda, Maryland, USA, http://rsb.info.nih.gov/ij/, 1997-2004

3.3.1 Influence on peroxisome abundance

First, we analyzed the peroxisomal abundance, comparing the expression of all Pex11 proteins to cells transfected with mCherry-SKL only. Two major questions were raised, namely i) whether the absolute number of peroxisomes changes and ii) whether the relative fraction of each category differs from cells transfected only with a peroxisomal marker protein.

Figure 13-Figure 15 summarize the data collected for all Pex11 proteins from yeast, plant and man. Each table (Figure 13C-Figure 15C) shows the numbers themselves, highlighting the most important category. The absolute numbers are represented as bars in Figure 13A-Figure 15A, whereas the relative abundance based on the total number of peroxisomes per cell are shown in Figure 13B-Figure 15B.

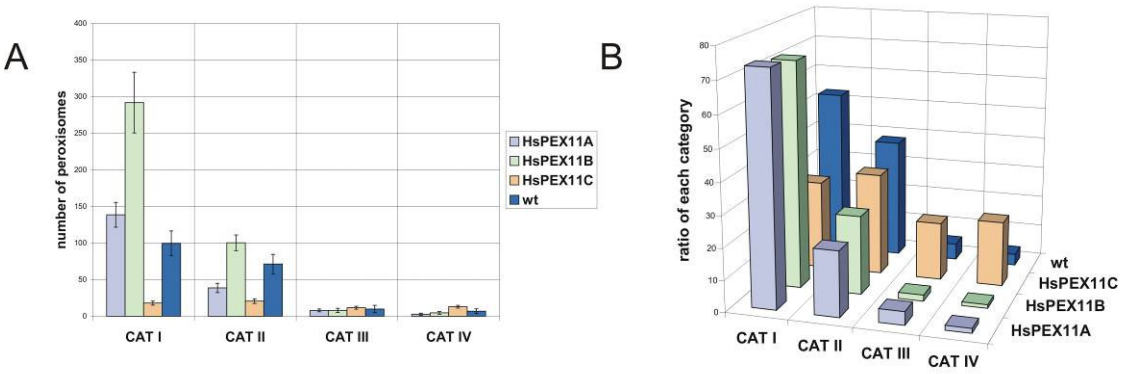

C

category		HsPEX11	HsPEX11	HsPEX11	wt
I	%	**74 ± 4**	**72 ± 4**	28 ± 4	53 ± 7
	total	**139 ± 17**	**292 ± 41**	18 ± 3	100 ± 17
II	%	21 ± 4	25 ± 3	33 ± 4	38 ± 7
	total	39 ± 6	100 ± 11	21 ± 3	71 ± 13
III	%	4 ± 1	2 ± 1	18 ± 3	5 ± 2
	total	8 ± 2	8 ± 3	12 ± 2	10 ± 5
IV	%	1 ± 1	1 ± 0	**21 ± 3**	4 ± 2
	total	3 ± 1	5 ± 2	**13 ± 2**	7 ± 3

Figure 13: analysis of the abundance of peroxisomes in cells overexpressing GFP-HsPex11α, β and γ; (A) total abundance of peroxisomes per widest focal plane/ cell, (B) relative distribution (sum of all peroxisomes=100%), (C) the exact numbers and standard deviations; n=50 cells;

The blue bars in Figure 13-Figure 15 show the absolute and relative distribution of peroxisomes in wild type cells, i.e. cells transfected with a peroxisomal marker only. These cells contained approximately 90% peroxisomes in categories I and II, ~200 peroxisomes in total in the widest focal plane. The categories III and IV are hardly present.

Overexpression of GFP-HsPex11α induced a shift towards smaller peroxisomes, as visible in Figure 13A/B. While the number of peroxisomes in category I increased, it decreased in category II as compared to wild type cells. The total abundance did not change. In contrast, GFP-HsPex11β expression led to an increase of both categories, but hardly altered the relative

distribution of the peroxisomes compared to cells expressing GFP-HsPex11α. More than 400 peroxisomes were counted in one cell's widest focal plane. When GFP-HsPex11γ was expressed the number of peroxisomes in category I and II was considerably reduced but cells showed only minor changes in the other categories. However, due to the reduced total number of peroxisomes (approximately 100/ widest focal plane/ cell) the relative distribution reveals a severe increase in bigger peroxisomes, which here contribute to a fifth of the total peroxisome number. Notably, only cells containing big or clustered peroxisomes were counted since this phenotype was present in more than 80% of the transfected cells.

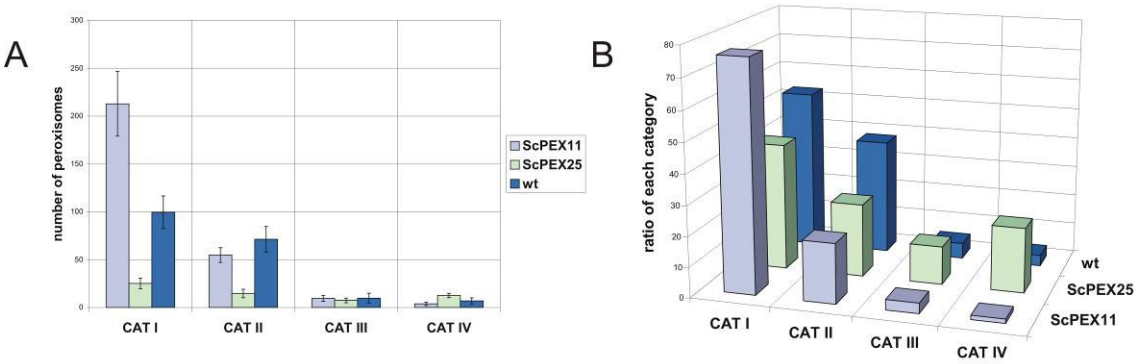

C

category		ScPEX11	ScPEX25	wt
I	%	**76** ± **6**	42 ± 6	53 ± 7
	total	**213** ± **34**	25 ± 6	100 ± 17
II	%	20 ± 4	24 ± 6	38 ± 7
	total	55 ± 8	15 ± 4	71 ± 13
III	%	3 ± 1	13 ± 5	5 ± 2
	total	10 ± 3	7 ± 2	10 ± 5
IV	%	1 ± 1	**21** ± **1**	4 ± 2
	total	4 ± 2	**13** ± **1**	7 ± 3

Figure 14: analysis of the abundance of peroxisomes in cells overexpressing GFP-ScPex11 and 25; (A) total abundance of peroxisomes per widest focal plane/ cell, (B) relative distribution (sum of all peroxisomes=100%), (C) the exact numbers and standard deviations; n=50 cells;

Figure 14 shows the summary of the statistical evaluation of the yeast Pex11 proteins. Expression of GFP-ScPex11 led to more peroxisomes in such way, that a strong increase of category I was detected, while the other categories remained unchanged. Analysis of the relative distribution underlines this fact even better. Expression of GFP-ScPex25 led to nearly the same distribution as in cells expressing GFP-HsPex11γ. Though a slight shift toward smaller peroxisomes was observed in comparison to cells expressing GFP-HsPex11γ.

The analysis of all plant Pex11 proteins is summarized in Figure 15. Expression of GFP-AtPex11-1 caused a decrease in category II and an increase in category I. This, together with slightly more peroxisomes in category IV might result in the presumption that more big peroxisomes are present.

A strong shift towards big peroxisomes together with a decrease in all other categories was induced by expressing GFP-AtPex11-2. For GFP-AtPex11-3 expression the distribution of peroxisomes was comparable to that of wild type cells, though a slight increase in category I can be noted. Interestingly, expression of GFP-AtPex11-4 only led to marginally more peroxisomes in category IV and approximately the same amount in category II and III. This however, was enough to present some tubule-like structures as visible in Figure 11D (arrow). Clearly, expression of GFP-AtPex11-5 gave rise to a strong shift towards small and more peroxisomes. These findings will be further analyzed in section 3.3.3.

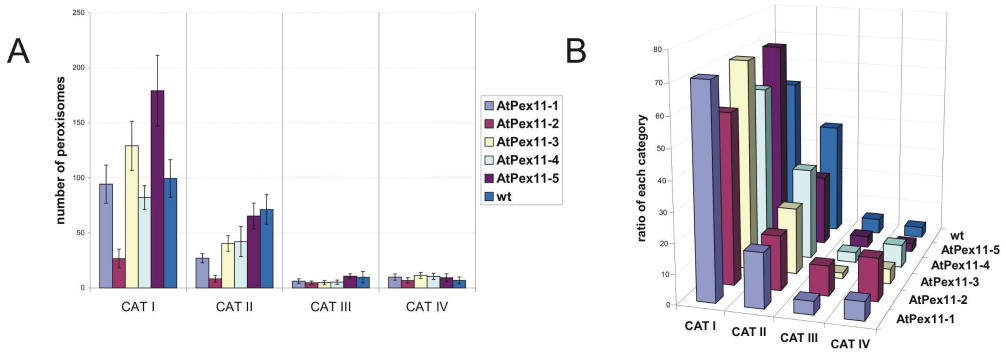

C

category		AtPex11-1	AtPex11-2	AtPex11-3	AtPex11-4	AtPex11-5	wt
I	%	71 ± 4	57 ± 8	71 ± 4	58 ± 9	**69 ± 6**	53 ± 7
	total	94 ± 17	27 ± 9	129 ± 22	82 ± 11	**179 ± 32**	100 ± 17
II	%	18 ± 3	18 ± 5	22 ± 3	31 ± 9	24 ± 5	38 ± 7
	total	27 ± 4	8 ± 3	40 ± 7	42 ± 14	65 ± 12	71 ± 13
III	%	4 ± 1	10 ± 3	2 ± 1	3 ± 1	4 ± 1	5 ± 2
	total	6 ± 2	5 ± 2	5 ± 2	5 ± 2	11 ± 2	10 ± 5
IV	%	6 ± 2	**14 ± 5**	5 ± 1	8 ± 2	3 ± 1	4 ± 2
	total	10 ± 3	**7 ± 3**	11 ± 3	11 ± 3	9 ± 4	7 ± 3

Figure 15: analysis of the abundance of peroxisomes in cells overexpressing GFP-AtPex11-1 to -5; (A) total abundance of peroxisomes per widest focal plane/ cell, (B) relative distribution (sum of all peroxisomes=100%), (C) the exact numbers and standard deviations; n=50 cells;

3.3.2 Influence on peroxisome size

We further analyzed the area covered by the peroxisomes of each category. Here, the same categories as described in section 3.3 (Table 2) were used.

A

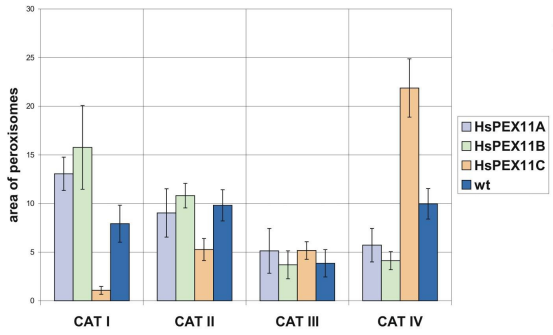

B

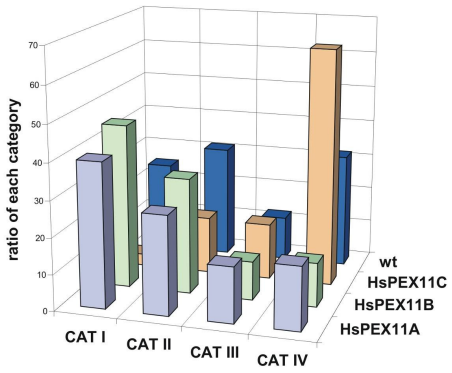

C

category		HsPEX11A	HsPEX11B	HsPEX11C	wt
I	%	**40 ± 5**	**45 ± 7**	3 ± 1	25 ± 5
	total	**13 ± 2**	**16 ± 4**	1 ± 0	8 ± 2
II	%	**27 ± 7**	**32 ± 5**	16 ± 3	31 ± 4
	total	**9 ± 2**	**11 ± 1**	5 ± 1	10 ± 2
III	%	15 ± 6	11 ± 4	16 ± 2	12 ± 4
	total	5 ± 2	4 ± 1	5 ± 1	4 ± 1
IV	%	17 ± 5	12 ± 3	**65 ± 4**	32 ± 5
	total	6 ± 2	4 ± 1	**22 ± 3**	10 ± 2

Figure 16: analysis of the covered area [µm^2] of peroxisomes in cells overexpressing GFP-HsPex11α, β and γ; (A) total area of peroxisomes per widest focal plane/ cell, (B) relative distribution (sum of area of all peroxisomes=100%), (C) the exact numbers and standard deviations; n=50 cells;

Again, all peroxisomes in the widest focal plane were considered and the area of all peroxisomes of each category was summed up. This enabled us to detect any minor changes concerning the size of peroxisomes within each category.

Figure 16 shows the statistics for the overexpressed human Pex11 proteins in HEK293T cells. In our experiments with GFP-HsPex11α, peroxisomes of category I and II covered the majority of all. This is in agreement with the counted abundance of the peroxisomes. Astonishingly, in the case of GFP-HsPex11β we observed approximately the same relative distribution as with GFP-HsPex11α, although a strong increase in the number of peroxisomes in category I was indicated before. Noteworthy, the covered area when GFP-HsPex11γ was expressed doubled as compared to wild type cells.

Similarly to GFP-HsPex11α and β, the majority of peroxisomal area is covered by peroxisomes of category I for GFP-ScPex11 (Figure 17). Cells expressing GFP-ScPex25 presented an even more pronounced shift to category IV as compared to cells expressing GFP-HsPex11γ.

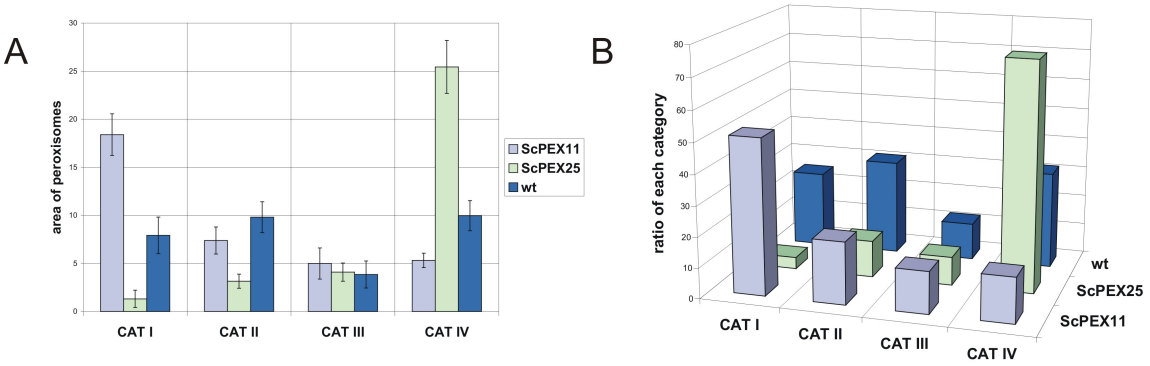

C

category		ScPEX11	ScPEX25	wt
I	%	**51 ± 5**	4 ± 3	25 ± 5
	total	**18 ± 2**	1 ± 1	8 ± 2
II	%	20 ± 3	12 ± 3	31 ± 4
	total	7 ± 1	3 ± 1	10 ± 2
III	%	14 ± 4	9 ± 2	12 ± 4
	total	5 ± 2	4 ± 1	4 ± 1
IV	%	15 ± 2	**75 ± 4**	32 ± 5
	total	5 ± 1	**25 ± 3**	10 ± 2

Figure 17: analysis of the covered area [µm^2] of peroxisomes in cells overexpressing GFP-ScPex11 and 25; (A) total area of peroxisomes per widest focal plane/ cell, (B) relative distribution (sum of area of all peroxisomes=100%), (C) the exact numbers and standard deviations; n=50 cells;

The expression of the plant Pex11 fusion proteins presented quite adverse results with regard to the covered peroxisomal area. The measurements are summarized in Figure 18. However, the total area covered by all peroxisomes of all categories did not change significantly throughout the cells expressing either of the used proteins (about 33µm^2).

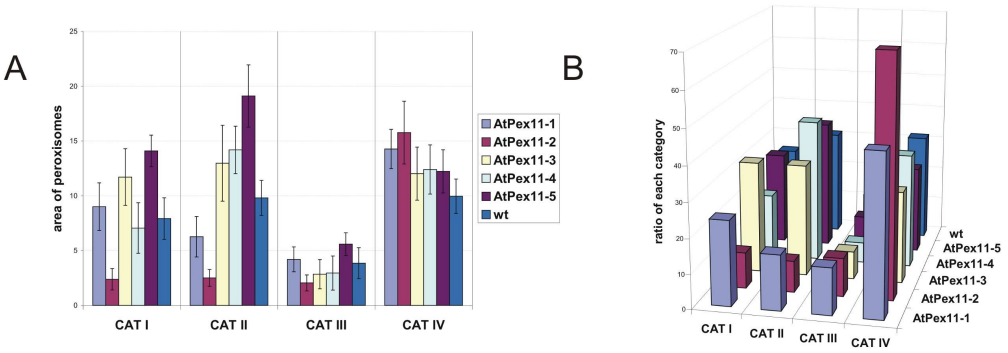

C

category		AtPex11-1	AtPex11-2	AtPex11-3	AtPex11-4	AtPex11-5	wt
I	%	24 ± 5	10 ± 4	33 ± 6	19 ± 7	27 ± 4	25 ± 5
	total	9 ± 2	2 ± 1	12 ± 3	7 ± 2	14 ± 1	8 ± 2
II	%	16 ± 5	9 ± 3	33 ± 4	42 ± 5	38 ± 6	31 ± 4
	total	6 ± 2	3 ± 1	13 ± 3	14 ± 2	19 ± 3	10 ± 2
III	%	14 ± 4	11 ± 3	8 ± 3	6 ± 4	9 ± 2	12 ± 4
	total	4 ± 1	2 ± 1	3 ± 1	3 ± 2	6 ± 1	4 ± 1
IV	%	46 ± 6	69 ± 6	27 ± 7	34 ± 6	26 ± 5	32 ± 5
	total	14 ± 2	16 ± 3	12 ± 2	12 ± 2	12 ± 2	10 ± 2

Figure 18: analysis of the covered area [µm^2] of peroxisomes in cells overexpressing GFP-AtPex11-1 to -5; (A) total area of peroxisomes per widest focal plane/ cell, (B) relative distribution (sum of area of all peroxisomes=100%), (C) the exact numbers and standard deviations; n=50 cells;

3.3.3 A correlation appears between peroxisomal size and number

Special interest has to be drawn at the correlation between the abundance and the size of peroxisomes. Since we used categories with a certain range, the covered area of peroxisomes might still vary within one category. For instance, there could exist fewer peroxisomes of category IV in a cell A that are bigger, and therefore cover a larger area than more peroxisomes of category IV in a cell B. In contrast, more peroxisomes in category I could also cover a smaller area than fewer but slightly bigger ones. The exact criteria defining the four categories can be found in Table 2.

A significant index is easily accessible by dividing the mean size by the mean abundance of the peroxisomes in each category. The result is the area per peroxisome, giving a realistic view of size-changes within categories.

The red-coloured numbers in Table 3 for the expression of HsPex11α and β explain the differences observed when comparing the abundance and the size of peroxisomes. The number of peroxisomes was higher for HsPex11β while the covered area stayed the same. This can only be explained by a different mean size of peroxisomes of category II which was doubled for HsPex11α. The most frapping differences occur in category IV, clearly due to its broad definition.

	wt	HsPex11A	HsPex11B	HsPex11C	ScPex11	ScPex25
cat I	0,08	0,09	0,05	0,06	0,09	0,05
cat II	0,14	0,23	0,11	0,26	0,13	0,22
cat III	0,39	0,65	0,39	0,44	0,52	0,55
cat IV	1,45	2,04	0,89	1,68	1,39	2,02

	AtPex11-1	AtPex11-2	AtPex11-3	AtPex11-4	AtPex11-5
cat I	0,10	0,09	0,09	0,09	0,08
cat II	0,23	0,30	0,32	0,34	0,29
cat III	0,68	0,43	0,59	0,56	0,52
cat IV	1,44	2,30	1,05	1,17	1,32

Table 3: average area of a typical peroxisome of each category for each used Pex11 protein; unit: [µm^2]

Overall, our results underline statistically the colocalization experiments and expand our knowledge by quantifying the relative differences in number and size of peroxisomes between the overexpression of the different Pex11 fusion proteins in human cells.

3.4 Effects of overexpressed Pex11 proteins over time

The analysis of the tagged Pex11 proteins was always performed about 22-24 hours after transfection. Since peroxisomes are versatile organelles, observing the dynamics of their proliferation, growth and adaptation may be better suited to study the different effects allied with overexpression of Pex11 proteins. The best technique is by far live cell imaging, however, huge datasets are created when using this strategy. Therefore, it is absolutely necessary to narrow the timeframe to some distinct interesting points. Then, live observation is ultimately applicable with acceptable amounts of data.

In order to achieve this, we decided to investigate the GFP-tagged Pex11 fusion proteins under the same conditions as before (see section 3.1) at different time points, namely 22h, 30h and 46h after transfection.

3.4.1 Effects of human Pex11 proteins overexpression change over time

Neither peroxisomal abundance nor size nor shape changed in cells cotransfected with plasmids expressing the peroxisomal matrix marker proteins, GFP-Scp2 and mCherry-SKL over the observed time frame (Figure 19D). The pattern of overexpressed GFP-HsPex11α did not change much over the observed timepoints; however, some increase in the peroxisomal abundance could be noticed (Figure 19A). The size of peroxisomes did not change in these cells. In contrast, when GFP-HsPex11β was overexpressed, the peroxisomal number, size and shape varied dramatically. The strong induction of peroxisome proliferation 22h after transfection shifted towards the formation of clusters observed 24h later.

This was obviously achieved via an intermediate step (see Figure 20, crop of Figure 19). Here, the peroxisomal number decreased significantly as compared to 22h after transfection.

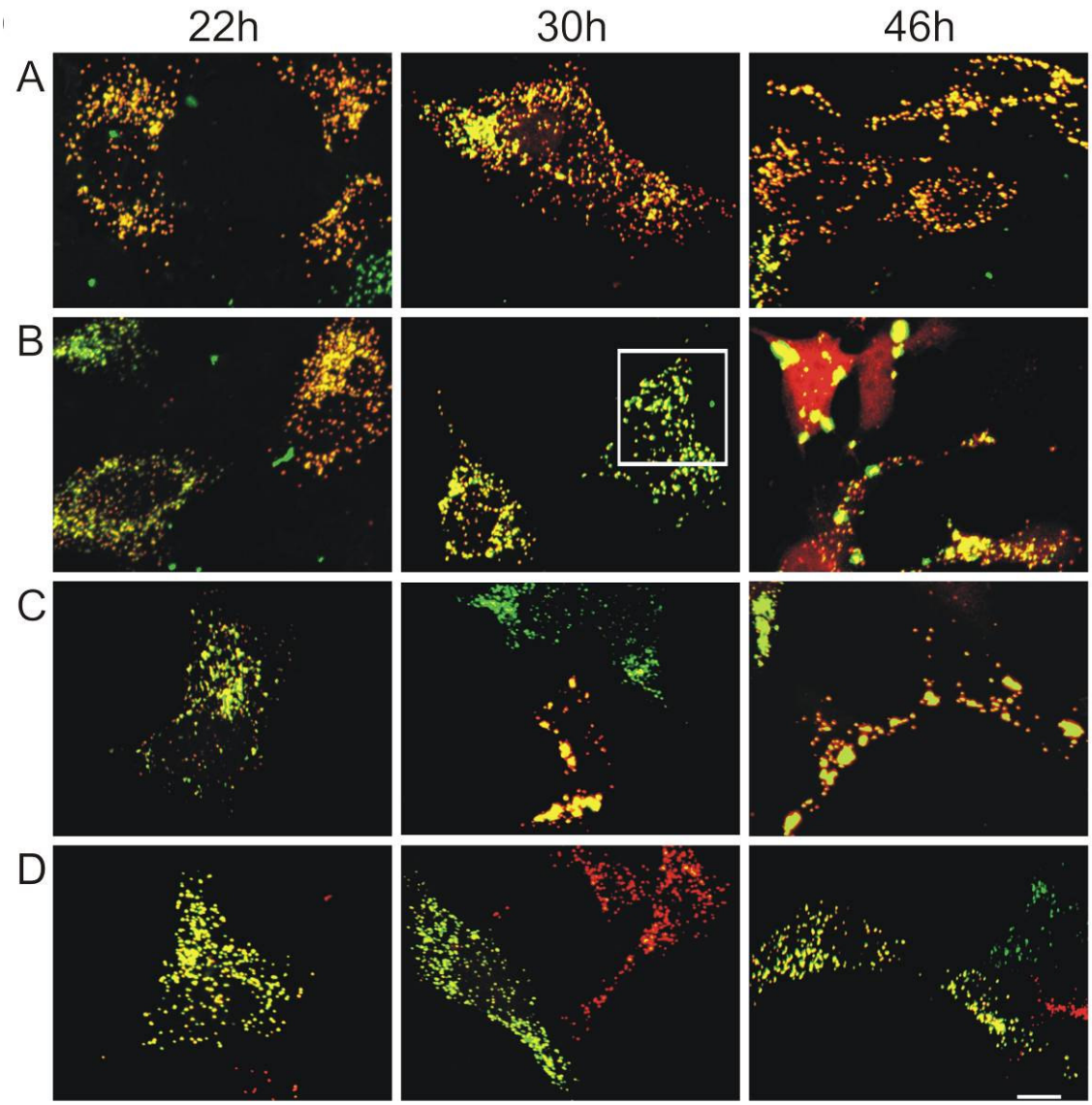

Figure 19: time-dependent expression of human GFP-Pex11 protein fusion constructs; (A) GFP-HsPex11α showed no significant change over time, although some increase in peroxisome number was observable, (B) GFP-HsPex11β induces strong cluster formation after 46h, for zoomed region of interest see Figure 20; (C) GFP-HsPex11γ stimulates peroxisomal clusters to grow and/or fuse to enlarged groups of peroxisomes, images are projected stacks, red channel (A-D): mCherry-SKL, bar: 10µm

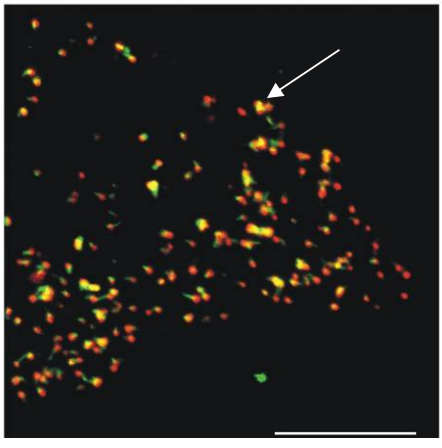

Figure 20: outlined area of Figure 19, cell overexpressing GFP-HsPex11β 30h after transfection; The green spots colocalize with the distinct red punctae (mCherry-SKL) and moreover, form a short tail which partly connects two red structures; sometimes, green fluorescence is observed as junction of more than two peroxisomes (arrow); bar: 10µm

Moreover, the individual peroxisomes (seen in red) seemed to be interconnected by a green structure, building up junctions for two or even more peroxisomes (see arrow in Figure 20 and Figure 21). A closer look at higher magnification on those structures revealed that in the majority of the cells some “ring-like” structures were visible only in the green channel (arrowheads in Figure 21), while red peroxisomal matrix marker, mCherry-SKL, stayed punctuate. Additionally, a green ring around a red dot could be observed (asterisks and crop in Figure 21) demonstrating that GFP-HsPex11β principally localized at the membrane. Whether the green rings observed represent an early step in peroxisome formation remains to be demonstrated.

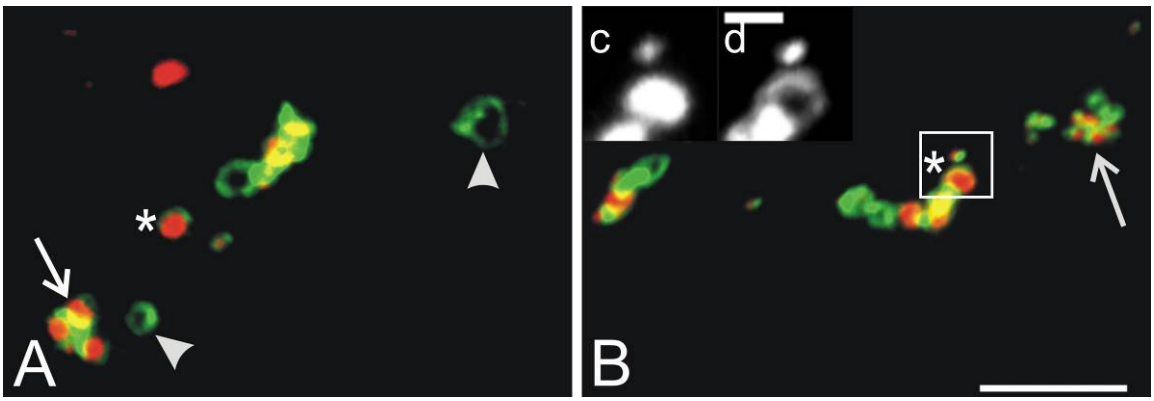

Figure 21: (A) and (B) highly magnified regions of interest of cells overexpressing GFP-HsPex11β 30h after transfection; red: mCherry-SKL; arrows mark junctions between multiple peroxisomes, arrowheads highlight ring structures and asterisks notate green encircled peroxisomes, bar: 5µm, (c) and (d) one region has been cropped and transformed in grey, where (c) represent the red channel and (d) the green one; bar: 1µm; all images are projected stacks

However, the above mentioned solely green ring- structures seemed to be an effect due to high overexpression, since it could be shown that all human Pex11 proteins as well as ScPex11 and ScPex 25 were able to form such structures upon high overexpression (data not shown). Nevertheless, only overexpressed GFP-HsPex11β led to interconnected peroxisomes 30h after transfection. This was not observable with any other protein. Remarkably, these structures all disappeared 46h after transfection, where some peroxisomal clusters could be observed together with some small peroxisomes. Here, the peroxisomal marker mCherry-SKL was also visible in the cytosol, though to a less extent so that the peroxisomes stayed brighter marked (data not shown).

Overexpressed GFP-HsPex11γ showed the clustering after 22h to some extent as observed before (Figure 6C). Again, the majority of the cells showed this phenotype, the rest of the cells contained normal-sized peroxisomes (shown in Figure 19C as compared to clusters shown before in Figure 6C). This changed over the time in such way, that all cells presented

enlarged or clustered peroxisomes. This shift was clearly observable as the percentage and the size of clusters per cell was growing continuously at each time point.

3.4.2 Overexpression effects of yeast proteins of the Pex11 family change over time

The overexpressed GFP-ScPex11 protein induced the formation of many peroxisomes already 22h after transfection. This did not change over time as visible in Figure 22A. Here, the morphology, size and abundance were not affected as compared to time point 22h.

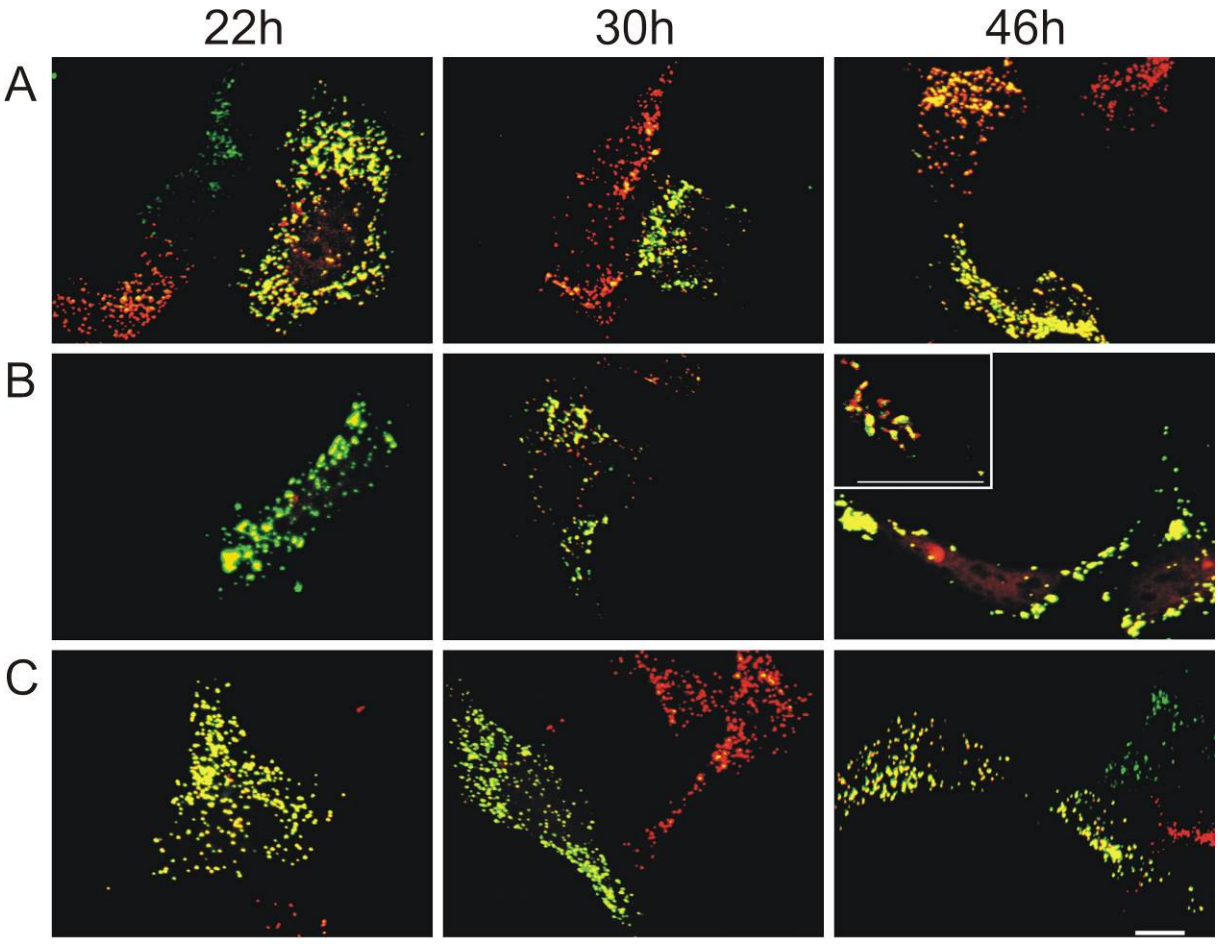

Figure 22: time-dependent expression of the yeast GFP-ScPex11 and GFP-ScPex25 fusion proteins; (A) GFP-Pex11 shows no significant change over time whereas (B) the clustering observed after overexpressing GFP-Pex25 increases, (C) GFP-Scp2; red channel (A-C): mCherry-SKL, images are projected z- stacks, bars: 10µm

The overexpressed GFP-ScPex25 which induced some clustering even 22h after transfection induced this clustering together with tubule-formation extensively until 46h after transfection (see Figure 22B). The smaller window in Figure 22B/46h shows an enlarged cell area which presents tubule-like structures.

3.5 SNAP-tag technology – a tool to study protein dynamics

The concept of tagging has allowed to establish new ways to analyze protein functions. A tag makes it possible to follow a protein *in vivo* via live-cell imaging, to detect it in a Western blot or to isolate and purify it via a column. Whatever task a tag is assigned with, several requirements have to be fulfilled. A fluorescent tag such as GFP should be as small as possible, not interfere with the protein's function, be photostable and have a short maturation time. Moreover, the quantum yield, the extinction coefficient and pH (in)sensitivity play a role, too.

Several new approaches have arisen since the cloning of the gene coding for avGFP including fluorescent peptide ligands, photoactivatable and photoswitchable fluorescent dyes (Chapman et al., 2005, Griffin et al., 1998; Shaner et al., 2007).

In our experiments, we searched for a tag that would enable us to perform both, imaging and biochemical experiments. Finally, we chose the SNAP® tag due to its multiple advantages. SNAP® stands for a protein, namely the human O^6-alkylguanine-DNA-alkyltransferase (hAGT). It transfers irreversibly the alkyl group from its substrate O^6-alkylguanine-DNA, to its reactive cysteine residue (Figure 23). Combined biochemical and structural-biological methods led to a proposed reaction mechanism (Figure 23, Daniels et al., 2004).

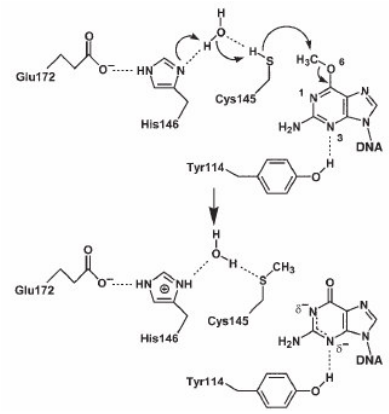

Figure 23: proposed reaction mechanism of hAGT (Daniels et al., 2004).

The essential role of hAGT in DNA damage repair has been studied extensively making this protein a functionally clarified one (Daniels and Tainer, 2000, Wibley et al., 2000, Xu-Welliver et al., 1999, Xu-Welliver et al., 2000, Xu-Welliver and Pegg, 2000). Additionally, hAGT represents an interesting target for pharmaceutical screens. Since alkylated DNA can induce apoptosis, chemotherapeutic strategies based on DNA-alkylating agents (e.g. temozolomide) have a reduced efficiency due to the endogenous hAGT reversing the effects

of such drugs. Therefore, medics inhibiting hAGT increase dramatically the effects of DNA-alkylating drugs (Ragg et al., 2000, Cai et al., 2000, Damoiseaux et al., 2001; Griffin et al., 2000, Meikrantz et al., 1998).

All these studies on hAGT revealed that the specificity for its substrate only requires the structure O^6-benzylguanine (BG). Therefore, any fluorescent dye coupled on BG would lead to a specific labelling of hAGT. The endogenous hAGT has been mutated several times to eliminate the disadvantages it may have when serving as a tag. Its intrinsic affinity for DNA was efficiently reduced, its activity for BG substrates was increased and its size was minimized by removing non-essential amino acid residues (Juillerat et al., 2003, Gronemeyer et al., 2006, Heinis et al., 2006). This enables to work in cells that are not deficient for hAGT.
One drawback of this approach still remains: Since the enzyme hAGT is not longer valuable after the transfer reaction, it is ubiquitinylated and degraded by the cell. However, the measured decrease of fluorescence in labelled living cells is about 50% after 7 hours (Keppler et al., 2004b, Srivenugopal et al., 1996).

The idea of using hAGT as a tag was first introduced in 2003 (Keppler et al., 2003) and has continuously been refined by developing new substrates over the years (Keppler et al., 2006; Keppler et al., 2004a; Keppler et al., 2004b).
An enormously valuable feature of the SNAP® tag (provided by Covalys) is the versatility to any BG substrate offered, be it in living cells, fixed cells or a BG immobilized on a surface, which makes protein purifications easily possible (Kindermann et al., 2003).
We expanded this technology by appending the SNAP® tag with a tobacco etch virus (TEV) protease cleavage site in order to pull down purified proteins from a matrix.
Eventually, our SNAP®-TEV tag will represent a useful tag for any kind of imaging and protein purification procedures.

3.5.1 Peroxisomal dynamics in live cell imaging

Several fluorescent dyes are available for imaging the SNAP® protein. We chose a red and a green label (TMR-Star and BG505, respectively), since these suited well with our peroxisome marker proteins (Figure 24).
To achieve our goals, we cloned N-terminally SNAP-TEV-tagged Pex11 fusion proteins, and evaluated then. We expressed SNAP-TEV-HsPex11α and γ in HEK293T cells, also expressing GFP-Scp2 and labelled the cells with the TMR-Star dye.

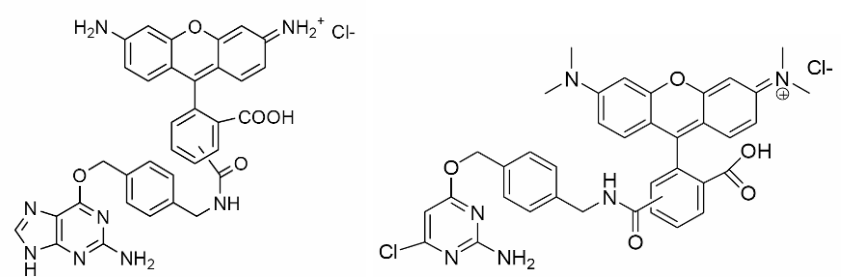

Figure 24: fluorescent labels for the SNAP® tag used; (A) BG-505, exc: 504nm, em: 532nm, (B) TMR-Star, exc:554nm, em:580nm

As control for the SNAP® technology, we transfected a plasmid encoding SNAP®-tagged cytochrome oxidase 8A (Cox8A), a mitochondrial protein. Cells were imaged alive with the

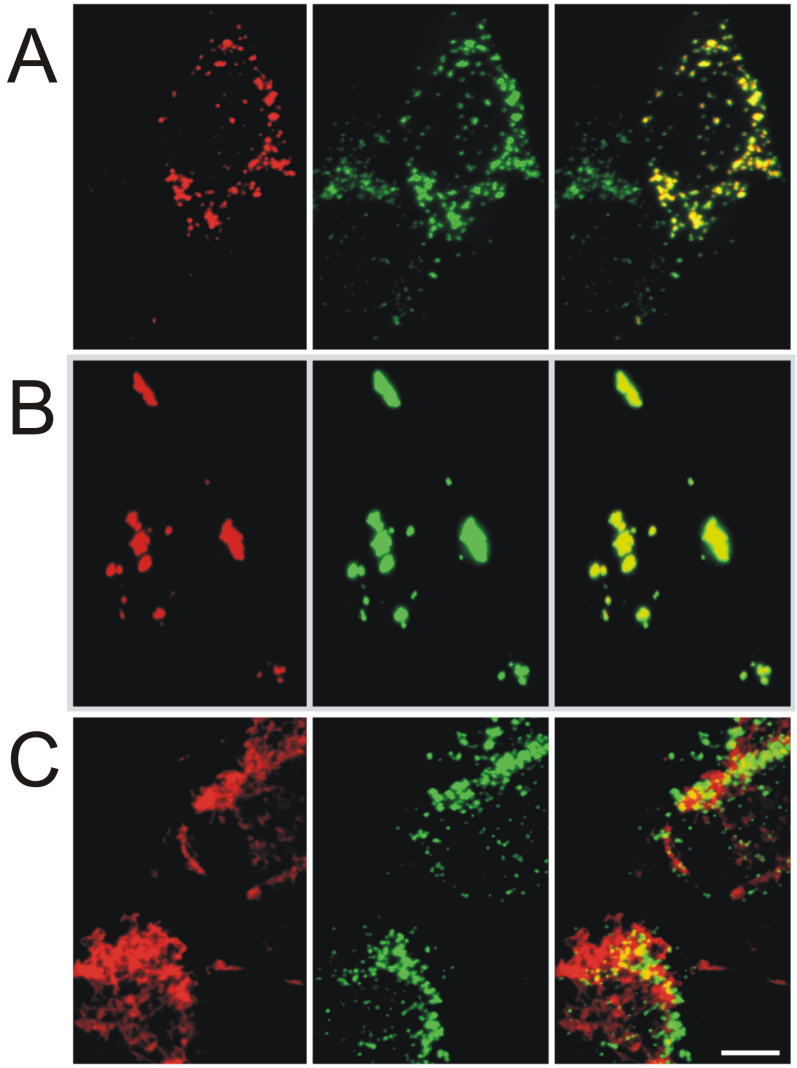

Figure 25: live cell imaging of HEK293T cells expressing labelled SNAP fusion proteins 24 hours after transfection, (A) SNAP-TEV-HsPex11α, (B) SNAP-TEV-HsPex11γ, (C) Cox8a-SNAP, (A-C) coexpressed with GFP-Scp2, images are projected z-stacks of one time frame, bar: 10µm

Zeiss DuoScan (Figure 25, see methods section for details). The control cells in Figure 25C presented a normal morphology. The mitochondrial network was properly established. Peroxisomal abundance, size and shape were comparable to cells transfected with mCherry-SKL or GFP-Scp2 only (Figure 6). Moreover, cells overexpressing SNAP-TEV-HsPex11α or γ showed identical peroxisome number and size as cells overexpressing the GFP tagged Pex11 proteins (Figure 6). Similar results were obtained with fixed cells labelled prior fixation. Evaluation of the BG-505 dye revealed that this dye was not that sensitive, bright and photostable than the red TMR-Star. Therefore, combining GFP-Scp2 with a red labelled SNAP® tag proved as best choice.

3.5.2 Establishing stable cell lines

For further study using the SNAP® tag, it is absolutely necessary to establish stably expressing cell lines for each Pex11 construct. We chose to establish stably transfected HEK293T cells expressing either mCherry-SKL, GFP-Scp2, SNAP-TEV-HsPex11α and SNAP-TEV-HsPex11γ. Briefly, HEK293T cells (passage 11) were transfected, one day after the appropriate selective agent was added. When most cells had died, each dish was split and diluted into a 96-well in such way, that one single cell was present in one well. These cells were grown to confluency, transferred to a 48-well. After repeated growth and splitting, cells were ready in passage 18.

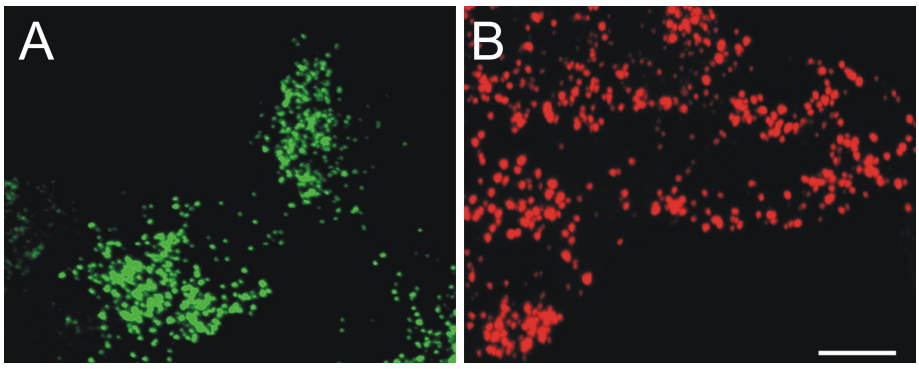

Figure 26: HEK293T cells stably expressing (A) GFP-Scp2 and (B) mCherry-SKL, images are projected z-stacks, bar: 10µm

The clones expressing the peroxisomal marker proteins GFP-Scp2 and mCherry-SKL were successfully tested (see Figure 26), now called HEK293T$^{GFP\text{-}Scp2}$ and HEK293T$^{mCherry\text{-}SKL}$, respectively. Every single cell presented wild-type like peroxisomes with very bright

fluorescence. Fortunately, every single clone exhibited a similar fluorescent pattern as compared to cells transiently transfected with the respective peroxisome marker. The emission was significantly brighter for HEK293T$^{mCherry-SKL}$ resulting in bigger peroxisomes as compared to HEK293T$^{GFP-Scp2}$, since the images were aquired using the same settings.

3.6 Study on domains and possible posttranslational modifications of Pex11 proteins

Elucidating the molecular role of the Pex11 proteins involves multiple approaches. Among those already employed, testing the importance of certain domains on the protein function could provide a first hint where to focus on while pinpointing the specific function in peroxisomal proliferation.

After scrutinizing the three human Pex11 proteins bioinformatically, we identified two putative phosphorylation sites for HsPex11α as well as the putative transmembrane domains for HsPex11α and β.

3.6.1 Mutations of putative phosphorylation sites affects the phenotype

We identified a double phosphorylation site at serine 159/ serine 161 of HsPex11α via a bioinformatical search (PhosphoELM, http://phospho.elm.eu.org/, Diella et al., 2004; Diella et al., 2008). The mutation of these serines to alanines (S→A) blocks possible phosphorylation and mimicks the unphosphorylated state whereas the mutation to aspartates resembles the phosphorylated state due to the high negative charges present. HsPex11α could be regulated via phosphorylation events, maybe another functional control together with a possible redox-sensitive dimerization (Marshall et al., 1996). We introduced both double mutations in HsPex11α, now called HsPex11α$^{S→A}$ and HsPex11α$^{S→D}$. We observed the expression of both proteins N- terminally tagged with GFP in HEK293T cells (Figure 27).

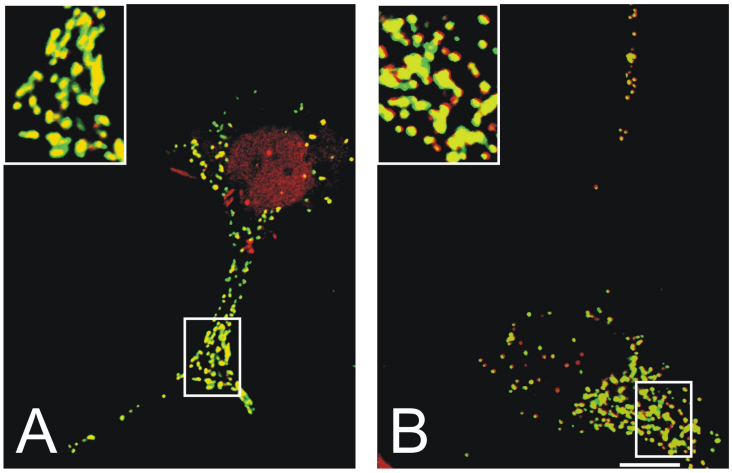

Figure 27: HEK293T cells expressing (A) GFP-HsPex11α$^{S\rightarrow A}$ and (B) GFP-HsPex11α$^{S\rightarrow D}$; (A) showing interconnected peroxisomal tubules, whereas in (B) the peroxisomal structures are more clustered and enlarged. images are projected stacks, (A-B) cotransfection with mCherry-SKL, bar: 10µm

The expression of GFP-HsPex11α$^{S\rightarrow A}$ caused peroxisomal tubule-formation, where the formed tubules are strongly interconnected (Figure 27A). In contrast, the overexpressed S→D mutation of HsPex11α led to a distinct phenotype, where the peroxisomes appeared more clustered than elongated. Of course, the endogenous HsPex11α was still present among the other members of the Pex11 protein family, whose interplay remains obscure. Despite these facts, the phenotypes observed make it necessary to investigate the singly mutated HsPex11α.

3.6.2 The transmembrane domain is important for localization and function

The careful bioinformatical scrutiny of the various Pex11 proteins revealed a transmembrane domain (TMD) for HsPex11α and β near the C-terminus (Kyte-Doolittle plot in Figure 28, Kyte and Doolittle, 1982). As easily visible in Figure 28, the hydropathy plots of HsPex11α and β are quite similar, whereas HsPex11γ exhibits different hydrophilic properties. Deletion of 60 base pairs of the cDNA coding for HsPex11α (aa 220-239) and 78 base pairs of the respective cDNA for HsPex11β (aa 230-255) would delete those TMDs, thus retaining the earlier discussed KxKxx motif of HsPex11α and the RxKx motif of HsPex11β. The real nature of the mPTS is yet unclear, it is only verified that one TMD is required for insertion into the peroxisomal membrane.

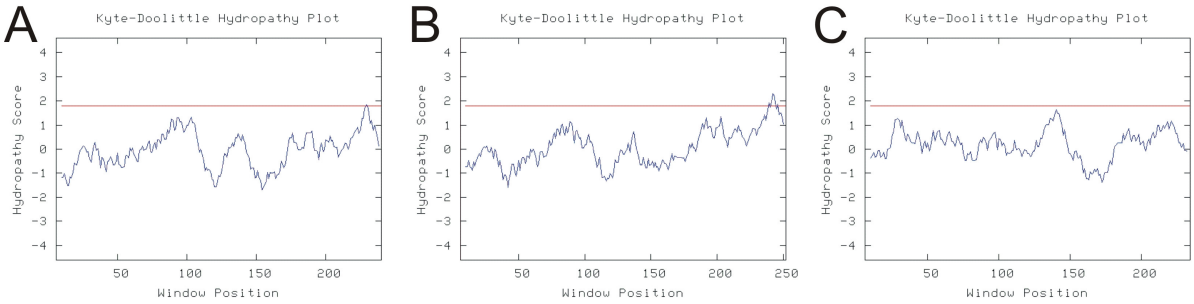

Figure 28: Kyte-Doolittle plots for the full-length human Pex11 proteins, (A) HsPex11α, (B) HsPex11β and (C) HsPex11γ, crossing the red line indicates a highly possible putative transmembrane domain, window size for A-C: 19 amino acids

We deleted the above indicated amino acids of HsPex11α and HsPex11β, now called HsPex11α$^{\Delta 20}$ and HsPex11β$^{\Delta 26}$, respectively, by means of PCR and expressed these proteins as N-terminal GFP-fusions in HEK293T cells stably expressing mCherry-SKL (HEK293T$^{mCherry\text{-}SKL}$).

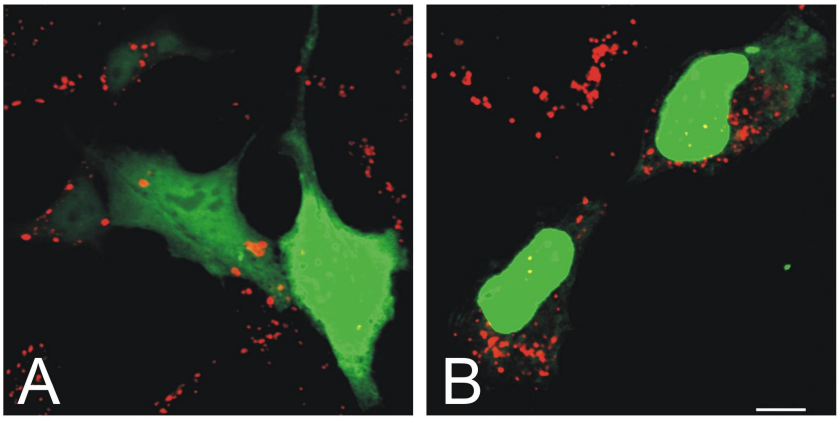

Figure 29: C-terminal deletion mutants of HsPex11α and β missing the putative TMD in HEK293T cells stably expressing mCherry-SKL; (A) GFP-HsPex11α$^{\Delta 20}$ and (B) GFP-HsPex11β$^{\Delta 26}$; (A-B) images are projected stacks, bar: 10µm

GFP-HsPex11α$^{\Delta 20}$ did not colocalize to peroxisomes, it was found in the cytosol. Interestingly, the cells expressing this truncated version of HsPex11α contained fewer and larger peroxisomes as compared to the surrounding cells only expressing the marker protein. Moreover, the expression level of GFP-HsPex11α$^{\Delta 20}$ seemed to negatively correlate with the peroxisome number (Figure 29A). This fact was not observable in cotransfection experiments, since the loss of red fluorescence from the marker proteins could be interpreted as reduced labeling of peroxisomes. This bias was eliminated in cells stably expressing the mCherry-SKL. Colocalization experiments in HEK293T$^{mCherry\text{-}SKL}$ cells with untruncated Pex11

proteins of either used kingdom showed the same results as presented before (see section 3.1). These findings could correlate localization and functionality of HsPex11α.

We further tested whether other organelles were affected as well by overexpressed GFP-HsPex11α$^{\Delta 20}$ by analyzing the nucleus, the golgi, the mitochondria and actin as important part of the cytoskeleton. We could not find any differences between cells overexpressing GFP-HsPex11α$^{\Delta 20}$ or the peroxisomal matrix marker GFP-Scp2 only. Further tests will include the ER, tubulin and a marker for the peroxisomal membrane, PMP70. The latter will show, whether only the import of PTS1-dependent proteins is inhibited or whether peroxisomal number is reduced at all.

The overexpressed GFP-HsPex11β$^{\Delta 26}$ behaved similarly in HEK293T$^{\text{mCherry-SKL}}$ cells, as it was found in the cytosol and the nucleus, sometimes forming aggregates. However, cells overexpressing GFP-HsPex11β$^{\Delta 26}$ presented a normal peroxisomal abundance and morphology comparable to cells only expressing mCherry-SKL (Figure 29B).

3.6.3 ScPex11 possibly forms redox-sensitive homodimers in human cells

It has been reported before that a possible redox-sensitive homo-dimerization of ScPex11 might regulate its function in the proliferating machinery in yeast cells (Marshall et al., 1996). CbPex11 contains only one cysteine, which is not fully conserved in ScPex11 that contains three cysteine residues. However, comparing the surrounding amino acids of each cysteine of ScPex11 to the one in CbPex11 reveals one similar cysteine, cys3. Marshall et al. introduced a cysteine to alanine (C→A) mutation in ScPex11 and expressed it under the Pex11-promoter in a *pex11* mutant yeast strain. The morphology and abundance of the yeast peroxisomes were affected significantly, since more and clustered peroxisomes were present (Marshall et al., 1996).

We already demonstrated that the yeast ScPex11 protein sorts to peroxisomes in human cells. Moreover, upon overexpression of this protein, the cells contained about 55% more peroxisomes than cells expressing only mCherry-SKL.

We introduced the same mutation in ScPex11 by changing the codon three from TGT(cys) to GCT(ala). Overexpressing an N-terminally GFP-tagged version of this protein in HEK293T$^{\text{mCherry-SKL}}$ cells induced clustering and elongation of peroxisomes (Figure 30). In some cases many small peroxisomes were present as well in the cell, which could represent the amount of overexpression in each cell.

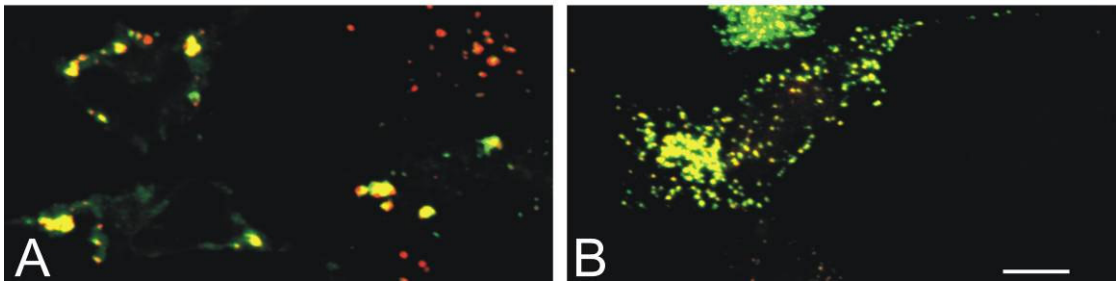

Figure 30: overexpressed GFP-ScPex11$^{C\rightarrow A}$ in HEK293T$^{mCherry\text{-}SKL}$ cells; (A) clustering and elongation of peroxisomes are present in cells expressing this protein, (B) some cells contain additionally small peroxisomes, image is a projected stack, bar: 10µm

The results of our study in human cells are similar to those observed from Marshal et al. in *Candida boidinii*, which could reflect an universal mode of regulation for the Pex11 proteins from yeast and human cells.

4 Discussion

Generally, the proliferation of all organelles is ultimately required for cell division and growth of cells, organisms and therefore life. Peroxisomes, though little in size, perform multiple important tasks. As they participate in the lipid metabolism and detoxify hydrogen peroxide via their enzymatic machinery, they are essential for most eukaryotic cells. Indeed, human cells containing aberrant peroxisomes or missing these organelles are hardly viable. Thus, most peroxisomal biogenesis disorders are lethal for humans.

Peroxisomes adapt to given environmental conditions or cellular requirements rapidly, making these organelles versatile. One important path of peroxisome proliferation is given by the fission of preexisting peroxisomes (Figure 31). Several proteins are involved in this multi-step process.

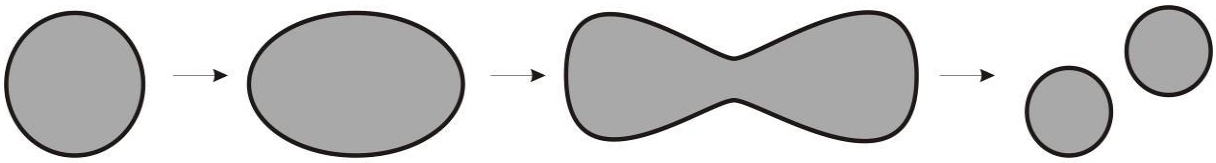

Figure 31: schematic drawing of the peroxisomal proliferation by fission

Among those proteins the Pex11 protein family plays an important role. In humans, three genes coding for HsPex11α, β and γ have been identified (Abe and Fujiki, 1998, Abe et al., 1998, Tanaka et al., 2003). Although, many years have passed since then, major questions have not been resolved yet. Why are there more than one Pex11 protein in a given organism? What is the difference in their function, do they work together or to what extent are they distinct? In plants, the five AtPex11 proteins are known to be expressed in different tissues at different levels and act at strongly regulated time points (Orth et al., 2007, Lingard et al., 2008). However, even single cell organisms such as baker's yeast contain three proteins of the Pex11 family. All together, the sequences of these different Pex11 proteins are quite conserved.

In humans, HsPex11α is – in contrast to the other two proteins – inducible. Pex11β seems to play a major role within the constitutively working division machinery. An interaction between HsPex11β and Fis1 could be proven biochemically (Li and Gould, 2003, Kobayashi et al., 2007). The function of HsPex11γ has not been elucidated, yet. However, it is the only member of the human Pex11 protein family, that induces clustering and not division of peroxisomes upon overexpression (this study, Li et al., 2002a). It certainly has to be

clarified whether an untagged version of this protein leads to the same effects on peroxisomes as its tagged counterparts.

Here, we could show the colocalization of overexpressed GFP-tagged Pex11 proteins from three different kingdoms with a peroxisomal matrix marker protein in human HEK293T cells. Overexpression of GFP-HsPex11α or β induced peroxisomal proliferation as more peroxisomes were visible as compared to cells tranfected only with the peroxisomal marker protein (Figure 6). In contrast, overexpressed GFP-HsPex11γ led to larger and clustered peroxisomes. It has been reported that in yeast, peroxisomes stick together after fission. The separation may require the function of the proteins ScPex28-29 (Figure 3, Vizeacoumar et al., 2003). In agreement with these published data, our observations could be a hint for proliferation as well.

However, many other explanations are possible; it could be that HsPex11γ is such a powerful proliferating factor, that the fission machinery is overwhelmed. It might also be that HsPex11γ is actively inhibiting the fission machinery or at least the separation process. It had been shown, that the knockdown of some proteins of the peroxisomal/mitochondrial fission machinery in human cell results in elongation – "sausage-like" – of peroxisomes. Our 3D reconstitutions enable to judge whether more than one peroxisome are involved in one cluster induced by overepxressed GFP-HsPex11γ. It seems, that there were more peroxisomes present in most clusters as observable via the 3D contours of the clusters (Figure 10). Still, they were connected to each other and not well separated. However, though this clustering was present in the majority of the cells, some cells contained an equal amount of peroxisomes of about the same size as compared to cells transfected only with mCherry-SKL.

Interestingly, overexpressed yeast and plant GFP-Pex11 fusion proteins sorted to human peroxisomes in HEK293T cells (Figure 7/ Figure 8). Here we could show that the presented phenotypes resemble at least partly the overexpression of human GFP-Pex11 fusion proteins. For instance, overexpressed GFP-ScPex25 induced clusters comparable to HsPex11γ, whereas GFP-ScPex11 led to a strong increase of the peroxisomal abundance as did HsPex11α. Among the plant proteins, overexpressed GFP-AtPex11-3, -4 and -5 induced peroxisomal proliferation. Overexpressed GFP-AtPex11-1 mildly and GFP-AtPex11-2 strongly induced cluster formation.

Obviously, there exist common elements in the overexpression phenotypes of the GFP-Pex11 fusion proteins of the three kingdoms. Still, the implications of cluster formation on molecular function need to be investigated further. If the fission machinery cannot cope with the activity of certain Pex11 proteins, why are rather clusters than elongated peroxisomes

observable? If some Pex11 proteins act as inhibitors of peroxisomal proliferation, do they block the fission process itself or the concerted elongation of peroxisomes driven by other Pex11 proteins?

Most of the Pex11 proteins from each studied kingdom are membrane-bound or -associated proteins. Some might exhibit a full TMD. The import of PMPs is not fully understood, yet. As summarized by Brown and Baker in 2003, the theory is now accepted that PMPs exhibiting a single TMD contain a patch of positively charged amino acids adjacent to this TMD though no consensus sequence could be identified. In PMPs that contain more than one membrane spanning domain, the cooperation of multiple regions within the protein and a loop on either side of one TMD is required for correct localization (Brown and Baker, 2003). The common element is at least one TMD being essential for insertion. Moreover, a complete mechanism for the insertion of PMP into the peroxisomal membrane has not been found, either. Two putative pathways have been postulated; i) the PMP is translated on free polysomes, interacts with Pex19 and is then inserted with the help of other proteins such as Pex3 or ii) PMPs are sorted via the ER, bud at defined regions, maybe marked by the presence of Pex3, and eventually fuse with existing peroxisomes demanding PMPs (for review see Tabak et al., 2008).

We may conclude from our colocalization studies that whichever mechanism might be true it is conserved throughout the three studied kingdoms. All investigated Pex11 proteins sorted to peroxisomes, each of them resulting in a slightly different phenotype suggesting their possible functionality in human cells. Either the mPTS is widely recognized without any species- or even kingdom-specificity or a more subtle signal is responsible for being recognized by the import machinery and finally, being inserted in the peroxisomal membrane.

Either way, the membrane topology and orientation of each protein has to be investigated. Some experiments have already been performed, e.g. ScPex11 is proposed to face the peroxisomal matrix with both, its N- and C- terminus in yeast (Marshall et al., 1996). We seek to investigate this topic if the orientation changes when expressed in human cells by means of biochemical redox-sensitive crosslinking (e.g. PEG-maleimide, see below). This experiment would enable to not only determine the topology of the studied protein in the membrane but as well to analyze its redox-sensitive residues outside the membrane.

4.1 Peroxisome membrane dynamics

We were able to quantify the abundance and the size of peroxisomes in HEK293T cells. We compared the overexpression phenotypes of all studied GFP-Pex11 fusion proteins to cells

transfected with mCherry-SKL only. Basically, we could confirm the data already evaluated visually. Due to the complex counting strategy, we decided to use only one focal plane (width: 0.5µm) of a cell, where the most peroxisomes could be detected. Of course, more peroxisomes than counted via this method are present in a cell. However, since we compared numbers and sought to outline trends rather than presenting absolute numbers this strategy was useful. Especially, the area of a peroxisome was actually obtained by measuring the area of the fluorescent dot. Still, this procedure was applicable because we only compared areas within each category. We divided the peroxisomes into four categories (Table 2) with growing size in order to easily observe shifts in the distribution due to overexpressed GFP-Pex11 proteins. We showed that big and clustered peroxisomes occurred predominately upon overexpression of GFP-HsPex11γ or GFP-ScPex25, a fact that was even more pronounced when looking at the area occupied by the enlarged peroxisomes (Figure 13/ Figure 14/ Figure 16/ Figure 17). This clustering was also induced by overexpressed GFP-AtPex11-1 and -2. Especially GFP-AtPex11-2 expression led to the formation of very few large peroxisomes. Here, no increase in number could be detected compared to cells transfected with mCherry-SKL only. However, these few peroxisomes covered more than twice the area than did the larger peroxisomes in cells transfected with mCherry-SKL only. This discrepancy may be attributed to internal variations within the defined categories. We defined four categories each with a certain range. Therefore, the size can vary within each category, particularly in category IV due to its wide range (Table 2). In order to overcome this problem to some extent, we calculated the mean size of a typical peroxisome of each category (Table 3).

	wt	HsPex11A	HsPex11B	HsPex11C	ScPex11	ScPex25
cat I	*0,08*	118%	68%	75%	109%	66%
cat II	*0,14*	169%	78%	186%	98%	157%
cat III	*0,39*	164%	99%	113%	133%	140%
cat IV	*1,45*	141%	61%	116%	96%	139%

	AtPex11-1	AtPex11-2	AtPex11-3	AtPex11-4	AtPex11-5
cat I	120%	112%	114%	108%	99%
cat II	168%	219%	233%	245%	212%
cat III	171%	110%	149%	141%	132%
cat IV	99%	159%	73%	81%	91%

Table 4: average area of a peroxisome of each category as percentage compared to peroxisomes of cells transfected with mCherry-SKL only; unit (wt): [µm^2]

The values expressed as percentage compared to that of cells only transfected with mCherry-SKL allow to better perceive the differences (Table 4). Notably, the standard deviations

behind these values have to be considered, too. Yet, since the relative average size of peroxisomes derives as means of means their standard deviations are not listed in Table 4. Most importantly, the overall average peroxisomal area covered in the widest focal plane was in most case approximately the same in each cell. Despite all the discussed drawbacks of the size determination via fluorescence measurements, our observations point directly at the issue of membrane dynamics. Where do peroxisomes get their membranes from? Are vesicles delivering lipids engulfed by a peroxisome just before it divides? Or does a mature "ready-for-fission"- peroxisome first fuse with an immature one? Here, live cell imaging certainly will provide new insights, since it should be possible to observe the events of peroxisome fission especially when forced by an overexpressed protein acting as a proliferating agent.

4.2 HsPex11β – a construction site for new peroxisomes

We scrutinized the behaviour of peroxisomes over time, upon expression of each GFP-Pex11 protein fusion. Especially, overexpressed GFP-HsPex11β induced various changes in peroxisome shape and size. First, many peroxisomes are formed which then form tubules and subsequently large fluorescent structures. We found complete colocalization of the GFP signal and the mCherry-SKL signal. However, the tubules observed showed massive green fluorescence within two or more red structures. This finding was reproducible. Similar structures were observable at more or less the same time points. This could be interpreted in several ways. It seems very unlikely that this behaviour just occurs as a result of overexpression. In that case, on the one hand the finding would not be as exactly reproducible and on the other hand similar plasmids coding for other Pex11 proteins would behave comparably, which was not the case (e.g. Figure 19A&C, Figure 22). Therefore, it is most likely that a correlation exists between the function of HsPex11β and the observed structural changes of the peroxisomes. Again, the question might arise whether cluster formation is a consequence of an overwhelmed fission machinery.

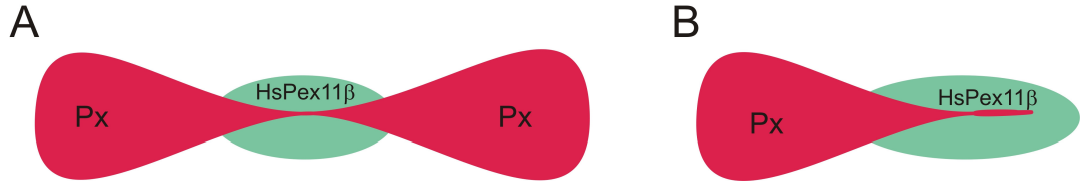

Figure 32: schematic drawing of the possible participation of HsPex11β in the elongation step; (A) two peroxisomes connected by a tunnel formed at the site of HsPex11β, (B) HsPex11β induces tubule formation at one specific site on a peroxisome, Px: peroxisome

Though more detailed studies are necessary, much evidence points at this idea. In the schematic drawing shown in Figure 32A we propose that the structures observed represent connections between dividing peroxisomes. HsPex11β could form a tube-like structure around the channel formed by the budding peroxisome. The green fluorescence concentrates at one distinct point and of course, the channel would be very thin exhibiting a too weak signal for detection. Figure 32B shows a possible explanation for the observation of single peroxisomes exhibiting a green tail (visible in Figure 20). It could represent a state immediately prior or post fission. As stated before, it has been shown that HsPex11β recruits Fis1 to the peroxisomal membrane which itself interacts with Dlp1 (Kobayashi et al., 2007). Dynamin-like proteins have been reported as possible mechanochemical machines, facilitating the budding of vesicles (for review see Praefcke and McMahon, 2004). At least, it has been shown that Dlp1 and Fis1 are part of the mitochondrial and peroxisomal fission machinery (Koch et al., 2005). It would be reasonable to think that HsPex11β, the initial regulator of this process, provokes the budding of peroxisomes at one defined membrane region. However, some structures in Figure 21 consist of more than two peroxisomes. The overexpression of HsPex11β might disregulate the whole process and consequently force this budding effect at more than just one site.

Importantly, we have to consider that dynamin related proteins are also involved in fusion processes, such as e.g. mitofusins in mitochondrial fusion. It could be that the intermediate step observed with HsPex11β represents a fusion of pre-existing peroxisomes. Further speculation might give rise to the question whether the peroxisomal clusters induced by overexpressed GFP-HsPex11γ are indices for dividing or fusing peroxisomes.

However, the role of the other two Pex11 proteins has to be considered beyond that speculation. Nevertheless, HsPex11β, being the non-inducible form, could be responsible for fission via the constitutive pathway, whereas HsPex11α might only be present upon induction as reaction to e.g. oxidative stress. Interestingly, the highest levels of Pex11α were found in liver tissue (Li et al., 2002a).

4.3 HsPex11α contains an essential transmembrane domain

We could show that the deletion of 20aa (aa 220-239) of HsPex11α is necessary for localization to peroxisomes, since we observed a cytosolic GFP-signal upon overexpression of GFP-HsPex11$\alpha^{\Delta 20}$ in HEK293T cells (Figure 29). Moreover, we observed a negative

correlation between GFP-HsPex11α$^{\Delta 20}$ expression levels and the abundance of peroxisomes. The peroxisomal number was strongly reduced in cells expressing this truncated version of HsPex11α, whereas other organelles were not affected. Since the endogenous proteins of the Pex11 family were still present, the truncation seemed to exert a dominant negative effect. Interestingly, truncated HsPex11β being similar to HsPex11α in the Kyte-Doolittle plot, behaved similarly when overexpressed in HEK293T cells as well. Its localization is cytosolic and nuclear. However and most importantly, peroxisomal abundance and morphology was not effected upon overexpression of GFP-HsPex11β$^{\Delta 26}$. It is noteworthy that the KxKxx motif of HsPex11α and the RxKx motif of HsPex11β were still present in the mutated versions of these proteins, allowing a possible function or regulation of these ER-related motifs to be exerted.

Maybe the transmembrane domain does not only control the localization, but also the function of HsPex11α. After insertion into the membrane, HsPex11α could get phosphorylated, which might inhibit its redox-sensitive homodimerization and/ or enable other interactions. When not needed anymore, the phosphate could be removed and HsPex11α might be able to dimerize. This could cause a change in its conformation; the HsPex11α might no longer be stably inserted into the membrane, and upon removal could be degraded in the cytosol. Therefore, overexpression of HsPex11α$^{\Delta 20}$ leads to non-dividing peroxisomes, though these are actually needed. Of course, the exact localization needs to be determined. We will perform experiments using PEG/ maleimide in the presence and absence of DTT in order to answer these questions. Here, methyl-PEG-maleimide reacts with thiols making a pegylated protein heavier and thus visibly shifting its band on a SDS-PAGE gel. mPEG is not membrane permeable, therefore allowing to assess the reactive cysteine residues outside the membrane. By cautiously varying the reaction conditions, we will be able to determine redox-sensitive thiol groups of the Pex11 proteins since the mentioned reaction can be moderated by redox-reactive SH reagents that are i) small, hydrophilic impermeant or ii) small membrane-permeant in order to block available cysteines prior to pegylation (Lu and Deutsch, 2001).

It remains to be clarified, why the endogenously expressed proteins are not overruling the phenotype of aberrant peroxisomes. This mutation must have a dominant negative effect, possibly affecting the other proteins as well maybe through dimerization with α or β or other members of the peroxisome proliferation machinery. Here, HsPex11γ could take over the control and act as inhibitor of peroxisomal fission leading to this dramatic phenotype. Another possible role for HsPex11γ could be to regulate HsPex11α and β. Given, that HsPex11β was responsible for the constitutively promoted fission process and HsPex11α acted as additional

stimulator when needed, HsPex11γ could bind to those two proteins, maybe inhibiting their interactions with other proteins, necessary for fission.
Especially the redox-sensitivity of the model proposed above is supported by the phenotype of the overexpressed GFP-ScPex11^{cod3} which led to enormous clustering and enlargement of peroxisomes (Figure 30).
Whatever process is taking place in the cell to promote proliferation of peroxisomes, it is a highly regulated one.

4.4 Conclusion and future aims

Our analysis of ten proteins of the Pex11-family in human cells has already provided interesting hints on the conservation of the peroxisomal proliferation machinery between yeast, plant and human cells. In future experiments we will focus on the dynamics of peroxisomal biogenesis by implementing live cell imaging, biochemical experiments and other cell biological approaches.
We established a technique for live cell imaging to observe peroxisome fission and the participation of each protein *in vivo*. Moreover, the SNAP-TEV-tag introduced provides the opportunity for protein purification as well. A remarkable feature of this tag lies in its ability to form a covalent bondage between its reactive cysteine and the substrate. We will use this for a multi-color assay in live cell imaging. We will label our protein of interest at time point zero with one fluorescent dye. After several hours of observation, the newly synthesized protein will be labeled with another dye. This step can be repeated several times. The only drawbacks are the degradation of the labeled SNAP protein and the limited amount of separable fluorescent dyes. However, we have a large time window of about seven to ten hours where a labeled SNAP tag is still stable. Alternatively, we can always observe the cells labelled with different dyes after fixation. Live observations will certainly enable us to get an even closer look on the function of the proteins of the Pex11 family.
Furthermore, we plan to perform coimmunoprecipitation experiments in order to isolate interaction partners of each human Pex11 protein. Here, the already known binding partners could prove as good positive controls (e.g. Pex19 for HsPex11α and Fis1 for HsPex11β). A very interesting topic in the context of evolutionary conservation of the peroxisomal proliferation machinery will be the scrutiny for interaction partners of yeast and plant Pex11 proteins in human cells. Finally, we seek to compare the found interaction partners of every Pex11 protein in each organism. Some interesting truncations will be investigated, too.

We will establish an additional approach by testing the effect of siRNA against the human Pex11 proteins. We designed and cloned two siRNAs per PEX11 cDNA into the plasmid pSilencer 2.1 U6 hygro, which enables us to use these vectors for small hereditary RNA (shRNA) experiments. Here, we will be able to investigate the effects in long-term studies and to verify whether the viability of cells with any knocked-down Pex11 protein is affected. In addition to the necessary tests including western and northern blotting, we designed a scrambled 19-mer siRNA in order to exclude plasmid-derived phenotypes. Since the used vector contains a hygromycin resistance, we can use this system together with our established HEK293T$^{mCherry\text{-}SKL}$ or HEK293T$^{GFP\text{-}Scp2}$ cell line.

A quite important role is attributed to the host system used. We decided to perform the colocalization studies in HEK293T cells. They are easily to transfect, grow fast and require only conventional medium. Despite the fact that these cells were derived from embryonic kidney tissue the real type of tissue to which HEK293T cells belong remains rather obscure. Indeed, recent publications propose that an immature neuronal tissue instead of epithelial cells was taken for the generation of HEK cells (Shaw et al., 2002) This group found many proteins in HEK293T cells, that are commonly present in neuronal tissue. Overall, HEK cells are well suitable if one needs a host for proteins but does not want to study the cell itself. In our study the cellular behavior is important since we aim at analyzing the Pex11 proteins in a reasonable cellular context. We will therefore perform our future cell biological experiments in fibroblasts as these represent well established cells to study peroxisomes.

Additionally, we will expand our knowledge of the importance of certain domains and putative phosphorylation sites. Since we investigated only the double mutant (HsPex11α S159D/S161D and S159A/S161A) by now, the effects of the respective single mutations promise deeper insight into a possible regulation of HsPex11α.

At a later point, we want to analyze the effects of different substances inducing oxidative stress on the regulation of Pex11 proteins. Here, it will be interesting to compare “young” to “old” cells, observing their capability to handle oxidative stress with regard to peroxisome proliferation.

The analysis of the peroxisomal proliferation machinery in human cells might provide insight into a new mode of organelle proliferation based on constitutive and inducible fission processes and, potentially, on a close interaction with the ER. As mentioned above, HsPex11α contains a dilysine motif, known to be able to recruit coatomer (Passreiter et al., 1998). Similarly, the C-terminus of RnPex11-1 contains a KxKxx motif. CHO-mutants,

defective for the coatomer, presented tubuled, elongated peroxisomes upon introduction of RnPex11-1 (Anton et al., 2000). As a consequence, a possible role for a cargo or retrograde transport from peroxisomes to the ER has been suggested (Lay et al., 2006).

Eventually, our work may bring forth new aspects and strategies to analyze membrane dynamics and organelle proliferation at a molecular level, stimulating further studies.

5 Materials

5.1 Buffers

FSB

10mM KOAc
10% v/v glycerol
10mM KCl
50mM $CaCl_2$
pH=6.2 with HAc

LYSIS BUFFER (for human tissue)

20mM Tris HCl pH 7.5
0.5mM EDTA disodium salt
120mM KCl
1mM DTT
10% v/v glycerol
+protease inhibitor cocktail (as recommended)

10xPBS

1.3M NaCl
0.07M Na_2HPO_4
0.3M NaH_2PO_4

10xPBST

PBS + 0.05% v/v Tween-20

TBE

89mM Tris
89mM boric acid
2.5mM EDTA disodium salt
pH 8.2 (with HCl)

TBS(T)

50mM Tris
150mM NaCl
(0.05% v/v Tween 20)

TE

10mM Tris
1mM EDTA disodium salt
pH 7.7 with HCl

Buffers for alkaline lysis (DNA preparation)

P1
50mM Tris HCl pH 7.5
10mM EDTA disodium salt
100µg/ml RNAse A

P2
200mM NaOH
1% w/v SDS

P3
3M KOAc
pH 5 with HAc

DNA PAGE gel

6% v/v acrylamide/ bisacrylamide solution (39:1, provided by BioRad)
4% v/v glycerol
15µl TEMED
15µl APS
in TBE

DNA PAGE sample buffer

50% v/v glycerol
50% v/v H_2O
0.01% w/v bromphenol blue

STOP solution

4M urea
50% w/v sucrose
5mM EDTA disodium salt
0.01% w/v bromphenol blue

5.2 SDS PAGE/ Western blot solutions

10% separation gel (use 7.5ml)

1.5M Tris HCl pH 8.8	2.5ml
30% acrylamide/ bisacrylamide solution (provided by BioRad)	3.3ml
dH_2O	4.1ml
10%SDS	100µl
mix and degas with vacuum pump	
20% APS	15µl
TEMED	15µl

5% stacking gel (use ~2.5ml)

1.5M Tris HCl pH 6.8	1.25ml
30% acrylamide/ bisacrylamide solution (provided by BioRad)	0.8ml
dH_2O	2.9ml
10%SDS	50µl
mix and degas with vacuum pump	
20% APS	15µl
TEMED	7.5µl

2x SDS Sample Buffer

125mM Tris
4% w/v SDS
10% v/v 2-mercaptoethanole (1.43M)
20% v/v glycerol
0.01% w/v bromphenol blue

5x SDS Sample Buffer

the same applies as for 2x SDS Sample Buffer, but 2.5fold higher concentrated

2x SDS Sample Buffer with urea

100mM Tris
4M urea
4% w/vSDS
40% v/v glycerol
3.5% v/v 2-mercaptoethanole (250mM)
0.01% w/v bromphenol blue

running buffer

25mM Tris

500mM glycin
10% w/v SDS

transfer buffer

25mM Tris
500mM glycin

stripping buffer

2M $MgCl_2$
100mM acetic acid

Ponceau S staining solution

0.2% w/v PonceauS
3% w/w trichloracetic acid (TCA)

5.3 Cell culture

Dulbecco's modified Eagle's medium (DMEM)

supplemented with 1%L-Gln, 10% FCS (fetal calf serum) and 1% Penicilline/ Streptomycin ("full medium")

inorganic salts mg/l

$CaCl_2$ (dry)	200
$Fe(NO)_3 \cdot 9H_2O$	0.10
KCl	400
$MgSO_4$	97.70
NaCl	6400
$NaH_2PO_4 \cdot H_2O$	125
$NaHCO_3$	3700

other components mg/l

D-glucose	4500
phenolred	15
sodium pyruvate	110

amino acids mg/l

L-arginine HCl	84
L-cystine	48
L-glutamine	584 (added separately)

glycine	30
L-histidine HCl H_2O	42
L-isoleucine	105
L-leucine	105
L-lysine HCl	146
L-methionine	30
L-phenylalanine	66
L-serine	42
L-threonine	95
L-trypthophane	16
L-tyrosine	72
L-valine	94

vitamins mg/l

D-calcium pantothenate	4
choline chloride	4
folic acid	4
myo- inositol	7.2
nicotinamide	4
pyridoxal HCl	4
riboflavin	0.4
thiamine HCl	4

penicillin/streptomycin solution and FCS added separately

trypsin splitting solution

0.5mg/ml trypsin, 0.22mg/ml EDTA (Titriplex III) in PBS

fixation solution

4% formaldehyde in PBS

freezing medium

DMEM + 1%L-gln + 10% DMSO + 15% FCS

permeabilization solution

0.3% Triton X-100 in PBS

blocking solution for immunostaining

1% BSA in PBST

mounting medium

2.4g mowiol 4-88 (partly hydrolyzed polyvinylalcohol)
6.0g glycerol
6.0ml dH_2O
12.0ml 0.2M Tris HCl pH 8.5

each additive added with one hour mixing in between; final incubation at 50°C for 2 hours with slight shaking; then 25mg/ml DABCO (1,4-Diazabicyclo-(2,2,2)octan) as bleaching-inhibitor were added, storage at -20°C
for staining the nuclei (through staining the DNA) DAPI (4',6-diamidino-2-phenylindol) was directly added to the mounting medium. Alternatively, coverslips were finally incubated in Hoechst dye solution (Hoechst 33342, 1µg/ml, 5', RT), washed and mounted.

5.4 E.coli media

Luria Broth (LB)

1% w/v bacto trypton
0.5% w/v yeast extract
0.5% w/v NaCl
0.5% w/v D-glucose
pH 7.2 with NaOH

add if resistance was given
30mg/l Kanamycin
100mg/l Ampicillin
20mg/l Tetracycline

3% w/v agar for plates

SOC

2% w/v bacto tryptone
0.5% w/v yeast extract
10mM NaCl
2.5mM KCl
10mM $MgCl_2$
10mM $MgSO_4$
20mM D-glucose

YT

1.6% w/v bacto tryptone
1% w/v yeast extract
0.5% w/v NaCl

5.5 Plasmids and Oligonucleotides

5.5.1 Plasmids

name	description
pCB234	pDEST53-GFP+
pCB322	pSilencer 2.1-U6 hygro (EGFP)
pCB344	pENTR4
pCB368	pCMV-mCherry-SKL
pCB391	pDEST53-SNAPTEVTEV
pCB402	pmCherry-ER
pCB430	pcDNA-DEST53
pCB435	pEGFP-HsmSCP2
209	EXP53-GFP-HsPEX11B
214	EXP53-GFP+-yPEX11delta stop
215	HsPEX11A+STOP in pENTR4
216	HsPEX11B+STOP in pENTR4
217	HsPEX11C+STOP in pENTR4
218	EXP53-GFP+-HsPEX11A+STOP
219	EXP53-GFP+-HsPEx11B+STOP
220	EXP53-GFP+-HsPEx11C+STOP
222	EXP53-GFP+-yPEX25+STOP
224	EXP53-GFP+-yPEX27+STOP
227	S-A HsPEX11A+STOP in pENTR4, StrategyIII
228	S-D HsPEX11A+STOP in pENTR4, StrategyIV
229	HsPEX11B delta 78bp +STOP in pENTR4, Strategy VI
231	EXP53-S-A HsPEX11A+STOP, StrategyIII
232	EXP53-S-D HsPEX11A+STOP , StrategyIV
233	EXP53-HsPEX11B delta 78bp +STOP, Strategy VI
234	EXP53-codon 3 MUT yPEX11+STOP, StrategyVII
235	EXP53-AtPEX11-1
236	EXP53-AtPEX11-2
237	HsPEX11A delta60bp +STOP in pENTR4
238	EXP53+-AtPEX11-3
239	EXP53+-AtPEX11-4
240	EXP53+-AtPEX11-5
241	EXP53+-HsPEX11Adelta60bp
242	EXP53+-yPEX11delta54bp
243	EXP53+-SNAPTEVTEV-HsPEX11A
244	EXP53+-SNAPTEVTEV-HsPEX11C

Table 5: plasmids used in this study

5.5.2 Oligonucleotides/ Primers

name	sequence
CB109	TTAGCTAGCGGTACCATGGTGAGCAAGGG
CB110	CTAGATCTTTATAATTTGGACAGGTGGTGGCGCTTGTACAGCTCGTCCATGCC
CB127	GATCCCAGATTCGACAACTGGAGATTCAAGAGATCTCCAGTTGTCGAATCTGTTTTTTTGGAAA
CB128	AGCTTTTCCAAAAAACAGATTCGACAACTGGAGATCTCTTGAATCTCCAGTTGTCGAATCTGG
CB129	GATCCACACGCAAGAGCATATGTGTTCAAGAGACACATATGCTCTTGCGTGTTTTTTTGGAAA
CB130	AGCTTTTCCAAAAAAACACGCAAGAGCATATGTGTCTCTTGAACACATATGCTCTTGCGTGTG
CB131	GATCCGAGCTGTTCACCTATCAGATTCAAGAGATCTGATAGGTGAACAGCTCTTTTTTGGAAA
CB132	AGCTTTTCCAAAAAAGAGCTGTTCACCTATCAGATCTCTTGAATCTGATAGGTGAACAGCTCG
CB133	GATCCACAAGTGCACATGTGTCTCTTCAAGAGAGAGACACATGTGCACTTGTTTTTTTGGAAA

CB134	AGCTTTTCCAAAAAAACAAGTGCACATGTGTCTCTCTCTTGAAGAGACACATGTGCACTTGTG
CB135	GATCCCTCAGCCACTGCAGGACCATTCAAGAGATGGTCCTGCAGTGGCTGAGTTTTTTGGAAA
CB136	AGCTTTTCCAAAAAACTCAGCCACTGCAGGACCATCTCTTGAATGGTCCTGCAGTGGCTGAGG
CB137	GATCCAGTGTACGCGCACACCCACTTCAAGAGAGTGGGTGTGCGCGTACACTTTTTTTGGAAA
CB138	AGCTTTTCCAAAAAAAGTGTACGCGCACACCCACTCTCTTGAAGTGGGTGTGCGCGTACACTG
CB139	GATCCTCCTCAGCATGTACCAGGCTTCAAGAGAGCCTGGTACATGCTGAGGATTTTTTGGAAA
CB140	AGCTTTTCCAAAAAATCCTCAGCATGTACCAGGCTCTCTTGAAGCCTGGTACATGCTGAGGAG
CB141	GATCCGTAGACACGCACGCTCTCTTTCAAGAGAAGAGAGCGTGCGTGTCTACTTTTTTGGAAA
CB142	AGCTTTTCCAAAAAAGTAGACACGCACGCTCTCTTCTCTTGAAAGAGAGCGTGCGTGTCTACG
CB983a	GATCCGAGAAATCAGCATCCCAGGTTCAAGAGACCTGGGATGCTGATTTCTCTTTTTTGGAAA
CB984a	AGCTTTTCCAAAAAAGAGAAATCAGCATCCCAGGTCTCTTGAACCTGGGATGCTGATTTCTCG
CB985	GATCCAGAGGGCACATGCATACACTTCAAGAGAGTGTATGCATGTGCCCTCTTTTTTTGGAAA
CB986	AGCTTTTCCAAAAAAAGAGGGCACATGCATACACTCTCTTGAAGTGTATGCATGTGCCCTCTG
CB987	GATCCGAACCTTTGTGATATCCTGTTCAAGAGACAGGATATCACAAAGGTTCTTTTTTTGGAAA
CB988	AGCTTTTCCAAAAAAGAACCTTTGTGATATCCTGTCTCTTGAACAGGATATCACAAAGGTTCG
CB989	GATCCAGCAAGTGTGTCTCTATCTTTCAAGAGAAGATAGAGACACACTTGCTTTTTTTTGGAAA
CB990	AGCTTTTCCAAAAAAAGCAAGTGTGTCTCTATCTTCTCTTGAAAGATAGAGACACACTTGCTG
CB991	GAGCTCTCTGACACCATGGACAAAGACTGCGAAATGAAG
CB996	GGAGCGAGAATTTGTATTTTCAGGGTGAGCTATCCGAAAATCTCTATTTTCAGAGTGAGCCATGGGAGCT
CB997	CCCATGGCTCACTCTGAAAATAGAGATTTTCGGATAGCTCACCCTGAAAATACAAATTCTCGCTCCAGCT
CB998	AGCTGGAGCTCCCATGGCTCACTC
Pex11A-Hs-5	CCATGGACGCCTTCACCCG
Pex11A-Hs-6	CTCGAGCTAACGGGTCTTCAGCTTCATCTGAGG
Pex11A-Hs-7	ATCTTGGGCTGCGGCTTTCTCTTTCTTTGCCCTGTCACA
Pex11A-Hs-8	GAGAAAGCCGCAGCCCAAGATCCTCTTTGGTTCAGTGTGGCT
Pex11A-Hs-9	ATCCTGATCAGCATCTTTCTCTTTCTTTGCCCTGTCACA
Pex11A-Hs-10	GAGAAAGATGCTGATCAGGATCCTCTTTGGTTCAGTGTGGCT
Pex11A-Hs-11	GGCTCGAGCTAACGGGTCTTAAGCTTCATCTGAGGAGGATTGGATTTATAGATCCCCAG
Pex11B-Hs-5	CCATGGACGCCTGGGTCCG
Pex11B-Hs-6	CTCGAGTCAGGGCTTGAGTCGTAGCCAGG
Pex11B-Hs-7	GGTCTAGATATCTCGAGTCAGGGCTTGAGACGTCGCCAGAGGCCTAGTTTGTCCAG
Pex11G-Hs-1	TGGATCCGGATGGCGTCGCTGAGCGGCCTGG
Pex11G-Hs-2	CTCGAGTCAGGGGGTAGTGGCCTCGGCCT

Table 6: oligonucleotides used in this study

5.6 Human cell lines

HEK293T human embryonic kidney cells (Invitrogen)

6 Methods

6.1 Molecular biology

6.1.1 Restriction digest

Digests were performed according to the manufacturer's instruction unless otherwise stated. Usually one unit enzyme was used per microgram DNA.

6.1.2 Ligation

Ligation was performed using Invitrogen's Rapid Ligation Kit® according to the manufacturer's instructions. The amount of vector-DNA and insert-DNA was adjusted to come as close as possible to the ideal molar ratio of 1:3 (vector:insert) depending on the length of the insert. The usual incubation time was 20-30 minutes unless otherwise stated.

6.1.3 PCR

The usual PCR mixture was

1µl template (appropriate dilution of 1:100 - 1:1000)
2µl of each primer (10µM)
5µl of appropriate 10x buffer
1µl dNTPs (10mM)
1µl polymerase
38µl TE (pH 8.0).

All components were mixed and the solution was overlaid with 50-70µl of mineral oil to prevent vapour diffusion. PCR was performed with Pfu polymerase (30cycles), because Pfu exhibits a proof reading activity. For TA-cloning (e.g. in pGEM-T) PCR was continued with Taq polymerase (five cylces). The temperature setting was

first cycle	95°C	5'	
30 cycles	95°C	1'	
	-	1'	annealing temperature had to be adjusted to primers' T_m
	72°C	2'/kb	if Pfu turbo was used the time could be halved
last cycle	72°C	10'	

The water phase of the PCR was loaded on an agarose gel for analyzing the DNA content.

6.1.4 Gateway® reaction

The gateway® technology provided by Invitrogen was used to create tagged proteins very conveniently. The tag is part of the destination vector, while the protein of interest is coded in the entry vector. Both vectors contain att-sites localized in such way that after the recombination performed by an enzyme mix, called clonase, the gene of interest is in frame with the tag. This product is called expression vector. The possibility to create a manifold of expression vectors by this recombination out of few educts saves time.
The usual mixture and conditions were

1µl of destination vector (150 ng/µl DNA)
1µl of entry vector (150 ng/µl DNA)
2µl clonase enzyme mix
1µl 10x clonase buffer
5µl TE pH 8.0

for 2 hours at RT. After subsequent treatment with Proteinase K (10', 37°C), the produced expression vector was transformed by electroporation.

6.1.5 Agarose gel electrophoresis

Agarose gel electrophoresis was performed to separate DNA fragments. STOP solution was added to the DNA before loading onto the gel (1% agarose (Biozym or Sigma) in TBE with 0.05‰ ethidiumbromid).
Standard parameters: 100V (fixed), buffer: TBE

6.1.6 DNA PAGE

PAGE was performed to analyze small DNA fragments in the range of 20-100bp. Samples were mixed with DNA PAGE sample buffer and loaded onto gel with Fermentas' o'Gene low range DNA ladder®. Electrophoresis was performed with TBE as running buffer ($170V_{max}$, 50mA). For visualization of the DNA the gel was incubated in 0.05‰ ethidium bromide in TBE for 30 minutes followed by a destaining in TBE for 15 minutes.

6.1.7 DNA purification

DNA fragments were separated on a 1% agarose gel. The gel piece containing the DNA of interest was cut out with a scalpel and transferred to a tube. Gel extraction and DNA elution was performed with Nucleospin Extract II® (Macherey & Nagel) according to the manufacturer's instruction. The DNA amount after elution was analyzed by agarose gel electrophoresis.

6.1.8 DNA precipitation

The DNA solution was filled up to at least 100µl. Two volumes of i-propanol and $1/10^{th}$ volume of 3M sodiumacetate was added. DNA was precipitated at -80°C and pelleted (10', 13000rpm, 4°C). The pellet was once washed in 70% v/v ethanol (-20°C), dried well, e.g. with a vacuum centrifuge (10', 8000rpm, 40°C), and resuspended in TE.

6.1.9 Plasmid- DNA preparation *E.coli* (alkaline lysis)

A colony was inoculated and grown in 3ml of appropriate selective medium at 37°C over night, 1.5ml were harvested and centrifuged (1', 13000rpm, RT). The cell pellet was resuspended in 300µl buffer P1 (see buffer section), subsequently 300µl buffer P2 and 300µl of buffer P3 were added with mixing steps in between. In order to remove all cell debris and proteins the solution was centrifuged (10', 13000rpm, RT). The supernatant was transferred cautiously into a new tube, 650µl of 2-propanol were added, mixed and incubated for 10 minutes at room temperature. Then the suspension was centrifuged (10', 13000rpm, 4°C). The DNA pellet was washed with 70% ethanol (4°C) once, dried well and resuspended in 50µl TE.

6.1.10 Plasmid- DNA preparation *E.coli* (Promega Kit)

A colony was inoculated and grown in 3ml of appropriate selective medium at 37°C over night, 1.5ml were harvested and centrifuged (1', 13000rpm, RT). The following steps were performed according to the manufacturer's instructions.

6.1.11 Alignment for sequences

In the case a plasmid was checked by sequencing, the obtained sequence was compared to the correct one by using a multiple alignment program available via http:// baboon.math.berkeley.edu/mavid/ (Bray and Pachter, 2003; Bray and Pachter, 2004).

6.1.12 Transformation into *E.coli*

6.1.12.1 Preparation of chemically competent *E.coli*

Cells were inoculated in YT or LB medium O/N at 37°C. Subsequently 1ml of this culture was grown in 100ml YT medium to OD_{600}=0.8 and centrifuged (3700rpm, 12', 4°C). The cell pellet was washed in 15ml icecold FSB and incubated for 10 minutes on ice. After a further centrifugation step (3700rpm, 10', 4°C), cells were resuspended in 8ml icecold FSB, aliquoted and stored at -80°C.

6.1.12.2 Chemical transformation of *E.coli*

DNA (in case of ligation: 10-15µl, in case of retransformation: 1-3µl of a suitable dilution) was added to 100µl of competent cells and incubated for 10-15 minutes at 4°C. This solution was heat shocked for 45 seconds at 42°C and immediately put on ice for 5 minutes. 1ml of YT medium was added, the solution was incubated for 30-45 minutes at 37°C for revival, centrifuged (30'', 7000rpm, RT) and plated onto appropriate selective medium.

6.1.12.3 Preparation of electrocompetent *E.coli*

Cells were prepared as described for chemically competent E.coli, but were washed and resuspended in dH_2O instead of FSB.

6.1.12.4 Transformation of *E.coli* by electroporation

50µl of electrocompetent cells were mixed with 2µlof DNA avoiding bubbles and transferred to a clean and sterile cuvettes (washed with soap & 70% EtOH, UV treatment for 30'). In order to avoid a short-circuit the cuvettes had to be wiped off prior to placing in the pulse controller. Pulse conditions were 1.7V, 25µF capacitance and 200Ω resistance resulting in an ideal time constant of about 3.4-4.3s. 1ml of SOC was added to the cuvettes and after resuspending the suspension, cells were transferred into a tube and revived 30 minutes at 37°C. Subsequently cells were pelleted (7000rpm, 1', RT) and plated onto appropriate selective medium.

6.2 Biochemistry

6.2.1 Bradford assay

An appropriate dilution of the sample was mixed with an 1:5 dilution of Bradford's reagent and incubated at 30°C for 10-20'. Photometric absorption was measured at 595nm.

6.2.2 SDS PAGE

6.2.2.1 Gel preparation

The separation gel was prepared first: All components, but APS and TEMED, were mixed and degassed for 10'. After addition of APS and TEMED (icecold) the solution was carefully filled in between the prepared glass plates and overlaid with i-amylalcohol. During polymerization the stacking gel had been prepared like the separation gel. After polymerization, the alcoholic layer was removed, the stacking gel solution was filled in and the comb was pulled in tightly avoiding bubbles.

6.2.2.2 Sample preparation

Samples were mixed with sample buffer (SB), incubated for 5' at 95°C and centrifuged (13000rpm, 5', RT).

6.2.2.3 Electrophoresis

The system was set up, the gel was fixed in the chamber. After removal of the comb, the slots were washed with dH_2O and the chamber was filled with running buffer (RB). The prepared samples were loaded into the slots and the voltage had been applied (40mA constant, 170V max.) until the blue front reached the bottom of the gel.

6.2.2.4 Western blotting (semi-dry)

The stacking gel was cautiously removed and the separation gel was shortly incubated in transfer buffer before it was situated onto a nitrocellulose (NC) membrane of appropriate size. In order to guarantee enough transfer buffer during the whole blotting process a stack of filter papers was placed on the bottom and on the top between the electrodes of the blotting apparatus. Voltage had been applied (60mA constant (1.5mA/cm^2), 25V max.) for two hours. The membrane was then washed once in TBST, incubated in blocking solution for one hour, subsequently briefly washed and incubated with the primary antibody for 2 hours at RT. Incubation with the secondary antibody was performed for 1.5-2 hours following a washing procedure (3x for 15' each in TBST). The detection assay was performed using Pierce Super Signal West Pico Chemiluminescent Substrate (HRP) or BioRad Immunstar WesternC® for more sensitive detection.

6.2.2.5 Stripping a NC-membrane

In some cases it was necessary to perform a second assay (e.g. another antibody) on the same NC membrane. Therefore the antigen-antibody interaction had to be weakened and then eliminated. The membrane was incubated with stripping buffer 10' at RT and washed in TBST O/N or at least 3 times for 15'. The membrane was then treated as described before.

6.2.2.6 PonceauS staining

The NC membrane was incubated in PonceauS staining solution for 1 to 2 minutes, subsequently destained in dH_2O for higher contrast. For complete destaining the NC membrane was incubated in TBST.

6.3 Cell culture

6.3.1 Growing conditions

Cells were grown in DMEM + L-glutamine + FCS + penicillin/ streptomycin (referred to as "full medium") at 37°C with 5% v/v CO_2 (incubator: Binder CB150). Any sterile operations were performed in a laminar flow hood (Holten LaminAir, HB2438).

dish diameter	volume of medium
10 cm or 75cm^2 flask	10 ml
3 cm (6-well)	2 ml
12-well	1 ml
24-well	750µl
48-well	500µl
96-well	100µl

6.3.2 Splitting/ dry

All medium was removed and cells were washed with PBS once. 1.5 ml trypsin EDTA solution was added and removed immediately. The cells were incubated for 5 minutes at 37°C and the appropriate amount of full medium was added to dilute the cells. They were thoroughly resuspended and transferred to a new dish.

6.3.3 Splitting/ wet

The same applies as for dry splitting, but trypsin was not removed. After resuspending the cells, they were centrifuged (700rpm, 4', RT) and resuspended in the appropriate amount of full medium in order to dilute.

6.3.4 Freezing

Cells were split as described before and resuspended in freezing medium. Cells were frozen in aliquots of 1600µl for at least 24h at -80°C in a cool box containing isopropanol for a constant freeezing gradient, then transferred in liquid nitrogen.

6.3.5 Thawing

The cryotube (containing 1.5ml of cell suspension) was put at 37°C in order to thaw the cells as quickly as possible. The thawed solution was then diluted with 5ml DMEM, centrifuged

(700rpm, 3', RT), resuspended in 7ml of full medium and transferred to a 25cm^2 flask (T25) for incubation.

6.3.6 Transfection with FuGene 6 (Invitrogen)

First, cover slips (12mm glass circles, Sigma) had to be prepared. They were left in HNO_3/H_2SO_4 (1:2) O/N, washed in dH_2O 10 times, then incubated in 1g/l EDTA for three hours before getting thoroughly rinsed with dH_2O 10 times. Prepared cover slips were stored in 95% ethanol.
For microscopy, cells were grown directly on cover slips or, for whole cell extracts seeded in 100mm dished. Cells were prepared and transfected according to the manufacturer's instructions. Usual parameters (unless otherwise stated): total amount of DNA: 1µg, 3µl FuGene, incubation time: 20h

6.3.7 Whole-cell extracts (lysis with sample buffer)

Cells were washed once with PBS, 20µl of 2x sample buffer with urea (each 6-well) preheated at 95°C was added and cells were scraped with a sterile cell scraper and transferred to a new tube. In case of a slimy consistence the extracts were sonicated twice (75% intensity, 50% cycle time, 7'', 4°C). An aliquot was loaded onto a SDS-PAGE gel.

6.3.8 Whole cell extracts (lysis with lysis buffer)

Cells were trypsinized (wet method) and resuspended in appropriate volume of lysis buffer (usually 100-200µl for 100mm dish). After breaking the cells for 15' at 4°C on a rocking platform, they were additionally treated with a mini-eppendorf-potter and/or sonicated.

6.3.9 Optimizing antibiotic selection conditions ("antibiotic titration")

Some substances inhibit the growth of a wide range of prokaryotic and eukaryotic cells. Nevertheless they are called antibiotics. It was necessary to determine the ideal concentration of each antibiotic for each cell line. An equal number of cells (about 20.000) was seed into every well of a 6-well and incubated for 24 hours before the antibiotic treatment was started: Cells were washed, the medium is changed and different amounts of the antibiotic solution are added to each well, recurring every three days. Cells were inspected for viability every day. The optimal antibiotic concentration should cause massive cell death after 4-7 days and kill all cells within 10-14 days. This concentration was used to keep cells on selective conditions, but to initiate selection the concentration was doubled.

6.3.10 Establishing stable cell lines after plasmid transfection

Cells were transfected as described above. One day after the transfection cells were split in different densities and incubated for 24h before the selective agent was added. Then growth and apoptosis was observed while changing the medium (with antibiotic) every 2-3 days.

After all nontransfected cells were killed, the 100mm dish were split in a 96-well and diluted in such way, that only one cell remained in one well. Medium with selective agent was changed every 2-3 days until cells reached full density. Dense cells were split and transferred to a 48-well followed by subsequent growth and splitting until the cells fully covered a 100mm dish.

6.3.11 4-PBA treatment

Cells were seeded in normal density and incubated 10 days in full medium supplemented with 5mM final concentration sodium 4-phenylbutyrate (provided by Calbiochem).

6.3.12 siRNA/ shRNA

Suitable 19-mer siRNA fragments were designed using the software OligoEngine Workstation 2. The fragments with the highest potency and fewest BLAST hits (nucleotide blast, BLASTN, Altschul et al., 1997) were chosen. A negative control was designed for each siRNA by scrambling its oligonucleotides.
All siRNA were cloned into pSilencer 2.1-U6 hygro (BamHI, HindIII) and sequenced.

6.3.13 Labeling the SNAP®-tag

Medium was removed from cells expressing SNAP fusion proteins and the labelling solution was added directly onto the cells (1:200 dilution of stock; stock: 400µM TMR-Star or 1mM BG-505 in DMSO) and incubated for 15' (TMR-Star) or 30' (BG-505) at 37°C. Then, cells were washed twice and incubated with full medium for 30' to remove unreacted substrate leaching out of the cells followed by a last washing step. Then, cells were ready for live cell imaging or fixing.

6.3.14 SNAP® -vista technology

For direct labeling the SNAP® fusion proteins on a SDS-gel, 2µl labeling solution was added to 18µl of sample in lysis buffer (recommended composition of lysis buffer identical with lysis buffer described above) and incubated for 20' at RT in the dark. Then, sample buffer was added and the SDS-gel was run. After running, the bands were made visible by excitation with an UV-illuminator.

6.4 Microscopy

6.4.1 Fixation of human cells with formaldehyde

Cells were washed twice in PBS for five minutes, incubated for 10-15 minutes in fixing solution, washed in PBS three times for five minutes and embedded in 20-30µl moviol onto a micro slide.

6.4.2 Immunostaining

Cells were fixed as described above. Directly after fixing, cells were permeabilized in 0.1% TritonX-100 in PBS (10',RT). Then, cells were blocked in blocking solution. After washing (5',RT), cells were incubated with the primary antibody solution (PBST, 1h,RT) and after subsequent washing steps (3x 5',RT) stained with the secondary antibody solution (PBST,1h,RT). After a final washing procedure (3x 5',RT), cells were mounted as described above.

6.4.3 Fluorescent microscope

Zeiss Axioplan2, objective: Plan-ApoChrom 63x, 1.4, light source: Zeiss FluoArc +N HBO 103; CCD camera: Pursuit B/W monochrome PR1600 + DualView imager, software: Spot v4.6.

6.4.4 Confocal laser scanning microscope (CLSM)

Zeiss Axioplan2 + Zeiss LSM 510 META, objectives: Plan-ApoChrom 63x, 1.4; α-Plan-Fluar 100x, 1.45, software: Zeiss operating software AIM (expert mode), excitation by laser: 488nm for GFP, 561nm for dsRED and mCherry, 633nm for IR-dyes and 405nm for Hoechst. Emission settings: DsRed/ mCherry: HFT 405/488/561, NFT 515, LP 585; GFP: HFT 488, NFT 565, LP 505; Hoechst: HFT 405/488/561, NFT 490, BP 470-525; far red: HFT 405/514/633, NFT 565, LP 650

6.4.5 Live cell imaging

Live cell imaging was performed using the Zeiss LSM5 LIVE DuoScan system, objectives Plan-ApoChrom 63x, 1.4; software: Zeiss operating software AIM (expert mode), excitation by laser: 488nm for GFP, 535nm for dsRED and mCherry and 405nm for Hoechst. Emission settings as indicated above.

6.4.6 Image handling

Images were handled with Zeiss Image Software AIM® and ImageJ. Figures were arranged with Corel Draw 12.

6.4.7 Deconvolution and 3D reconstruction

Deconvolution and 3D rendering were performed with "Iterative Deconvolve 3D", "Diffraction PSF 3D" and "VolumeJ" (Abramoff and Viergever, 2002), plugins of ImageJ. A representative crop of each channel was deconvolved (low pass filter (for x and y dimension) 1.0, no Wiener filter, Z-direction low pass filter 1.0, maximum number of iterations 100, termination if mean delta is smaller than 0.01%) using the appropriate PSF. This was used as

input for 3D rendering (Raytrace algorithm, gradient no index, Scale 2.0, Classifier threshold 128.0, Classifier deviation 2.0). Finally, channels were coloured and merged.

6.4.8 Counting of peroxisomes

Images from the CLSM were filtered by a median filter (radius 1.0), despeckled (radius 1.0), converted to 8-bit and thresholded using the "Multithresholder", a plugin of ImageJ (threshold "Maximum Entropy"), to highlight the peroxisomal fluorescence. After applying the "Watershed" segmentation algorithm to separate neighbouring individual peroxisomes from each other, one cell was encircled manually and the particle analysis of ImageJ counted the number and area of each dot of a given category. Four categories have been set up (CAT I 0-0.35µm, CAT II 0.36-0.66, CAT III 0.37-0.95µm, CAT IV 0.96-3.6µm diameter) and 50 randomly chosen cells for each construct were counted.

7 Appendix

7.1 List of Figures

7.2 List of Tables

7.3 List of Abbreviations

‘	minute
‘’	second
aa	amino acid
BG	benzylguanine
CHO(-K1)	chinese hamster ovary cells, (K1)
CMV	cytomegalovirus
ER	endoplasmic reticulum
hAGT	human alkylguanine transferase
HEK	human embryonic kidney
mPTS	peroxisomal membrane targeting sequence
ORE	oleate-responsive element
PBA	sodium 4-phenylbutyrate
PMP	peroxisomal membrane protein
PPAR	peroxisome proliferator activated receptor
PPRE	peroxisome proliferator responsive element
PSF	point spread function
PTS	peroxisomal targeting sequence
Rb	rabbit
ROS	reactive oxygen species
RT	room temperature
TEV	tobacco etch virus
TMD	transmembrane domain

VLCFA	very long chain fatty acid

At	*Arabidopsis thaliana*
Cb	*Candida boidinii*
Hs	*Homo sapiens*
Sc	*Saccharomyces cerevisiae*

additionally, standardized usage of abbreviations of nucleotides and amino acids (one and three letter code) was applied

8 References

Abe, I., and Y. Fujiki. 1998. cDNA cloning and characterization of a constitutively expressed isoform of the human peroxin Pex11p. *Biochem Biophys Res Commun*. 252:529-33.

Abe, I., K. Okumoto, S. Tamura, and Y. Fujiki. 1998. Clofibrate-inducible, 28-kDa peroxisomal integral membrane protein is encoded by PEX11. *FEBS Lett*. 431:468-72.

Abramoff, M.D., and M.A. Viergever. 2002. Computation and visualization of three-dimensional soft tissue motion in the orbit. *IEEE Trans Med Imaging*. 21:296-304.

Albertini, M., P. Rehling, R. Erdmann, W. Girzalsky, J.A. Kiel, M. Veenhuis, and W.H. Kunau. 1997. Pex14p, a peroxisomal membrane protein binding both receptors of the two PTS-dependent import pathways. *Cell*. 89:83-92.

Altschul, S.F., T.L. Madden, A.A. Schaffer, J. Zhang, Z. Zhang, W. Miller, and D.J. Lipman. 1997. Gapped BLAST and PSI-BLAST: a new generation of protein database search programs. *Nucleic Acids Res*. 25:3389-402.

Anton, M., M. Passreiter, D. Lay, T.P. Thai, K. Gorgas, and W.W. Just. 2000. ARF- and coatomer-mediated peroxisomal vesiculation. *Cell Biochem Biophys*. 32 Spring:27-36.

Bascom, R.A., H. Chan, and R.A. Rachubinski. 2003. Peroxisome biogenesis occurs in an unsynchronized manner in close association with the endoplasmic reticulum in temperature-sensitive Yarrowia lipolytica Pex3p mutants. *Mol Biol Cell*. 14:939-57.

Bray, N., and L. Pachter. 2003. MAVID multiple alignment server. *Nucleic Acids Res*. 31:3525-6.

Bray, N., and L. Pachter. 2004. MAVID: constrained ancestral alignment of multiple sequences. *Genome Res*. 14:693-9.

Brocard, C., and A. Hartig. 2006. Peroxisome targeting signal 1: is it really a simple tripeptide? *Biochim Biophys Acta*. 1763:1565-73.

Brocard, C., and A. Hartig. 2007. Peroxins: A Proliferation Romance amongst Supposition and Disposition. *Dyn Cell Biol*. 1:1-11.

Brocard, C., F. Kragler, M.M. Simon, T. Schuster, and A. Hartig. 1994. The tetratricopeptide repeat-domain of the PAS10 protein of Saccharomyces cerevisiae is essential for binding the peroxisomal targeting signal-SKL. *Biochem Biophys Res Commun*. 204:1016-22.

Brocard, C., G. Lametschwandtner, R. Koudelka, and A. Hartig. 1997. Pex14p is a member of the protein linkage map of Pex5p. *Embo J*. 16:5491-500.

Brown, L.A., and A. Baker. 2003. Peroxisome biogenesis and the role of protein import. *J Cell Mol Med*. 7:388-400.

Cai, Y., M.H. Wu, M. Xu-Welliver, A.E. Pegg, S.M. Ludeman, and M.E. Dolan. 2000. Effect of O6-benzylguanine on alkylating agent-induced toxicity and mutagenicity. In Chinese hamster ovary cells expressing wild-type and mutant O6-alkylguanine-DNA alkyltransferases. *Cancer Res*. 60:5464-9.

Chapman, S., K.J. Oparka, and A.G. Roberts. 2005. New tools for in vivo fluorescence tagging. *Curr Opin Plant Biol*. 8:565-73.

Damoiseaux, R., A. Keppler, and K. Johnsson. 2001. Synthesis and applications of chemical probes for human O6-alkylguanine-DNA alkyltransferase. *Chembiochem*. 2:285-7.

Daniels, D.S., and J.A. Tainer. 2000. Conserved structural motifs governing the stoichiometric repair of alkylated DNA by O(6)-alkylguanine-DNA alkyltransferase. *Mutat Res*. 460:151-63.

Daniels, D.S., T.T. Woo, K.X. Luu, D.M. Noll, N.D. Clarke, A.E. Pegg, and J.A. Tainer. 2004. DNA binding and nucleotide flipping by the human DNA repair protein AGT. *Nat Struct Mol Biol*. 11:714-20.

De Duve, C. 1969. Evolution of the peroxisome. *Ann N Y Acad Sci*. 168:369-81.

De Duve, C., and P. Baudhuin. 1966. Peroxisomes (microbodies and related particles). *Physiol Rev*. 46:323-57.

Desai, M., and J. Hu. 2008. Light induces peroxisome proliferation in Arabidopsis seedlings through the photoreceptor phytochrome A, the transcription factor HY5 HOMOLOG, and the peroxisomal protein PEROXIN11b. *Plant Physiol*.

Diella, F., S. Cameron, C. Gemund, R. Linding, A. Via, B. Kuster, T. Sicheritz-Ponten, N. Blom, and T.J. Gibson. 2004. Phospho.ELM: a database of experimentally verified phosphorylation sites in eukaryotic proteins. *BMC Bioinformatics*. 5:79.

Diella, F., C.M. Gould, C. Chica, A. Via, and T.J. Gibson. 2008. Phospho.ELM: a database of phosphorylation sites--update 2008. *Nucleic Acids Res*. 36:D240-4.

Distel, B., R. Erdmann, S.J. Gould, G. Blobel, D.I. Crane, J.M. Cregg, G. Dodt, Y. Fujiki, J.M. Goodman, W.W. Just, J.A. Kiel, W.H. Kunau, P.B. Lazarow, G.P. Mannaerts, H.W. Moser, T. Osumi, R.A. Rachubinski, A. Roscher, S. Subramani, H.F. Tabak, T. Tsukamoto, D. Valle, I. van der Klei, P.P. van Veldhoven, and M. Veenhuis. 1996. A unified nomenclature for peroxisome biogenesis factors. *J Cell Biol*. 135:1-3.

Dyer, J.M., J.A. McNew, and J.M. Goodman. 1996. The sorting sequence of the peroxisomal integral membrane protein PMP47 is contained within a short hydrophilic loop. *J Cell Biol*. 133:269-80.

Einwachter, H., S. Sowinski, W.H. Kunau, and W. Schliebs. 2001. Yarrowia lipolytica Pex20p, Saccharomyces cerevisiae Pex18p/Pex21p and mammalian Pex5pL fulfil a common function in the early steps of the peroxisomal PTS2 import pathway. *EMBO Rep*. 2:1035-9.

Erdmann, R., and G. Blobel. 1995. Giant peroxisomes in oleic acid-induced Saccharomyces cerevisiae lacking the peroxisomal membrane protein Pmp27p. *J Cell Biol*. 128:509-23.

Erdmann, R., M. Veenhuis, D. Mertens, and W.H. Kunau. 1989. Isolation of peroxisome-deficient mutants of Saccharomyces cerevisiae. *Proc Natl Acad Sci U S A*. 86:5419-23.

Fagarasanu, A., M. Fagarasanu, G.A. Eitzen, J.D. Aitchison, and R.A. Rachubinski. 2006. The peroxisomal membrane protein Inp2p is the peroxisome-specific receptor for the myosin V motor Myo2p of Saccharomyces cerevisiae. *Dev Cell*. 10:587-600.

Fagarasanu, M., A. Fagarasanu, Y.Y. Tam, J.D. Aitchison, and R.A. Rachubinski. 2005. Inp1p is a peroxisomal membrane protein required for peroxisome inheritance in Saccharomyces cerevisiae. *J Cell Biol*. 169:765-75.

Fang, Y., J.C. Morrell, J.M. Jones, and S.J. Gould. 2004. PEX3 functions as a PEX19 docking factor in the import of class I peroxisomal membrane proteins. *J Cell Biol*. 164:863-75.

Frolov, A., T.H. Cho, J.T. Billheimer, and F. Schroeder. 1996. Sterol carrier protein-2, a new fatty acyl coenzyme A-binding protein. *J Biol Chem*. 271:31878-84.

Gandre-Babbe, S., and A.M. van der Bliek. 2008. The Novel Tail-anchored Membrane Protein Mff Controls Mitochondrial and Peroxisomal Fission in Mammalian Cells. *Mol Biol Cell*.

Gould, S.J., G.A. Keller, N. Hosken, J. Wilkinson, and S. Subramani. 1989. A conserved tripeptide sorts proteins to peroxisomes. *J Cell Biol*. 108:1657-64.

Gould, S.J., G.A. Keller, and S. Subramani. 1988. Identification of peroxisomal targeting signals located at the carboxy terminus of four peroxisomal proteins. *J Cell Biol*. 107:897-905.

Gould, S.J., and D. Valle. 2000. Peroxisome biogenesis disorders: genetics and cell biology. *Trends Genet*. 16:340-5.

Green, S. 1995. PPAR: a mediator of peroxisome proliferator action. *Mutat Res*. 333:101-9.

Griffin, B.A., S.R. Adams, and R.Y. Tsien. 1998. Specific covalent labeling of recombinant protein molecules inside live cells. *Science*. 281:269-72.

Griffin, R.J., C.E. Arris, C. Bleasdale, F.T. Boyle, A.H. Calvert, N.J. Curtin, C. Dalby, S. Kanugula, N.K. Lembicz, D.R. Newell, A.E. Pegg, and B.T. Golding. 2000. Resistance-modifying agents. 8. Inhibition of O(6)-alkylguanine-DNA alkyltransferase by O(6)-alkenyl-, O(6)-cycloalkenyl-, and O(6)-(2-oxoalkyl)guanines and potentiation of temozolomide cytotoxicity in vitro by O(6)-(1-cyclopentenylmethyl)guanine. *J Med Chem*. 43:4071-83.

Gronemeyer, T., C. Chidley, A. Juillerat, C. Heinis, and K. Johnsson. 2006. Directed evolution of O6-alkylguanine-DNA alkyltransferase for applications in protein labeling. *Protein Eng Des Sel*. 19:309-16.

Haan, G.J., R.J. Baerends, A.M. Krikken, M. Otzen, M. Veenhuis, and I.J. van der Klei. 2006. Reassembly of peroxisomes in Hansenula polymorpha pex3 cells on reintroduction of Pex3p involves the nuclear envelope. *FEMS Yeast Res*. 6:186-94.

Heinis, C., S. Schmitt, M. Kindermann, G. Godin, and K. Johnsson. 2006. Evolving the substrate specificity of O6-alkylguanine-DNA alkyltransferase through loop insertion for applications in molecular imaging. *ACS Chem Biol*. 1:575-84.

Hettema, E.H., W. Girzalsky, M. van Den Berg, R. Erdmann, and B. Distel. 2000. Saccharomyces cerevisiae pex3p and pex19p are required for proper localization and stability of peroxisomal membrane proteins. *Embo J*. 19:223-33.

Hoepfner, D., D. Schildknegt, I. Braakman, P. Philippsen, and H.F. Tabak. 2005. Contribution of the endoplasmic reticulum to peroxisome formation. *Cell*. 122:85-95.

Hogenboom, S., J.J. Tuyp, M. Espeel, J. Koster, R.J. Wanders, and H.R. Waterham. 2004. Mevalonate kinase is a cytosolic enzyme in humans. *J Cell Sci*. 117:631-9.

Honsho, M., and Y. Fujiki. 2001. Topogenesis of peroxisomal membrane protein requires a short, positively charged intervening-loop sequence and flanking hydrophobic segments. study using human membrane protein PMP34. *J Biol Chem*. 276:9375-82.

Hunt, J.E., and R.N. Trelease. 2004. Sorting pathway and molecular targeting signals for the Arabidopsis peroxin 3. *Biochem Biophys Res Commun*. 314:586-96.

Issemann, I., and S. Green. 1990. Activation of a member of the steroid hormone receptor superfamily by peroxisome proliferators. *Nature*. 347:645-50.

Juillerat, A., T. Gronemeyer, A. Keppler, S. Gendreizig, H. Pick, H. Vogel, and K. Johnsson. 2003. Directed evolution of O6-alkylguanine-DNA alkyltransferase for efficient labeling of fusion proteins with small molecules in vivo. *Chem Biol*. 10:313-7.

Kemp, S., H.M. Wei, J.F. Lu, L.T. Braiterman, M.C. McGuinness, A.B. Moser, P.A. Watkins, and K.D. Smith. 1998. Gene redundancy and pharmacological gene therapy: implications for X-linked adrenoleukodystrophy. *Nat Med*. 4:1261-8.

Keppler, A., C. Arrivoli, L. Sironi, and J. Ellenberg. 2006. Fluorophores for live cell imaging of AGT fusion proteins across the visible spectrum. *Biotechniques*. 41:167-70, 172, 174-5.

Keppler, A., S. Gendreizig, T. Gronemeyer, H. Pick, H. Vogel, and K. Johnsson. 2003. A general method for the covalent labeling of fusion proteins with small molecules in vivo. *Nat Biotechnol*. 21:86-9.

Keppler, A., M. Kindermann, S. Gendreizig, H. Pick, H. Vogel, and K. Johnsson. 2004a. Labeling of fusion proteins of O6-alkylguanine-DNA alkyltransferase with small molecules in vivo and in vitro. *Methods*. 32:437-44.

Keppler, A., H. Pick, C. Arrivoli, H. Vogel, and K. Johnsson. 2004b. Labeling of fusion proteins with synthetic fluorophores in live cells. *Proc Natl Acad Sci U S A*. 101:9955-9.

Kim, P.K., R.T. Mullen, U. Schumann, and J. Lippincott-Schwartz. 2006. The origin and maintenance of mammalian peroxisomes involves a de novo PEX16-dependent pathway from the ER. *J Cell Biol*. 173:521-32.

Kindermann, M., N. George, N. Johnsson, and K. Johnsson. 2003. Covalent and selective immobilization of fusion proteins. *J Am Chem Soc*. 125:7810-1.

Kobayashi, S., A. Tanaka, and Y. Fujiki. 2007. Fis1, DLP1, and Pex11p coordinately regulate peroxisome morphogenesis. *Exp Cell Res*. 313:1675-86.

Koch, A., G. Schneider, G.H. Luers, and M. Schrader. 2004. Peroxisome elongation and constriction but not fission can occur independently of dynamin-like protein 1. *J Cell Sci*. 117:3995-4006.

Koch, A., Y. Yoon, N.A. Bonekamp, M.A. McNiven, and M. Schrader. 2005. A role for Fis1 in both mitochondrial and peroxisomal fission in mammalian cells. *Mol Biol Cell*. 16:5077-86.

Kragt, A., T. Voorn-Brouwer, M. van den Berg, and B. Distel. 2005. Endoplasmic reticulum-directed Pex3p routes to peroxisomes and restores peroxisome formation in a Saccharomyces cerevisiae pex3Delta strain. *J Biol Chem*. 280:34350-7.

Kuravi, K., S. Nagotu, A.M. Krikken, K. Sjollema, M. Deckers, R. Erdmann, M. Veenhuis, and I.J. van der Klei. 2006. Dynamin-related proteins Vps1p and Dnm1p control peroxisome abundance in Saccharomyces cerevisiae. *J Cell Sci*. 119:3994-4001.

Kyte, J., and R.F. Doolittle. 1982. A simple method for displaying the hydropathic character of a protein. *J Mol Biol*. 157:105-32.

Lay, D., K. Gorgas, and W.W. Just. 2006. Peroxisome biogenesis: where Arf and coatomer might be involved. *Biochim Biophys Acta*. 1763:1678-87.

Lazarow, P.B. 1995. Peroxisome structure, function, and biogenesis--human patients and yeast mutants show strikingly similar defects in peroxisome biogenesis. *J Neuropathol Exp Neurol*. 54:720-5.

Lazarow, P.B., and Y. Fujiki. 1985. Biogenesis of peroxisomes. *Annu Rev Cell Biol*. 1:489-530.

Lemberger, T., B. Desvergne, and W. Wahli. 1996. Peroxisome proliferator-activated receptors: a nuclear receptor signaling pathway in lipid physiology. *Annu Rev Cell Dev Biol*. 12:335-63.

Li, X., E. Baumgart, G.X. Dong, J.C. Morrell, G. Jimenez-Sanchez, D. Valle, K.D. Smith, and S.J. Gould. 2002a. PEX11alpha is required for peroxisome proliferation in response to 4-phenylbutyrate but is dispensable for peroxisome proliferator-activated receptor alpha-mediated peroxisome proliferation. *Mol Cell Biol*. 22:8226-40.

Li, X., E. Baumgart, J.C. Morrell, G. Jimenez-Sanchez, D. Valle, and S.J. Gould. 2002b. PEX11 beta deficiency is lethal and impairs neuronal migration but does not abrogate peroxisome function. *Mol Cell Biol*. 22:4358-65.

Li, X., and S.J. Gould. 2002. PEX11 promotes peroxisome division independently of peroxisome metabolism. *J Cell Biol*. 156:643-51.

Li, X., and S.J. Gould. 2003. The dynamin-like GTPase DLP1 is essential for peroxisome division and is recruited to peroxisomes in part by PEX11. *J Biol Chem*. 278:17012-20.

Lingard, M.J., S.K. Gidda, S. Bingham, S.J. Rothstein, R.T. Mullen, and R.N. Trelease. 2008. Arabidopsis PEROXIN11c-e, FISSION1b, and DYNAMIN-RELATED PROTEIN3A Cooperate in Cell Cycle-Associated Replication of Peroxisomes. *Plant Cell*.

Lingard, M.J., and R.N. Trelease. 2006. Five Arabidopsis peroxin 11 homologs individually promote peroxisome elongation, duplication or aggregation. *J Cell Sci*. 119:1961-72.

Lu, J., and C. Deutsch. 2001. Pegylation: a method for assessing topological accessibilities in Kv1.3. *Biochemistry*. 40:13288-301.

Maier, A.G., S. Schulreich, M. Bremser, and C. Clayton. 2000. Binding of coatomer by the PEX11 C-terminus is not required for function. *FEBS Lett*. 484:82-6.

Marelli, M., J.J. Smith, S. Jung, E. Yi, A.I. Nesvizhskii, R.H. Christmas, R.A. Saleem, Y.Y. Tam, A. Fagarasanu, D.R. Goodlett, R. Aebersold, R.A. Rachubinski, and J.D. Aitchison. 2004. Quantitative mass spectrometry reveals a role for the GTPase Rho1p in actin organization on the peroxisome membrane. *J Cell Biol*. 167:1099-112.

Marshall, P.A., J.M. Dyer, M.E. Quick, and J.M. Goodman. 1996. Redox-sensitive homodimerization of Pex11p: a proposed mechanism to regulate peroxisomal division. *J Cell Biol*. 135:123-37.

Marshall, P.A., Y.I. Krimkevich, R.H. Lark, J.M. Dyer, M. Veenhuis, and J.M. Goodman. 1995. Pmp27 promotes peroxisomal proliferation. *J Cell Biol*. 129:345-55.

McCartney, A.W., J.S. Greenwood, M.R. Fabian, K.A. White, and R.T. Mullen. 2005. Localization of the tomato bushy stunt virus replication protein p33 reveals a peroxisome-to-endoplasmic reticulum sorting pathway. *Plant Cell*. 17:3513-31.

McCollum, D., E. Monosov, and S. Subramani. 1993. The pas8 mutant of Pichia pastoris exhibits the peroxisomal protein import deficiencies of Zellweger syndrome cells--the PAS8 protein binds to the COOH-terminal tripeptide peroxisomal targeting signal, and is a member of the TPR protein family. *J Cell Biol*. 121:761-74.

McGuinness, M.C., H. Wei, and K.D. Smith. 2000. Therapeutic developments in peroxisome biogenesis disorders. *Expert Opin Investig Drugs*. 9:1985-92.

Meikrantz, W., M.A. Bergom, A. Memisoglu, and L. Samson. 1998. O6-alkylguanine DNA lesions trigger apoptosis. *Carcinogenesis*. 19:369-72.

Moser, A.B., M. Rasmussen, S. Naidu, P.A. Watkins, M. McGuinness, A.K. Hajra, G. Chen, G. Raymond, A. Liu, D. Gordon, and et al. 1995. Phenotype of patients with

peroxisomal disorders subdivided into sixteen complementation groups. *J Pediatr*. 127:13-22.

Moser, H.W., A.E. Moser, I. Singh, and B.P. O'Neill. 1984. Adrenoleukodystrophy: survey of 303 cases: biochemistry, diagnosis, and therapy. *Ann Neurol*. 16:628-41.

Nakajima, T., G. Ichihara, M. Kamijima, S. Itohara, and T. Aoyama. 2002. Functional activation of peroxisome proliferator-activated receptor alpha (PPARalpha) by environmental chemicals in relation to their toxicities. *Nagoya J Med Sci*. 65:85-94.

Neuberger, G., M. Kunze, F. Eisenhaber, J. Berger, A. Hartig, and C. Brocard. 2004. Hidden localization motifs: naturally occurring peroxisomal targeting signals in non-peroxisomal proteins. *Genome Biol*. 5:R97.

Neuberger, G., S. Maurer-Stroh, B. Eisenhaber, A. Hartig, and F. Eisenhaber. 2003. Motif refinement of the peroxisomal targeting signal 1 and evaluation of taxon-specific differences. *J Mol Biol*. 328:567-79.

Neuspiel, M., A.C. Schauss, E. Braschi, R. Zunino, P. Rippstein, R.A. Rachubinski, M.A. Andrade-Navarro, and H.M. McBride. 2008. Cargo-selected transport from the mitochondria to peroxisomes is mediated by vesicular carriers. *Curr Biol*. 18:102-8.

Niederhoff, K., N.M. Meindl-Beinker, D. Kerssen, U. Perband, A. Schafer, W. Schliebs, and W.H. Kunau. 2005. Yeast Pex14p possesses two functionally distinct Pex5p and one Pex7p binding sites. *J Biol Chem*. 280:35571-8.

Novikoff, P.M., and A.B. Novikoff. 1972. Peroxisomes in absorptive cells of mammalian small intestine. *J Cell Biol*. 53:532-60.

Orth, T., S. Reumann, X. Zhang, J. Fan, D. Wenzel, S. Quan, and J. Hu. 2007. The PEROXIN11 protein family controls peroxisome proliferation in Arabidopsis. *Plant Cell*. 19:333-50.

Osumi, T., T. Tsukamoto, S. Hata, S. Yokota, S. Miura, Y. Fujiki, M. Hijikata, S. Miyazawa, and T. Hashimoto. 1991. Amino-terminal presequence of the precursor of peroxisomal 3-ketoacyl-CoA thiolase is a cleavable signal peptide for peroxisomal targeting. *Biochem Biophys Res Commun*. 181:947-54.

Passreiter, M., M. Anton, D. Lay, R. Frank, C. Harter, F.T. Wieland, K. Gorgas, and W.W. Just. 1998. Peroxisome biogenesis: involvement of ARF and coatomer. *J Cell Biol*. 141:373-83.

Pastori, G.M., and L.A. Del Rio. 1997. Natural Senescence of Pea Leaves (An Activated Oxygen-Mediated Function for Peroxisomes). *Plant Physiol*. 113:411-418.

Pause, B., R. Saffrich, A. Hunziker, W. Ansorge, and W.W. Just. 2000. Targeting of the 22 kDa integral peroxisomal membrane protein. *FEBS Lett*. 471:23-8.

Perichon, R., J.M. Bourre, J.F. Kelly, and G.S. Roth. 1998. The role of peroxisomes in aging. *Cell Mol Life Sci*. 54:641-52.

Platta, H.W., and R. Erdmann. 2007. Peroxisomal dynamics. *Trends Cell Biol*. 17:474-84.

Praefcke, G.J., and H.T. McMahon. 2004. The dynamin superfamily: universal membrane tubulation and fission molecules? *Nat Rev Mol Cell Biol*. 5:133-47.

Purdue, P.E., and P.B. Lazarow. 1995. Identification of peroxisomal membrane ghosts with an epitope-tagged integral membrane protein in yeast mutants lacking peroxisomes. *Yeast*. 11:1045-60.

Ragg, S., M. Xu-Welliver, J. Bailey, M. D'Souza, R. Cooper, S. Chandra, R. Seshadri, A.E. Pegg, and D.A. Williams. 2000. Direct reversal of DNA damage by mutant methyltransferase protein protects mice against dose-intensified chemotherapy and leads to in vivo selection of hematopoietic stem cells. *Cancer Res*. 60:5187-95.

Rottensteiner, H., A.J. Kal, B. Hamilton, H. Ruis, and H.F. Tabak. 1997. A heterodimer of the Zn2Cys6 transcription factors Pip2p and Oaf1p controls induction of genes encoding peroxisomal proteins in Saccharomyces cerevisiae. *Eur J Biochem*. 247:776-83.

Rottensteiner, H., A. Kramer, S. Lorenzen, K. Stein, C. Landgraf, R. Volkmer-Engert, and R. Erdmann. 2004. Peroxisomal membrane proteins contain common Pex19p-binding sites that are an integral part of their targeting signals. *Mol Biol Cell*. 15:3406-17.

Rottensteiner, H., K. Stein, E. Sonnenhol, and R. Erdmann. 2003. Conserved function of pex11p and the novel pex25p and pex27p in peroxisome biogenesis. *Mol Biol Cell*. 14:4316-28.

Sakai, Y., M. Oku, I.J. van der Klei, and J.A. Kiel. 2006. Pexophagy: autophagic degradation of peroxisomes. *Biochim Biophys Acta*. 1763:1767-75.

Santos, M.J., T. Imanaka, H. Shio, and P.B. Lazarow. 1988. Peroxisomal integral membrane proteins in control and Zellweger fibroblasts. *J Biol Chem*. 263:10502-9.

Schauss, A.C., J. Bewersdorf, and S. Jakobs. 2006. Fis1p and Caf4p, but not Mdv1p, determine the polar localization of Dnm1p clusters on the mitochondrial surface. *J Cell Sci*. 119:3098-106.

Shaner, N.C., R.E. Campbell, P.A. Steinbach, B.N. Giepmans, A.E. Palmer, and R.Y. Tsien. 2004. Improved monomeric red, orange and yellow fluorescent proteins derived from Discosoma sp. red fluorescent protein. *Nat Biotechnol*. 22:1567-72.

Shaner, N.C., G.H. Patterson, and M.W. Davidson. 2007. Advances in fluorescent protein technology. *J Cell Sci*. 120:4247-60.

Shaw, G., S. Morse, M. Ararat, and F.L. Graham. 2002. Preferential transformation of human neuronal cells by human adenoviruses and the origin of HEK 293 cells. *Faseb J*. 16:869-71.

Shimizu, M., A. Takeshita, T. Tsukamoto, F.J. Gonzalez, and T. Osumi. 2004. Tissue-selective, bidirectional regulation of PEX11 alpha and perilipin genes through a common peroxisome proliferator response element. *Mol Cell Biol*. 24:1313-23.

Smith, J.J., M. Marelli, R.H. Christmas, F.J. Vizeacoumar, D.J. Dilworth, T. Ideker, T. Galitski, K. Dimitrov, R.A. Rachubinski, and J.D. Aitchison. 2002. Transcriptome profiling to identify genes involved in peroxisome assembly and function. *J Cell Biol*. 158:259-71.

South, S.T., and S.J. Gould. 1999. Peroxisome synthesis in the absence of preexisting peroxisomes. *J Cell Biol*. 144:255-66.

Srivenugopal, K.S., X.H. Yuan, H.S. Friedman, and F. Ali-Osman. 1996. Ubiquitination-dependent proteolysis of O6-methylguanine-DNA methyltransferase in human and murine tumor cells following inactivation with O6-benzylguanine or 1,3-bis(2-chloroethyl)-1-nitrosourea. *Biochemistry*. 35:1328-34.

Subramani, S. 1998. Components involved in peroxisome import, biogenesis, proliferation, turnover, and movement. *Physiol Rev*. 78:171-88.

Subramani, S., A. Koller, and W.B. Snyder. 2000. Import of peroxisomal matrix and membrane proteins. *Annu Rev Biochem*. 69:399-418.

Subramanya, S., and K. Mensa-Wilmot. 2006. Regulated cleavage of intracellular glycosylphosphatidylinositol in a trypanosome. Peroxisome-to-endoplasmic reticulum translocation of a phospholipase C. *Febs J*. 273:2110-26.

Swinkels, B.W., S.J. Gould, A.G. Bodnar, R.A. Rachubinski, and S. Subramani. 1991. A novel, cleavable peroxisomal targeting signal at the amino-terminus of the rat 3-ketoacyl-CoA thiolase. *Embo J*. 10:3255-62.

Tabak, H.F., J.L. Murk, I. Braakman, and H.J. Geuze. 2003. Peroxisomes start their life in the endoplasmic reticulum. *Traffic*. 4:512-8.

Tabak, H.F., A. van der Zand, and I. Braakman. 2008. Peroxisomes: minted by the ER. *Curr Opin Cell Biol*. 20:393-400.

Tam, Y.Y., A. Fagarasanu, M. Fagarasanu, and R.A. Rachubinski. 2005. Pex3p initiates the formation of a preperoxisomal compartment from a subdomain of the endoplasmic reticulum in Saccharomyces cerevisiae. *J Biol Chem*. 280:34933-9.

Tam, Y.Y., J.C. Torres-Guzman, F.J. Vizeacoumar, J.J. Smith, M. Marelli, J.D. Aitchison, and R.A. Rachubinski. 2003. Pex11-related proteins in peroxisome dynamics: a role for the novel peroxin Pex27p in controlling peroxisome size and number in Saccharomyces cerevisiae. *Mol Biol Cell*. 14:4089-102.

Tanaka, A., K. Okumoto, and Y. Fujiki. 2003. cDNA cloning and characterization of the third isoform of human peroxin Pex11p. *Biochem Biophys Res Commun*. 300:819-23.

van den Bosch, H., R.B. Schutgens, R.J. Wanders, and J.M. Tager. 1992. Biochemistry of peroxisomes. *Annu Rev Biochem*. 61:157-97.

van Roermund, C.W., H.F. Tabak, M. van Den Berg, R.J. Wanders, and E.H. Hettema. 2000. Pex11p plays a primary role in medium-chain fatty acid oxidation, a process that affects peroxisome number and size in Saccharomyces cerevisiae. *J Cell Biol*. 150:489-98.

Veenhuis, M., M. Komori, F. Salomons, R.E. Hilbrands, H. Hut, R.J. Baerends, J.A. Kiel, and I.J. van der Klei. 1996. Peroxisomal remnants in peroxisome-deficient mutants of the yeast Hansenula polymorpha [corrected]. *FEBS Lett*. 383:114-8.

Veenhuis, M., M. Mateblowski, W.H. Kunau, and W. Harder. 1987. Proliferation of microbodies in Saccharomyces cerevisiae. *Yeast*. 3:77-84.

Vizeacoumar, F.J., J.C. Torres-Guzman, D. Bouard, J.D. Aitchison, and R.A. Rachubinski. 2004. Pex30p, Pex31p, and Pex32p form a family of peroxisomal integral membrane proteins regulating peroxisome size and number in Saccharomyces cerevisiae. *Mol Biol Cell*. 15:665-77.

Vizeacoumar, F.J., J.C. Torres-Guzman, Y.Y. Tam, J.D. Aitchison, and R.A. Rachubinski. 2003. YHR150w and YDR479c encode peroxisomal integral membrane proteins involved in the regulation of peroxisome number, size, and distribution in Saccharomyces cerevisiae. *J Cell Biol*. 161:321-32.

Wanders, R.J., and H.R. Waterham. 2006. Biochemistry of mammalian peroxisomes revisited. *Annu Rev Biochem*. 75:295-332.

Wang, X., M.J. Unruh, and J.M. Goodman. 2001. Discrete targeting signals direct Pmp47 to oleate-induced peroxisomes in Saccharomyces cerevisiae. *J Biol Chem*. 276:10897-905.

Wei, H., S. Kemp, M.C. McGuinness, A.B. Moser, and K.D. Smith. 2000. Pharmacological induction of peroxisomes in peroxisome biogenesis disorders. *Ann Neurol*. 47:286-96.

Wibley, J.E., A.E. Pegg, and P.C. Moody. 2000. Crystal structure of the human O(6)-alkylguanine-DNA alkyltransferase. *Nucleic Acids Res*. 28:393-401.

Wierzbicki, A.S., M.D. Lloyd, C.J. Schofield, M.D. Feher, and F.B. Gibberd. 2002. Refsum's disease: a peroxisomal disorder affecting phytanic acid alpha-oxidation. *J Neurochem*. 80:727-35.

Williams, C., M. van den Berg, and B. Distel. 2005. Saccharomyces cerevisiae Pex14p contains two independent Pex5p binding sites, which are both essential for PTS1 protein import. *FEBS Lett*. 579:3416-20.

Xu-Welliver, M., S. Kanugula, N.A. Loktionova, T.M. Crone, and A.E. Pegg. 2000. Conserved residue lysine165 is essential for the ability of O6-alkylguanine-DNA alkyltransferase to react with O6-benzylguanine. *Biochem J*. 347:527-34.

Xu-Welliver, M., J. Leitao, S. Kanugula, W.J. Meehan, and A.E. Pegg. 1999. Role of codon 160 in the sensitivity of human O6-alkylguanine-DNA alkyltransferase to O6-benzylguanine. *Biochem Pharmacol*. 58:1279-85.

Xu-Welliver, M., and A.E. Pegg. 2000. Point mutations at multiple sites including highly conserved amino acids maintain activity, but render O6-alkylguanine-DNA alkyltransferase insensitive to O6-benzylguanine. *Biochem J*. 347:519-26.

Yokota, S. 1993. Formation of autophagosomes during degradation of excess peroxisomes induced by administration of dioctyl phthalate. *Eur J Cell Biol*. 61:67-80.

Zhang, Y., and D.C. Chan. 2007. Structural basis for recruitment of mitochondrial fission complexes by Fis1. *Proc Natl Acad Sci U S A*. 104:18526-30.

SUMMARY

Peroxisomes are vital single membrane-bound organelles present in all eukaryotic cells. Their function is mainly associated with lipid metabolism and they enclose hydrogen peroxide-generating and degrading enzymes. Peroxisomes are highly versatile organelles that quickly adjust their shape, size, number and protein content according to the cellular requirements. In humans, defects in peroxisome biogenesis lead to devastating diseases such as the Zellweger syndrome. Over 30 proteins, the peroxins, are involved in peroxisome biogenesis. In the yeast *Saccharomyces cerevisiae*, peroxins of the PEX11-family, namely PEX11, PEX25 and PEX27, participate in peroxisome proliferation. Indeed, yeasts lacking *PEX11* present fewer and larger peroxisomes than wild type cells. Orthologues of the yeast PEX11-proteins, PEX11α, β, γ and PEX11-1 to -5 have been identified in human and plants, respectively.

We sought to analyze the regulation of peroxisome proliferation through the PEX11-protein families in yeast, plant and human cells. This thesis focuses on human cells, where we performed co-expression studies using mCherry-SKL as peroxisomal matrix marker. We statistically described the effects of the different overexpressed GFP-Pex11 fusion proteins on peroxisome size and number. To pinpoint the molecular role of the Pex11 proteins we analyzed the overexpression effects over time. We further analyzed Pex11 proteins harboring point mutations and domain deletions. Moreover, we established stable cell lines expressing either peroxisomal marker proteins or a SNAP-TEV tagged version of Pex11. This tag enables to perform live cell imaging as well as biochemical experiments.

Our analysis of ten proteins of the Pex11 family provided interesting hints on the conservation of the peroxisomal proliferation machinery between yeast, plant and human cells.

ZUSAMMENFASSUNG

Peroxisomen sind wichtige, von einer einzelnen Membran umgebene Organellen, die in allen eukaryotischen Zellen vorkommen. Ihre Funktion betrifft hauptsächlich den Lipidstoffwechsel; sie enthalten auch Wasserstoffperoxid generierende und abbauende Enzyme. Peroxisomen sind sehr wandlungsfähige Organellen, die ihre Form, Größe, Anzahl und Proteininhalt rasch an die zellulären Anfordernisse anpassen. Bei Menschen führen Defekte in der Peroxisomenbiogenese zu verheerenden Krankheiten, wie etwa das Zellweger Syndrom. Über 30 Proteine, die Peroxine, sind in die Peroxisomenbiogenese involviert. In der Hefe *Saccharomyces cerevisiae* nehmen die Peroxine der Pex11 Familie, nämlich Pex11, Pex25 und Pex27 an der peroxisomalen Proliferation teil. Tatsächlich sind in Hefen, disruptiert für das *PEX11* Gen, weniger und größere Peroxisomen vorhanden als in Wildtypzellen. Orthologe der Hefe-Pex11 Familie wurden in Säugetieren (Pex11α, β und γ) und Pflanzen (Pex11-1 bis -5) gefunden.

Wir analysierten die Regulation der peroxisomalen Proliferation durch die Pex11 Proteinfamilien in Hefe, Pflanzen und Menschen. Diese Arbeit beschäftigt sich mit humanen Zellen, wo wir Coexpressionsstudien mit mCherry-SKL, einem peroxisomalen Matrixmarker, durchgeführt haben. Des weiteren haben wir die Effekte der verschiedenen überexprimierten GFP-Pex11 Fusionsproteine auf die Größe und Anzahl der Peroxisomen statistisch beschrieben. Zudem analysierten wir die Überexpressionseffekte der GFP-Pex11 Fusionsproteine über einen größeren Zeitrahmen hinweg, um die molekulare Rolle der Pex11 Proteine genauer bestimmen zu können. Weiters untersuchten wir bestimmte Punktmutationen sowie Domänendeletionen einzelner Pex11 Proteine. Zusätzlich etablierten wir stabile Zelllinien, sowohl für die Expression eines peroxisomalen Matrixmarker-Proteins, als auch für SNAP-TEV getaggte Pex11 Fusionsproteine. Dieser Tag ermöglicht live cell imaging sowie biochemische Experimente.

Unsere Analyse von zehn Proteinen der Pex11 Familie hat interessante Hinweise auf die evolutionäre Konservierung der peroxisomalen Proliferationsmaschinerie zwischen Hefe, Pflanzen und Menschen geliefert.

Curriculum vitae

Johannes- Paul M. Koch

education:

since Sep 2007	working on diploma thesis ("Functional analysis of Proteins of the Pex11-family in human cells and their role in peroxisome proliferation"), University of Vienna, Dept. of Biochemistry, supervisor: Dr. Cécile Brocard
June 2006	first diploma-certificate summa cum laude
since 2003	studies of chemistry at the University of Vienna and studies of economics at the University of economics and business administration of Vienna
2002-2003	military service
2002	Matura at Schottengymnasium cum laude (in combination with a scholarly research paper, awarded with the first prize of the "Gesellschaft österreichischer Chemiker")
1994-2002	gymnasium (high school) Schottengymnasium Wien
2001	two weeks language course in Spain (Spanish)
2000	five weeks exchange student in Paris (French)
1998/99	six weeks in total language course in the U.K. (Cambridge)

employment:

2007	holiday internship/ Baxter AG, Orth a.d.Donau, GMP
since 2005	cashier/ Peek & Cloppenburg GmbH&CoKG, Vienna (weekly)
2005/06	tutor at the University of Vienna, Institute of Physical Chemistry
2005	holiday internship/ Austrian Research Center Seibersdorf, Systems Research GmbH
2004	holiday internship/ G.L. Pharma, quality control, GLP
2003&2002	holiday internship/ G.L. Pharma, assistant to the production manager
2001	salesman/ Vemap.Com, Vienna
2000	salesman/ McDonalds, Klosterneuburg

extracurricular activities:

since 2008	member of „Österreichische Gesellschaft für Biochemie und Molekularbiologie" (OEGBM)
since 2003	full member of the "Aktionsgemeinschaft Naturwissenschaften", a student fraction, elective offices: chairman of the chemistry board

poster: FEBS-IUBMB-2008, Athens ("Study on the Evolution of the Peroxisomal Proliferation Machinery in Yeast and Human Cells" Johannes Koch, Anja Huber, Andreas Hartig, Kornelija Pranjic, Friedrich Kragler, Cécile Brocard)

grants:

2006	"Leistungsstipendium aus den Sondervermögen" as well as "Leistungsstipendium aus den Mitteln des Bundesministeriums"of the University of Vienna
2008	FEBS- bursary grant for FEBS congress 2008 in Athens, GR